leti
innovation for industry

Annual Research Report 2013

Wellness sensors

Lab On chip

Microfluidics

Radiation Imaging

Optical Imaging

Neural Interfaces

Microtechnologies for Biology and Healthcare

Chemistry

Environment

Delivery Systems

DE LA RECHERCHE À L'INDUSTRIE
cea

Annual Research Report 2013

Microtechnologies for Biology and Healthcare

Leti is an institute of **CEA**, a French research-and-technology organization with activities in energy, IT, healthcare, defence and security.

By creating innovation and transferring it to industry, Leti is the bridge between basic research and production of micro- and nanotechnologies that improve the lives of people around the world.
Backed by its portfolio of 2,200 patents, Leti partners with large industrials, SMEs and startups to tailor advanced solutions that strengthen their competitive positions. It has launched more than 50 startups. Its 8,000m² of new-generation cleanroom space feature 200mm and 300mm wafer processing of micro and nano solutions for applications ranging from space to smart devices. Leti's staff of more than 1,700 includes 200 assignees from partner companies. Leti is based in Grenoble, France, and has offices in Silicon Valley, Calif., and Tokyo.

Visit www.leti.fr for more information

Microtechnologies for Biology and Healthcare research activities are mainly dedicated to Medical Imaging, In Vitro Diagnostic, Biosensors and Environment Monitoring fields of applications. These activities cover the design, integration and qualification of systems comprising sensors (for radiation, biochemical, neural activity or motion detection) or actuators, analog front end electronics, acquisition system, signal processing algorithms, data management and control software.

The design and fabrication of microfluidic components with embedded biological functions and associated systems is also addressed. This set of R&D works is achieved through strong partnerships with academic or industrial partners ranging from SMEs to large international companies. Bridging the gap between basic research and industrial developments, the collaborative projects main goal, is to introduce scientific achievements into innovative and successful new products.

Contents

Edito 5

Key figures 7

E-Books and
book chapters 9

Radiation Detection 11

Optical Imaging 19

Microfluidics 29

Sensors and
Medical Devices 37

Neural Interfaces 47

Nanotechnologies 51

PhD Degree Awarded 59

Edito

Daniel Vellou,
Head of Microtechnologies for Biology and Healthcare Division

President Hollande and French Minister of Industrial Renewal, Arnaud Montebourg, presented on Thursday, September 12th, their plan to build the « new industrial France ». The plan will support 34 strategic industrial priorities, implying sectors such as health, factory of the future, nanotechnologies, food, environments… which are our main application domains.

For instance, the French market of the health industries and technologies represents more than 200 000 employees and 75 billion euros. But 94% of the companies have less than 250 employees.

As a model of technology transfer to SMEs, the CEA-Leti has a key role to help these companies to grow and to become reference in Europe.

This document presents our major achievements in 2013, obtained through collaborative research conducted with large and small companies as well as academic teams.

Flowpad, a generic microfluidic platform, is a key realization. It answers the need to miniaturize and integrate laboratory procedure into a lab-on-chip and thanks to its modularity it can be adapted to a wide range of applications.
We worked closely with designers to be able to deliver a prototype ready to transfer to the industry, which is one of our main challenges of the next years.

We continue also our close collaboration with Clinatec, a unique biomedical translational technology center. We have developed a new optical device allowing a small area into the brain to be locally irradiated with near infrared light that could potential to slow down degeneration of dopaminergic cells in Parkinson disease.

The main objectives of next year remain miniaturization, multi-modality, prototypes "ready to transfer", going towards low-cost products and connected devices (m-health, e-health).

[1] Panorama d'une filière d'excellence: les industries et technologies de santé

Key Figures

134 Permanent researchers

88 PhDs, Post-docs and short term contracts

54 Book Chapters & Journals

47 Conferences & workshops

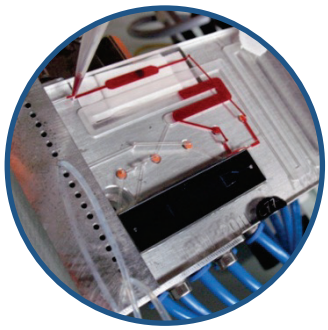

Clean rooms dedicated to surface chemistry and biochemistry

A dedicated chemistry platform for synthesis and formulation

36 Patents filed in 2013

352 Patents Portfolio

E-Books & Book chapters

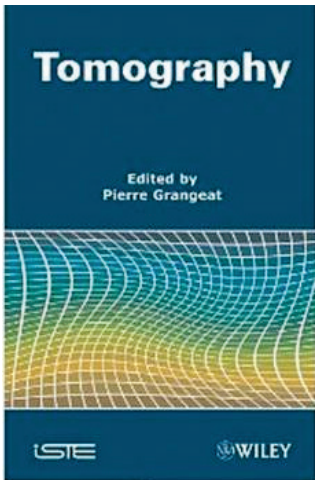

E-Book - Tomography
Grangeat P.

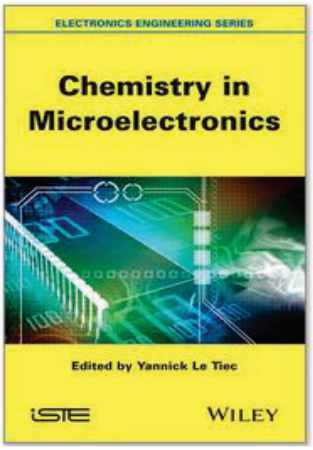

Chapter – Surface Functionalization for Micro-and nanosystems: Application to Biosensors
Hoang A., Marchand G., Nonglaton G., Texier-Nogues I., Vinet F.

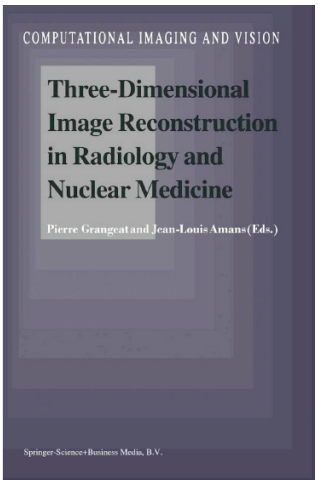

E-Book
Three-Dimensional Image Reconstructiopn in Radiology and Nuclear Medicine

Grangeat P., Amans J. L.

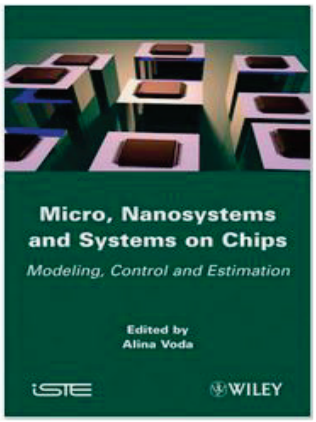

E-Book-Chapter
Fractional Order Modeling and Identification for Electrochemical Nano-biochip
Djouambi A., Voda A., Grangeat P., Mailley P.

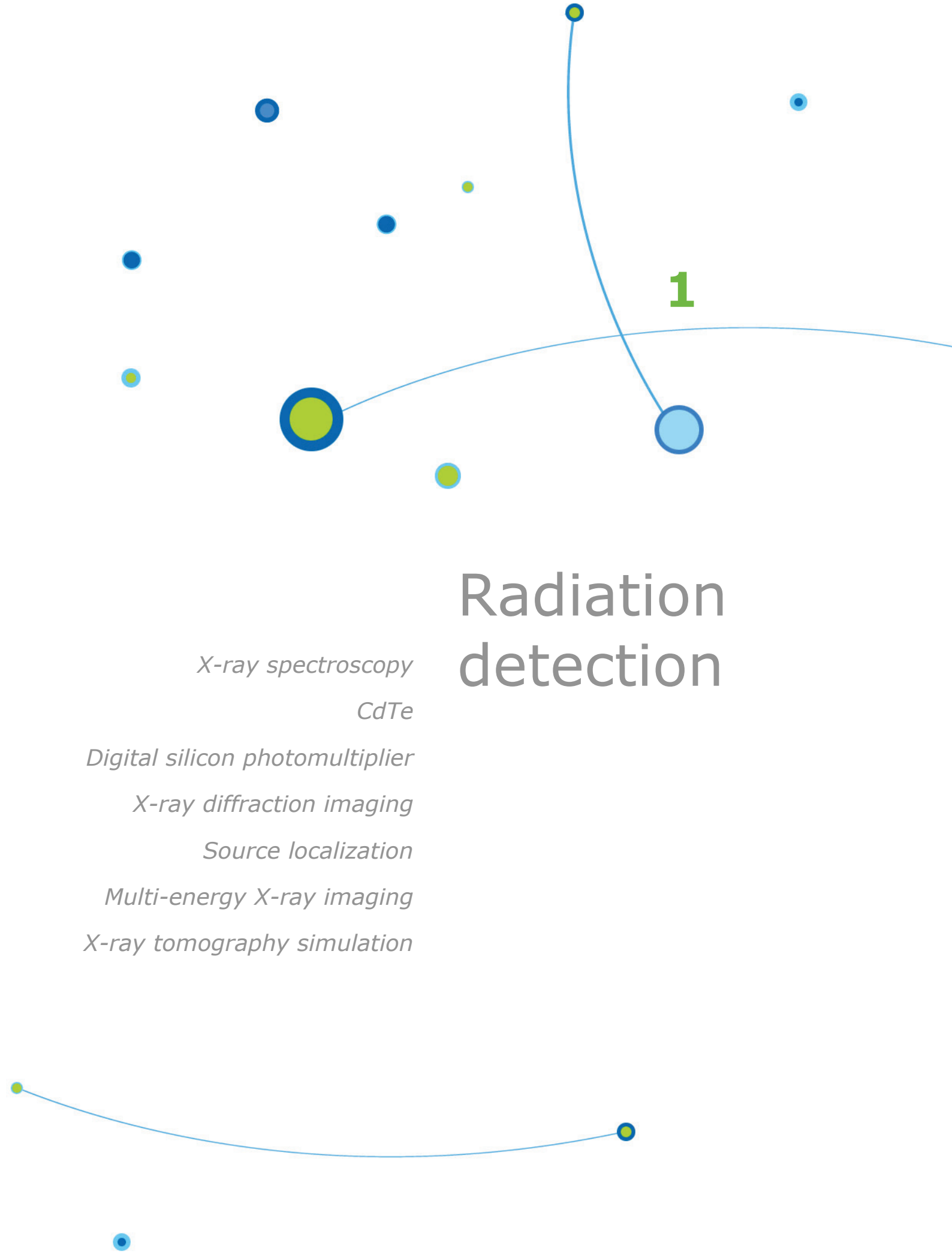

1

Radiation detection

X-ray spectroscopy

CdTe

Digital silicon photomultiplier

X-ray diffraction imaging

Source localization

Multi-energy X-ray imaging

X-ray tomography simulation

Comparing performances of a CdTe X-ray spectroscopic detector and an X-ray dual energy sandwich detector

Research topics: X-ray, CdTe detector, explosive detection

A. Gorecki, A. Brambilla, V. Moulin, E. Gaborieau, P. Radisson and L. Verger

ABSTRACT: Multi-Energy (ME) detectors are becoming a serious alternative to classical Dual-Energy Sandwich (DE-S) detectors for X-ray applications such as medical imaging or explosive control. The performances of these two detector technologies are compared between each other with simulations and experimental measurements. With the same photon statistics, the ME detector performs 3.5 times better than DE-S detector on a material distinction criterion. In case of explosive detection, the gain on the false detection rate is about 2.9.

So far, the devices used to detect explosive in the luggage work with **Dual Energy Sandwich (DE-S) detector**. These modules provide just low and high energy measurements which occur to be mixed. Today, MultiX (a spinoff of Thales) provides a **Multi Energy (ME) CdTe detector**, called **ME100**, based on technologies developed by LETI [2] [3]. ME100 detector works at room temperature and associates both **high count rate** (at 3.1 10^6 photons/mm²/s, the lost rate is about 8%) and **good energy resolution** (8.5 keV at 60 keV). It has 128 pixels (pitch 800µm) and provides a spectrum for each pixel: 128 channels for an energy range from 20 keV to 160 keV.

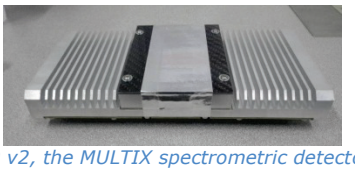

Figure 1: ME100 v2, the MULTIX spectrometric detector

To compare the performance of these two types of detector technologies, ME and DE-S, two materials "A" and "B" are chosen such that their spectral signatures are very close to each other. The **Distinction Criterion (DC)** is defined as follow:

$$DC = \sqrt{\sum_{i=1}^{n_{ch}} \frac{(\overline{mes}_{A,i} - \overline{mes}_{B,i})^2}{\sigma_{A,i}^2 + \sigma_{B,i}^2}}$$

Where $\overline{mes}_{A,i}$ and $\overline{mes}_{B,i}$ are the average of the measurements on the two materials in channel i, $\sigma_{A,i}$ and $\sigma_{B,i}$ the associated noise and n_{ch} is the number of channels, i.e. 2 for the DE-S detector and 128 for the ME detector. The higher the DC value, the better the distinction capacity of the detector between material A and B is.
DC was firstly computed from simulated data (using a detector model developed in [4]). The A and B materials are POM and PMMA. For each POM thickness and photon statistics, the PMMA thickness is found so that it minimizes the DC value as shown on figure 2.
For similar conditions, the ratio of DC values between the two types of detectors **is always around 3.5 in favor of ME detector**.

The simulated values of DC for ME and DE-S detectors have been confirmed experimentally. For the ME detector for instance, figure 3 displays DC values with the number of energy bins taken into account for 2 cm of POM and 2.5 cm of PMMA. Experimental and simulated curves show a good agreement and the DC value reaches 1.4, over the whole energy range, for both cases.

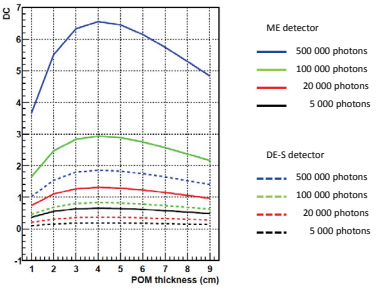

Figure 2: DC values for ME and DE-S detectors (simulation results)

For the DE-S detector, the comparison is harder. Indeed, the scintillator used in DE-S has a significant afterglow which acts as a filter on the measurements. So the noise values are underestimated and the DC value appears inordinately high. By taking into account the time constant of scintillator the simulation, the DC values for the DE-S detector are confirmed as well.

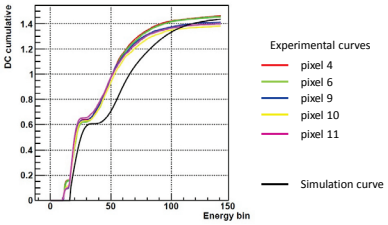

Figure 3: ME detector: comparison of experimental and simulation DC values

For the context of luggage inspection, we have converted this result in value of false detection rate (FDR): **ME detector is able to reduce FDR by a factor of 2.9 in relation to DE-S detector** for 4cm of POM**.**

Related Publications:
[1] A. Gorecki, A. Brambilla, V. Moulin, E. Gaborieau, P. Radisson and L. Verger, "Comparing performances of a CdTe X-ray spectroscopic detector and an X-ray dual-energy sandwich energy", 2013 JINST 8 P11011
[2] A. Brambilla, P. Ouvrier-Buffet, G. Gonon, J. Rinkel, V. Moulin, C. Boudou and L. Verger, "Fast CdTe and CdZnTe semiconductor detector arrays for spectroscopic X-ray imaging", IEEE T. Nucl. Sci. 60 (2013) 408.
[3] A. Brambilla, P. Ouvrier-Buffet, J. Rinkel, G. Gonon, C. Boudou and L. Verger, "CdTe linear pixel X-ray detector with enhanced spectrometric performance for high flux X-ray imaging", IEEE T. Nucl. Sci. 59 (2012) 1552.
[4] J. Tabary, P. Hugonnard and F. Mathy, SINBAD: "a realistic mutli-purpose and scalable X-ray simulation tool for NDT applications", Proc. Int. Symp. Digital Industrial Radiology CT (2007) [http://www.ndt.net/article/dir2007/papers/s4.pdf]

Effect of Dislocation Walls on Cadmium Telluride based X-ray Imagers

Research topics: Dislocations, CdTe, X-ray imager, transport properties

E. Gros d'Aillon, C. Buis

ABSTRACT: Microstructural defects in cadmium (zinc) telluride bulk crystals can affect the performances of Cd(Zn)Te-based X and gamma ray imagers. The effect of dislocation walls on the sensor dark current and photocurrent is shown, as well as the reduction of charge carrier transport properties.

Cadmium (Zinc) Telluride is the material of choice for X-ray and gamma ray detection in the medical imaging energy range. Images with good image quality are commonly produced in integration mode, were the X-ray flux is summed, or in counting mode, where each X-photon is individually counted at high rate However, defects in single crystals, such as inclusions and dislocations can induce charge transport inhomogeneities, resulting in image quality degradation, whatever the imaging mode.

A small imaging sensor prototype dedicated to mammography has been developed, based on a single crystal CdTe:Cl detector, hybridized through indium bump bonding to a CMOS readout circuit working in integration mode. It is an array of 200×200 pixels with 75 µm pitch. The Pt/CdTe/Pt detector has a thickness of 1 mm and a 16×16 mm² active area. The leakage-current of the semiconductor crystal as well as the gain of the sensor are measured for offset and sensitivity correction. Fig. 1 left shows a raw picture of a cowry shell measured under x-ray. Linear microstructures, with higher dark current and photocurrent, around one-pixel-wide (75 µm), are superimposed to the cowry image. These artifacts could be almost fully corrected using a linear model. However, some defects are still visible after correction because their behavior is not linear. Furthermore, some defects reappear over time because their effect is not stable over time (Fig. 1 right).

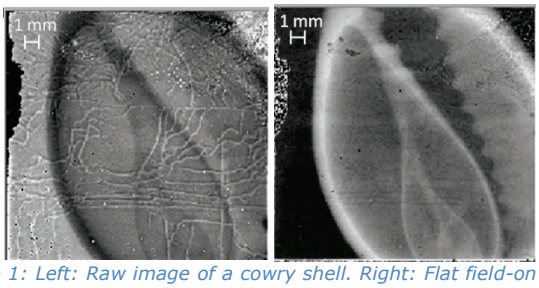

Figure 1: Left: Raw image of a cowry shell. Right: Flat field-on offset corrected image after 10 s irradiation.

In order to understand the origin of these linear defect, the sensor was disassembled and the CdTe:Cl crystal was mechanically polished to remove electrodes. The sample surface has been etched using a Nagawa solution in order to investigate the distribution of threading dislocations. The etchpits are arranged in lines to form subgrain boundaries, with several preferential directions which follow the crystal axis (Fig. 2 right). An exact correlation has been shown between the sensor dark-current, the sensitivity and the positions of the dislocation walls revealed at the surface of the sample (Fig 2) [1]. Dislocations induced small misorientations in the bulk crystal have also been measured using White Beam X-ray Diffraction Imaging (topography) measurements on the sample in transmission geometry, in the BM05 beamline of the European Synchrotron Radiation Facility. It shows that the dislocation walls thread the whole 1mm thickness of the sensor with an angle which range from 0 to 40°.

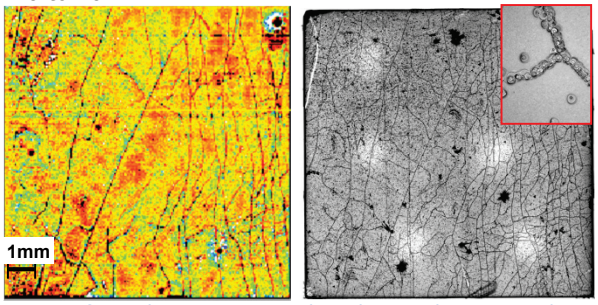

Figure 2: Left: Dark-current map CdTe:Cl X-ray detector. Right: Etch pits revealed on the (111) Cd face of the same CdTe:Cl crystal.

The effect of this dislocations walls on the charge carrier transport properties have been measured using an Ion Beam Induced Current facility (Fig. 3). We have shown that electron and holes mobility×lifetime products are reduced by respectively 15% and 20% by these extended defects [2].

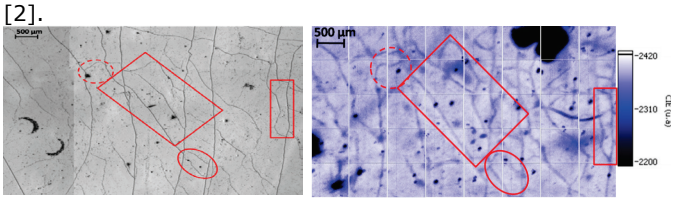

Figure 3: Left: Etch pits revealed with Everson solution on the (111)Te face of the CdTe:Cl crystal. Right: Electron charge collection efficiency map.

In order to solve this problem, the subgrain boundaries must be suppressed at the crystal growth level.

Related Publications:
[1] Effects of Dislocation Walls on Image Quality When Using Cadmium Telluride X-Ray Detectors, Buis, C., Marrakchi, G., Lafford, T.A., Brambilla, A., Verger, L., Gros d'Aillon, E. IEEE Trans. on Nucl. Sci., 60 (1), 2013, pp. 199-203.
[2] Effects of dislocation walls on charge carrier transport properties in CdTe single crystal, C. Buis, E. Gros d'aillon, G. Marrakchi, T. A. Lafford, A. Brambilla, L. Verger Nucl. Instr. And Meth. A, Vol. 735, 2014, pp 188-192

First Characterization of the SPADnet sensor: a Digital Silicon Photomultiplier for ToF-PET Applications compatible with MRI

Research topics: Gamma Detector, PET, SPADs, SiPM

E. Gros d'Aillon, L. Maingault, E. Charbon (TU Delft), Claudio Bruschini (EPFL), D. Stoppa (FBK), R. Henderson (Univ. Edin.), E. Lorincz (BUTE), L. Grant (STMicro), G. Nemeth (Mediso)

ABSTRACT: We present a new fully digital Silicon Photomultiplier fabricated in CMOS image sensor technology. It contains 16x8 pixels, 600µm pitch and is designed for use in Magnetic Resonance Imaging compatible Time-of-Flight Positron Emission Tomography (ToF-PET). The electro-optical properties of each 92160 Single Photon Avalanche Photodiodes within the array was measured. The sensor was optically coupled to LYSO scintillator crystals and the performance of this device for the PET application is assessed.

Current developments for Positron Emission Tomography follow two axes: The measurement of the gamma photons Time of Flight (ToF-PET), which improves the marker position determination, and the coupling of PET with a Magnetic Resonance Imaging scanner (PET-MRI), which provides soft-tissue contrast for attenuation correction without the patient dose induced by Computed Tomography scanners. Silicon Photomultipliers (SiPM) are insensitive to the strong magnetic field of the MRI, and are candidates to replace Photomultiplier Tubes (PMTs), for MRI compatible PET. Matching PMTs in terms of photon counting capability and timing performance, the system electronics is simplified thanks to aggressive integration. SiPMs are constituted by Single Photon Avalanche Photodiodes (SPAD), which are grouped in arrays to form pixels. Using CMOS technology, each SPAD is individually digitized: noisy SPADs can be disabled and timing information is generated on-chip; several photons can be time stamped, potentially enabling a more robust measurement process and better timing resolution.

SPADnet (http://spadnet.eu/) is a collaborative research project funded by the European Union. The first version of the SPADnet photosensor, a fully digital CMOS SiPM with 8×16 pixels, 600µm pitch, individually capable of photon time stamping and energy measurement, was fabricated (Fig. 1) [1]. Each pixel contains 720 SPADs and the array fill factor is 42.6%. The sensor also provides real-time output of the total detected energy at up to 100Msamples/s and on-chip discrimination of gamma events. The chips are 4-sides tileable using Through Silicon Via pads.

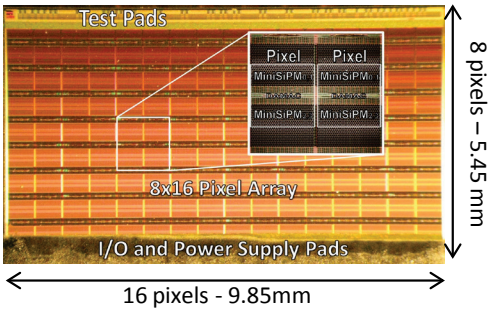

Figure 1: SPADnet-I chip micrograph

The electro-optical properties of each one of the 92k SPADs have been measured using 1.5V excess bias. The mean Dark Count Rate (DCR) is 24KHz and doubles every 17°C. Since these measurements, new devices with 10KHz mean DCR have been fabricated. The SPADs Photon Detection Probability (PDP) peaks at 32% at 450nm.

Several chips have been optically coupled to LYSO scintillator needles with dimensions suited for clinical and preclinical imaging (Fig. 2) without alignment between the scintillator pitch and the sensor pitch. In both cases, the energy resolution at 511keV is 13% FWHM. The 1.3 mm preclinical needles are clearly resolved (Fig. 3). The distortion on the edge of the image is due to the smaller sensor dimensions compared to the scintillator array. The coincidence timing resolution is better than 300ps FWHM.

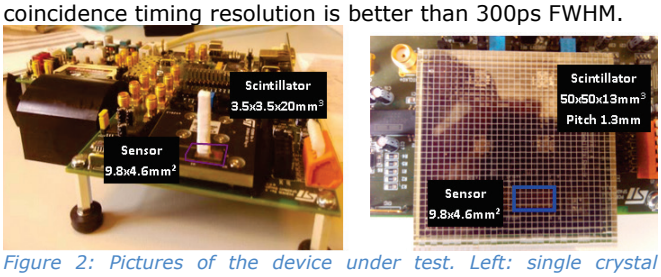

Figure 2: Pictures of the device under test. Left: single crystal needle. Right: array of LYSO crystals. The blue square represents the sensor

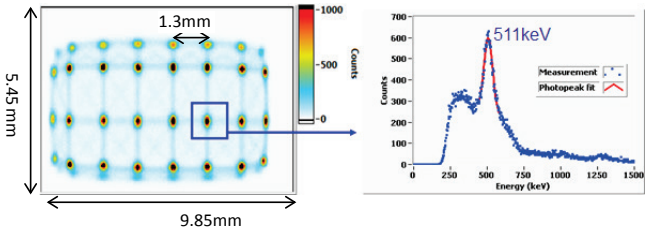

Figure 3: Left : images of scintillations. Right: energy spectrum from one single needle

The SPADnet sensor performance makes it suitable for MRI compatible ToF-PET. A larger version of this sensor is currently under fabrication and will be assembled in 5x5cm² tiles which will be integrated in a PET ring. This work, conceived within the SPADnet project, has been supported by the European Community within the European Community within the Seventh Framework Programme ICT Photonics.

Related Publications:
[1] C. Bruschini, E. Charbon, C. Veerappan, L.H.C. Braga, N. Massari, M. Perenzoni, L. Gasparini, D. Stoppa, R. Walker, A. Erdogan, R.K. Henderson, S. East, L. Grant, B. Jatekos, F. Ujhelyi, G. Erdei, E. Lörincz, L. André, L. Maingault, V. Reboud, L. Verger, E. Gros d'Aillon, P. Major, Z. Papp, G. Németh, "SPADnet : Embedded Coincidence in a Smart Sensor Network for PET Applications", Nucl. Instr. And Meth. A, Vol. 734, 2014, pp 122–126
[2] E. Gros d'Aillon, L. Maingault, L. André, V. Reboud, L. Verger, E. Charbon, C. Bruschini, C. Veerappan, D. Stoppa, N. Massari, M. Perenzoni, L. H. Braga, L. Gasparini, R. K. Henderson, R. Walker, S. East, L. Grant, B. Jatekos, E. Lorincz, F. Ujhely, G. Erdei, P. Major, Z. Papp, and G. Nemeth,"First Characterization of the SPADnet sensor: a Digital Silicon Photomultiplier for PET Applications", JINST 8(12) p. C12026, 2013.

IMADIF: An Autonomous CZT Module for X-ray Diffraction Imaging

Research topics: X-ray Imaging, diffraction, CdZnTe (CZT)

J.-M. Casagrande, G. Montémont, D. Kosciesza (Morpho), O. Monnet, S. Stanchina, L. Verger

ABSTRACT: A CZT-based detection module dedicated to X-ray diffraction imaging has been developed and produced on a small scale basis to be integrated in a cabin baggage scanning system prototype aimed at detecting illicit substances. The module shows a very good performance in efficiency, energy and spatial resolution in the 20-150 keV range. In addition to its mechanical compactness, it is completely autonomous since it includes calibration process and multi-parametric corrections..

The use of energy-dispersive X-Ray Diffraction (XRD) in security screening applications allows for highest detection and lowest false-alarm rates. So far, only Germanium-detectors have been used in commercially available XRD baggage-scanning systems, limiting the available detection area due to technical and commercial reasons, and as a consequence, the achievable throughput. In order to considerably improve the throughput of diffraction baggage scanner and thus enable XRD screening of cabin baggage, a new imaging architecture is based on the use of room temperature operated CZT detectors in replacement of cooled Germanium. CZT detectors allow to build compact and modular detection units (see Fig.1) and offer an energy resolution compatible with diffraction pattern identification.

Figure 1: External view of the detector module. Outline dimensions are 170 x 75 x 78 mm and power dissipation is 3.5 Watts.

In order to resolve Bragg peaks, good energy and spatial resolution are required. To do so, a 5 mm thick high resistivity CZT crystal of 660 mm² area is associated to low noise ASICs dedicated to 192 anodes and 12 cathodes readout and advanced multiparametric event corrections such as depth of interaction, charge sharing and induction sharing are performed using a FPGA circuit [1].

The FPGA also embeds a processor which controls the system, carries out all calibration, automated tests and acquisitions. Therefore, each module is a completely independent unit to ensure service friendliness, receiving only one voltage, a trigger and Ethernet for control and data transfer [2]. This autonomous module is then easy to manage and to integrate into a Cabin Baggage Scanning system which hosts 17 IMADIF detection units.

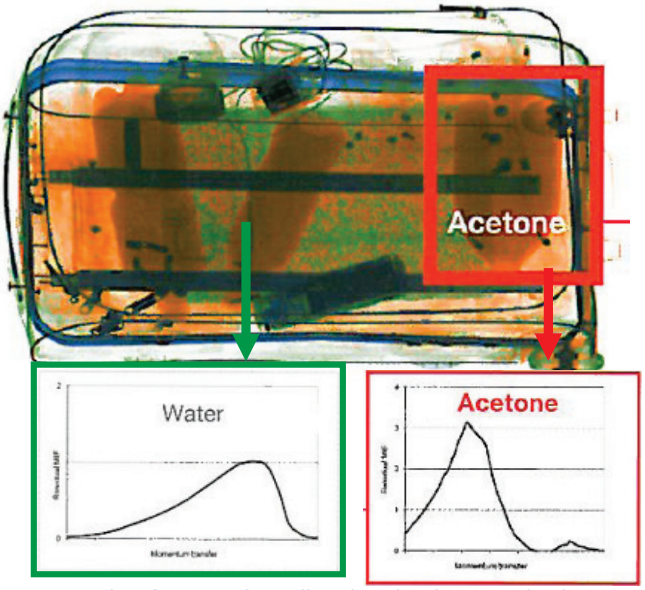

Figure 2: Identification of an illicit liquid substance thanks to its spectrometric signature

Around half hundred prototypes have been manufactured and statistics show quite stable and reproducible performance at room temperature: 73% average efficiency at 60 keV, energy resolution of 3.8% at 60 keV and 2.4% at 122 keV.

The IMADIF module performance allows the full system to discriminate illicit liquid substances **into** a baggage (see Fig.2) at a throughput of up to 600 bags per hour which represents a significant step in the current challenge in security screening applications.

Related Publications:
[1] G. Montémont, D. Kosciesza, O. Monnet, S. Stanchina, J.P . Schlomka, L. Verger, "An autonomous CZT Module for X-ray Diffraction", *IEEE NSS-MIC & RTSD Seoul 2013 - R02-2*
[2] D. Kosciesza, J.P. Schlomka, J. Meyer, G. Montémont, O. Monnet, S. Stanchina, L. Verger, "X-ray Diffraction imaging system for the detection of illicit substances using pixelated CZT-detectors", *IEEE NSS-MIC & RTSD Seoul 2013 – R12-6*

Source localization using a CZT coded aperture mask camera

Research topics: CZT detector, coded aperture, radioactive source localization

G. Montémont, O. Monnet, L. Maingault, S. Stanchina

ABSTRACT: Coded aperture imaging is known to be a sensitive technique allowing radioactive source localization. The image of a source projects the mask pattern of the detector array. By a decoding algorithm, the activity distribution in the field of view can be estimated accurately. We have design a system based on a 100x100 mm² CZT detector array. This dimensioning reaches a good trade-off between system portability and sensitivity.

We have developed a compact gamma-ray detection system comprising 16 CZT crystals of 25x25x5 mm [1,2]. It corresponds to a total detection volume of 50 cm3 of CZT (about 300 g with an average atomic number Z of 49) allowing a relatively sensitive whilst portable system.
CZT is a semiconducting detection material allowing the building of energy and position-sensitive detectors. Therefore, the system has imaging capabilities (128 x 128 pixels on a 10x10 cm² area) and spectral capabilities (5-10 % resolution at 122 keV). The implementation of these features relies on original solutions. First, detector design is based on an orthogonal coplanar strip readout architecture [3] allowing a reduction in the number of needed electronic channels. Second, signal digitizing is carried out using an asynchronous 1-bit modulation scheme allowing the simultaneous digitizing of any active channels [2].
The camera embeds a small computer running an operating system. This system is powered by a single 12V supply. It communicates using an Ethernet interface using standard networking protocols.
The whole system fits into a 15x15x25 cm housing and weights 4 kg (7kg with tungsten shield), see Fig. 1. In order to localize gamma-ray sources, it is possible to use it with various kinds of coded aperture masks. Additionally, an optical camera allows to localize precisely the source position in the field of view.

Figure 1 : Full camera with mask (left) and open view of the system with the detector array and readout electronic boards.

Coded aperture imaging relies on a deconvolution algorithm, that is mandatory to be able to interpret the image (decode the mask pattern). We have chosen to use a Maximum Likelihood Expectation-Maximization (MLEM) technique. The spatial (image) and spectral (isotope) estimations are performed jointly. This helps to separate clearly sources and to maximize the signal-to-noise ratio for each isotope. The decoding is performed online, in real time and the result, colored in function of the isotope type is directly overlaid with the optical image (see Fig. 2).

Figure 2 : Image of unattended luggages containing radioactive sources: two 241Am sources (60 nSv/h and 161 nSv/h) and one 57Co source (10nSv/h).

At low energy (57Co, 122keV), one typically need an accumulated dose of 10 pSv to localize a source. At higher energies (137Cs, 662keV), this threshold value increases to 50 pSv. In both cases, an activity of 1µSv/h is thus detectable in few seconds.
The obtained angular resolution is between 2 and 4° depending on the mask pattern used and the focal length (distance between mask and detector array).

Related Publications:
[1] F. Mathy & al., "Experimental tests of a 10x10cm CZT Imaging System for Gamma and µ-SPECT Imaging", IEEE NSS-MIC-RTSD, 2013.
[2] S. Stanchina & al., " Embedded Data Processing for an Autonomous 1010 cm CZT Imaging System Using Orthogonal Capacitive Strip Technology", IEEE NSS-MIC-RTSD, 2013.
[3] G. Montémont & al, "Simulation and Design of Orthogonal Capacitive Strip CdZnTe Detectors", IEEE Transactions on Nuclear Science, vol. 54, no. 4, p. 854-859, 2007.

Multi-Energy X-ray Imaging Detection for Waste Sorting

Research topics: X-ray imaging, waste sorting, environment

A. Brambilla, F. Marticke, J. Rinkel, G. Gonon, V. Moulin

ABSTRACT: The NOPTRIX-ME project was founded to evaluated the performance of an energy sensitive X-ray imaging detector for waste sorting. The ME 100 detector measures the energy distribution of X-rays transmitted by the analyzed materials, providing information on their chemical composition. This property was used to detect low concentrations of brominated and chlorinated flame retardants in polymers. The results obtained during the first phase of the project convinced us to produce a full scale demonstrator which will be operational end of 2014.

Recycling of waste has become a major economic and environmental issue. The market is growing rapidly and is based on advanced waste sorting technologies. Among them, X-Ray Transmission imaging (XRT) plays an important role due to its ability to provide real-time volumetric information on the chemical composition of the sorted waste. This feature makes it a unique technique for sorting polymers, metals, glass or batteries.

The NOPTRIX-ME project is a collaboration between CEA-LETI, Ecole des Mines d'Alès, Multix and Bertin to evaluated the interest of energy sensitive X-ray imaging for waste sorting. We used the ME100 detector developed by the Startup MULTIX in collaboration with the LETI. Based on a cadmium telluride linear sensor, ME100 can measure the energy distribution of transmitted X-ray flux giving information on the chemical composition of the analyzed materials. The fast read-out electronic provides high count rates up to 5 Mcounts/s in order to withstand strong X-ray fluxes encountered in NDT applications.

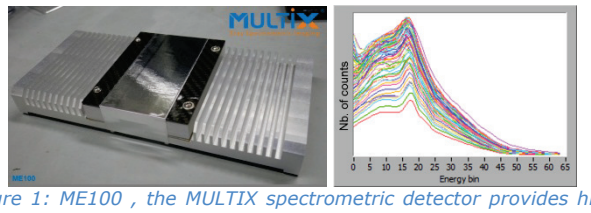

Figure 1: ME100 , the MULTIX spectrometric detector provides high resolution X-ray pulse-height spectra in real time from 128 pixel.

We focused our study on the sorting of plastic wastes. Undesired additives such as brominated and chlorinated flame retardant increase the mean atomic number of polymers thus modifying the energy spectrum of transmitted X-rays.
Figure 2 show the raw image transmitted by 3 mm thick polyethylene samples with 0%, 1% and 5 % Bromine shown figure 2. The bromine content modifies the mean atomic number and thus the energy distribution of the measured spectra. Samples with high bromine content appear dark gray due to the increased the X-ray absorption. However, samples with different thicknesses and bromine content can have the same absorption.

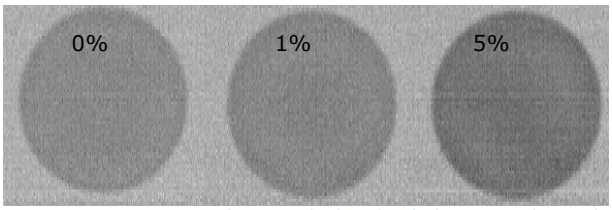

Figure 2: Raw images of 3 mm thick polyethylene samples with 0%, 1% and 5 % Bromine.

The ambiguity can be removed by using the energy information given by the measured X-ray pulse-height spectra. We have developed a method of treatment to estimate the concentration of Brome in the measured samples. In figure 3, the presence of bromine estimated with this method is represented in red while pure polyethylene is represented in green. The pure polyethylene sample can be discriminated from the other samples with bromine.

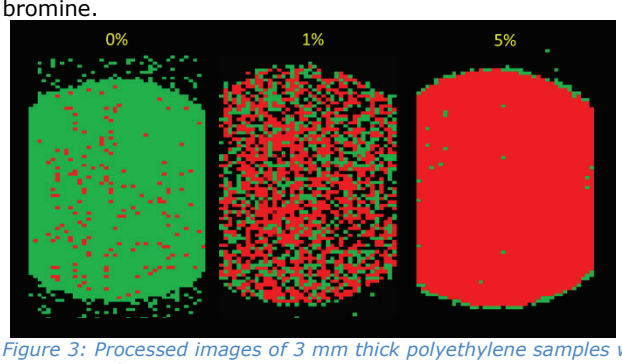

Figure 3: Processed images of 3 mm thick polyethylene samples with 0%, 1% and 5 % Bromine.

These results convinced the partners to continue the collaboration in the design and fabrication of a full scale waste sorting machine prototype. The detector will consist of 10 ME100 detector modules to achieve 1 meter detection width. The task of CEA is to define the conditions of use of the detector and to transfer the processing algorithms that discriminates polymers with undesired additives. The prototype will be installed at BERTIN and will serve as demonstrator for different industrial waste sorting applications.

Related Publications:
[1] Brambilla A., Ouvrier-Buffet P., Gonon G., Rinkel J., Moulin V., Boudou C., Verger L., "Fast CdTe and CdZnTe semiconductor detector arrays for spectroscopic X-ray imaging", (2013) IEEE Transactions on Nuclear Science, 60 (1), art. no. 6395225, pp. 408-415..
[2] Beldjoudi G., Rebuffel V., Verger L., Kaftandjian, V. Rinkel J., "An optimised method for material identification using a photon counting detector", (2012) Nuclear Instruments and Methods in Physics Research, Section A: Accelerators, Spectrometers, Detectors and Associated Equipment, 663 (1), pp. 26-36.
[3] Gorecki A., Brambilla A., Moulin V., Gaborieau E., Radisson P., Verger L., "Comparing performances of a CdTe X-ray spectroscopic detector and an X-ray dual-energy sandwich detector", (2013) Journal of Instrumentation, 60, P11011

Integration of the X-ray tomography simulation software Sindbad in the VIP (Virtual Imaging Platform) web platform

Research topics: Medical imaging, simulation, X-ray tomography

J. Tabary, P. Hugonnard, T. Glatard (INSA), C. Lartizien (INSA) & al.

ABSTRACT: The VIP Project (ANR-RNTL) has enabled the development of a web platform called VIP (Virtual Imaging Platform) that facilitates the sharing of object models and medical image simulators and provides access to distributed computing and storage resources. Several techniques are available, such as magnetic resonance imaging (MRI), positron emission tomography (PET), ultrasound imaging (U.S.) and X-ray tomography (CT). In this project, CEA-Leti has integrated in the platform VIP its X-ray tomography simulation software SINDBAD, developed in-house for over 15 years.

The **Virtual Imaging Platform (VIP)** is an open web platform accessible at http://vip.creatis.insa-lyon.fr for **multi-modality medical image simulation**. It targets (i) interoperability issues among simulators, (ii) the sharing of object models and (iii) the handling of heavy simulations by the use of Distributed Computing Infrastructures (DCIs). It has been designed to be extensible and it currently includes simulators of ultrasound (US) imaging, magnetic resonance imaging (MRI), positron emission tomography (PET) and computed tomography (CT). For the CT modality, **the simulation software SINDBAD** [1], developed at CEA-Leti for over 15 years, has been successfully integrated into VIP.

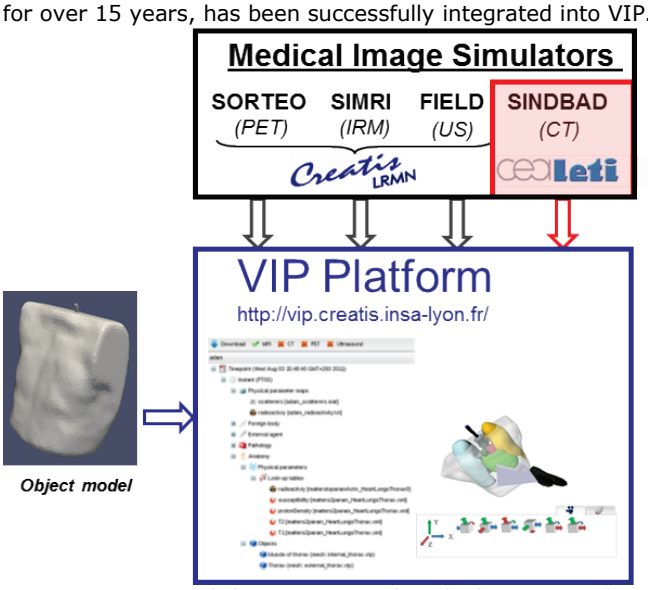

Figure 1: Diagram of the integration of medical image simulators into the VIP platform

A first necessary step to integrate SINDBAD and the other simulators into the VIP platform was to define **common ontologies**, including a same semantic object model representation and a same I/O data architecture. Thus, model files describing geometrical objects (represented as voxel maps or meshes) are annotated with concepts defined in the application ontology called **OntoVIP** [2]. OntoVIP integrates components describing representational objects (model layers, model layer parts, etc.) and their associated real-world entities (anatomical/pathological structures, foreign bodies, etc.). Fig. 1 shows a screenshot of the model repository and simulation scene interfaces.

A major asset of the VIP platform is to provide researchers with **powerful distributed computing and storage resources**. Indeed, computing time of simulations are optimized thanks to a splitting of the workflows on multi-grids. Concerning SINDBAD, simulations are split at two levels: splitting of a CT simulation into independent 2D simulations and splitting of analytical (primary radiation) and Monte-Carlo (scatter radiation) components of each 2D simulation. The reduction of the computing time, obtained thanks to the successful parallelization of SINDBAD into the VIP platform, was very significant with a speed up factor of 70. The work performed during the VIP project has enabled to simulate **realistic CT images**, using models such as XCAT [3] or ADAM models. For instance, Fig. 2 shows a multi-modality simulation of heart imaging, performed in the VIP platform and using the ADAM model.

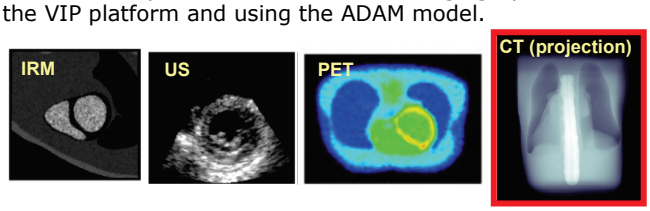

Figure 2: Multi-modality simulations of the ADAM model in the VIP platform

Today, VIP appears as a versatile, open-access platform for multi-modality medical image simulation. This tool can be very convenient for a large panel of users, particularly in conveying a combined understanding of both the fundamental operation of equipment and also its application in the clinical setting. At the beginning of 2013, the platform had 230 registered users who consumed 33 years of CPU time in 2011.

Next steps will be to finalize the development of a **user friendly interface** in order to enter more easily the input parameters, select and modify object models and visualize the resulted simulated images. Concerning SINDBAD, some additional modules such as **dosimetry calculation and reconstruction** will be very useful in future versions. Most **experimental validations** could also be considered soon by working in partnership with scanner manufacturers.

Related Publications:
[1] J. Tabary, P. Hugonnard, F. Mathy, "SINDBAD : a realistic multi-purpose and scalable X-ray simulation tool for NDT applications", Int. Symp. on DIR and CT, Lyon, June 2007
[2] B. Gibaud & al, "OntoVIP: an ontology for the annotation of object models used for medical image Simulation" in IEEE Second Conference on Healthcare Informatics, Imaging and Systems Biology, 2012.
[3] J. Tabary, S. Marache-Francisco, S. Valette, W. P. Segars, C. Lartizien, "Realistic X-Ray CT Simulation of the XCAT Phantom with SINDBAD", in IEEE NSS and MIC Conference, pp. 3980–3983, October 2009.

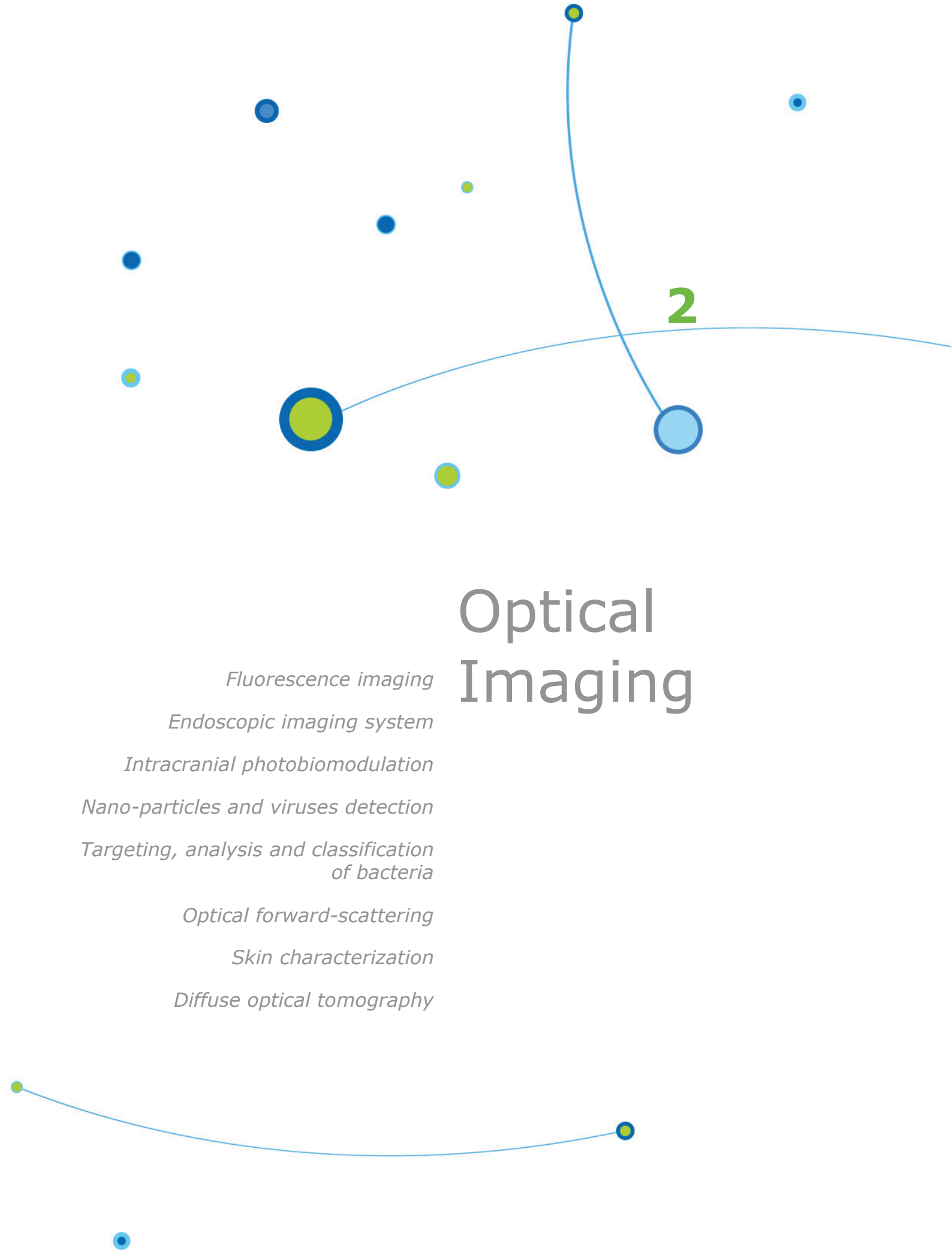

Optical Imaging

Fluorescence imaging

Endoscopic imaging system

Intracranial photobiomodulation

Nano-particles and viruses detection

Targeting, analysis and classification of bacteria

Optical forward-scattering

Skin characterization

Diffuse optical tomography

Laser line scanning illumination scheme for the enhancement of contrast and resolution of fluorescence reflectance imaging

Research topics: Diffuse optics, near infrared, molecular imaging, laser line illumination

F. Fantoni, L. Hervé, V. Poher, J.-M. Dinten

ABSTRACT: Intraoperative fluorescence imaging in reflectance geometry is an attractive imaging modality to noninvasively monitor the fluorescence targeted tumors but suffers from poor resolution due to the diffusive nature of photons in tissue. The proposed technique relies on the scanning of the medium with a laser line illumination and the acquisition of images at each position of excitation. We propose a detection scheme taking advantage of the stack of images acquired to enhance the resolution and the contrast of the final image. This technique has been validated on tissue-like phantoms with different levels of background fluorescence.

The attention to fluorescence reflectance imaging (FRI) has increased for the past few years due to the recent availability of fluorochromes which allow the study of gene expression, protein function and interactions, and a large number of cellular processes in a minimally invasive way.
FRI presents several advantages as it offers good sensitivity when the objects observed are close to the surface, is generally fast, the implementations are easy, low cost and compact. But on the other hand, it suffers from important limitations. One of them is due to the background noise caused by excitation leaks and fluorescence from superficial layers. While the natural fluorescence of tissues may be used as a mean of study it is an obstacle for FRI because it causes the depths addressed to be small (several millimeters): the detected signals decrease exponentially with depth while the background noise remains the same.
Our objective is to reduce as much as possible the effects of these parasite signals to improve the contrast and resolution of the fluorescent targets. To do so, we use a laser line illumination that scans the observed object. FRI is usually done with a wide-field illumination and detection (referred as WF-FRI), which means that both the fluorescent signal of interest and the background signal get excited and we cannot discriminate between the two. Our line scanning approach (referred as LS-FRI) gives access to more information because we acquire images for each position of the laser line on the medium studied. This information can be filtered in different ways to enhance the signal of interest.

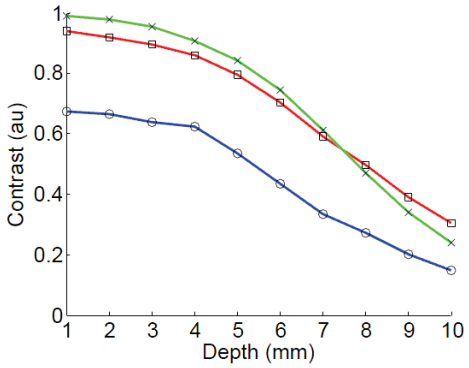

Figure 1: Comparison of the contrasts obtained for a fluorescent target at 10 different depths with WF-FRI (—) and both of our methods (LS-FRI1 (—) and LS-FRI2 (—))

Having access to images I_k for every position k of the excitation line allows us to select which part of the field to detect to enhance the contrast and resolution of the fluorescence signals. We can use the whole field of all the images, and sum them to obtain the equivalent of the WF-FRI image to use it as a basis that we want to improve. But we can also limit the detection to the area around the excitation to improve the signals. This first detection scheme is referred as LS-FRI1. The second detection scheme (referred as LS-FRI2) limits the detection to the area around the excitation as previously and uses the signal from the adjacent areas as an estimate of the unwanted background signal. As seen on Fig. 1 and 2, both methods improve the contrast and resolution.

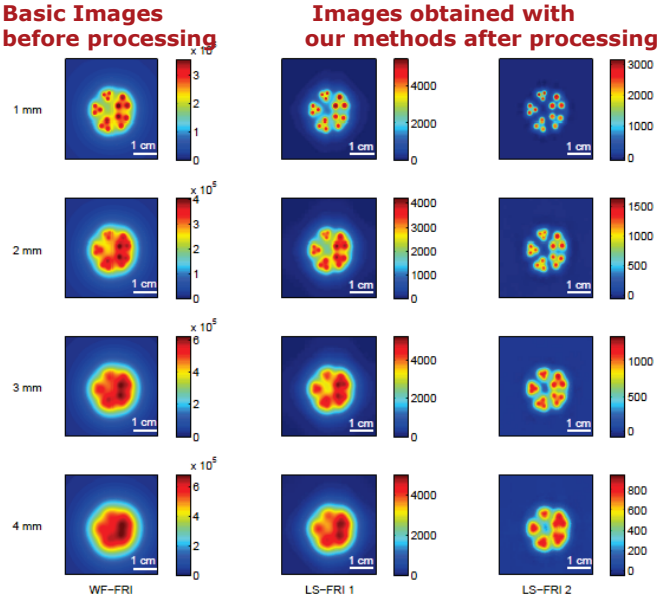

Figure 2: Images of a fluorescent target at four different depths from 1 mm to 4 mm obtained with the three methods

Other detection schemes are also being investigated. For each scheme a specific optical setup can be developed for real time implementation. We believe this method would enhance the use of fluorescence imaging in intraoperative surgery as it would allow a better detection and localization of fluorescence-targeted objects such as tumors.

Related Publications:
[1] F. Fantoni, L. Hervé, V. Poher, S. Gioux, J. I. Mars, J.-M. Dinten, "Laser line scanning illumination scheme for the enhancement of contrast and resolution for fluorescence reflectance imaging", Proc. SPIE 8572, Advanced Biomedical and Clinical Diagnostic Systems XI, 85720L (March 22, 2013)
[2] F. Fantoni, L. Hervé, V. Poher, S. Gioux, J. I. Mars, J.-M. Dinten, "Laser line scanning illumination scheme for the enhancement of contrast and resolution of fluorescence reflectance imaging", article submitted to Biomedical Optics Express

Novel Endoscopic Optical System for Simultaneous Color and Fluorescence Imaging

Research topics: Endoscopic Imaging, color Imaging, fluorescence-guided surgery

P. Le Coupanec, A. Daures, C. Emain, P. Rizo, J.-M. Dinten

ABSTRACT: The main challenge to the transition of surgery from open to endoscopy is the loss of anatomical information. Thus, in minimally invasive surgery (MIS), the rendering of the video color image is critical. Fluorescence imaging has been introduced and is complementing white light imaging, helping in targeting tumors and monitoring lymphatic and blood vessels. Today none endoscopic device commercialized allows both imaging modes simultaneously. We have developed an imaging system allowing simultaneous color and NIR fluorescence endoscopic imaging.

Introduction

Minimally invasive surgery (MIS) is an efficient and expanding technique for surgery. The main challenge to the transition of surgery from open to endoscopy is the loss of anatomical information as tissue palpation, texture recognition and 3D visualization are not possible through endoscopes. Doctors need a reliable video color image to compensate these lacks of information. White light imaging mode has been complemented by the introduction of fluorescence imaging which is helping in targeting tumors and monitoring lymphatic and blood vessels (SLN, Lymph nodes or vascularization). In laparotomy, fluorescence imaging has proven to be a valuable tool for physicians providing surgery guidance and efficient tissue differentiation and devices dedicated to laparoscopy begin to be commercialized.

System description and performances

We developed a novel imaging system allowing simultaneous color and NIR (800nm) fluorescence endoscopic imaging with optical performances in both modes comparable to commercialized non-simultaneous systems. This imaging system is derived from the miniaturized fluorescence image system previously developed [1] and technology to image NIR molecular probes with surgical field white light illumination and simultaneous fluorescence imaging. With such device, high quality illumination can be achieved with IRC above 90% (e.g. FluobeamTM ; Fluoptics, Grenoble).

Figure 1: Compact bi-modal camera head

The video flows resulting from parallel acquisitions can be performed with a minimum of 10 fps. Filtering on both the illumination and detection sides ensures high performance for color imaging without compromising sensitivity to the fluorescence signal. For optimal color image rendering, a color calibration method has been implemented to generate a displayable video flow with chromatic color difference (Delta E) comparable to white light illumination with the IRC levels obtained in open surgery.

A few preclinical testing, representative of surgery, on small and large animals were done using our bi-modal laparoscopic imaging system with ICG.

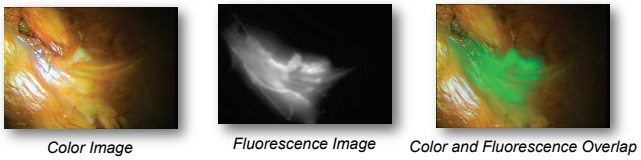

Figure 2: Display of bi-modal imaging modes

Simultaneous acquisition of the color and fluorescence video sequences is possible without compromising the color quality and the fluorescence sensitivity.

Conclusion

Simultaneous acquisition of the color and fluorescence video sequences offers better ease of use to the medical staff as there is no more need for a manual switch and mental registration between white light and fluorescence imaging modes. The functional information arising from the fluorescence signal can be superposed in real time to the color image or displayed next to it. Also the sensitivity of the fluorescence mode achieved so far is sufficient for a lot of common ICG applications already in use: hepatic surgery, cholecystectomy (bile duct visualization), anastomosis control and sentinel lymph node detection.

The whole system development has been designed to adapt easily onto rigid medical endoscopes and made following medical quality processes and regulations (ISO 13485 and IEC 60601-1).

Related Publications:
[1] S. Gioux, J-G. Coutard, M. Berger, H. Grateau, V. Josserand, M. Keramidas, C. Righini, J-L. Coll and J-M. Dinten, "FluoSTIC: miniaturized fluorescence image-guided surgery system", Journal of Biomedical Optics 17(10), 106014 (October 2012)

Intracranial photobiomodulation to improve dopaminergic cell survival in MPTP-treated mice

Research topics: near IR light treatment, neuroprotection, Parkinson disease

F. Perraut, C. Chabrol, C. Moro, A.L. Benabid, J. Mitrofanis, N. Torres, D. Ratel, F. Reinhart, X. de Jaeger, A. Bourgerette, M. Berger, F. Boizot

ABSTRACT: In collaboration with Clinatec (Pr. Benabid team) and the Pr. Mitrofanis team (University of Sydney, Australia), LETI/DTBS has designed a new optical device allowing a small area into the brain to be locally irradiated with near infra red light (670nm). This device will be used to evaluate near infrared irradiation potential to slow down degeneration of dopaminergic cells in Parkinson disease.

Introduction: Many studies have shown that red to infrared light (NIr) can be neuroprotective; that is, it can protect the central nervous system against stress from various origins. Near-infrared light treatment has been shown to improve cell survival and locomotive behavior in Parkinson disease, in particular, in various animal models of the disease. NIr protects dopaminergic cells of the substantia nigra pars compacta (SNc) from degeneration and preserves functional activity near to control levels. One potential problem associated with this treatment is related to the effective and reliable penetration of NIr through the thick human cranium, meningeal layers, and brain parenchyma to reach the SNc in the midbrain. This may present a limitation in the use of NIr as a long-term and reliable treatment in humans, particularly those suffering from Parkinson disease. There is a need to develop new and effective methods for delivering a strong NIr signal to deeper brainstem structures in humans, without secondary effects as heating. For this purpose, we have designed a novel LED–optical fiber device made to deliver NIr intracranially, within the brain.

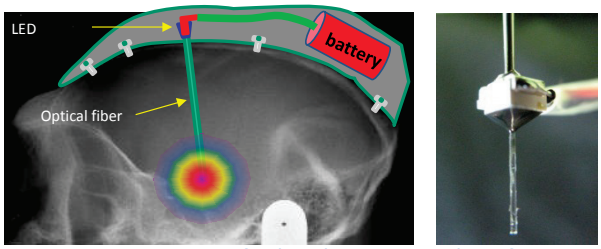

Figure 1: Diagram of the basic principle of intracranially photobiomodulation(left) and LED optical fiber device.

Thanks to a close collaboration, DTBS and Clinatec have developed a highly compact apparatus consisting of an optical fiber linked to an LED. A small, 3.5 x 2.7–mm 670-nm LED was aligned with and glued to an optical fiber having a tip diameter of 300 µm (Fig. 1): the light emitted by the LED is guided into the brain and emerges close to the SNc. An autonomous and compact power supply (battery, current regulator) was specifically designed for mice implants and linked through transcutaneous way . A prototype of passive package for monkey was also tested post mortem (fig2). All LED–optical fibers were tested for power output using a calibrated light sensor. This ensured that each device emitted a similar power at the output of the optical fiber(i.e. 0.16 mW at 20 mA, which was the maximum electronic power of the battery for this device).

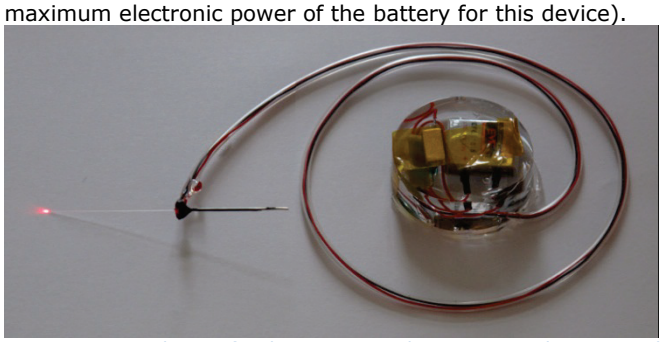

Figure 2: NIr device for large mammal. Battery and integrated regulator inside waterproof package.

Experiments were made on mice exposed to MPTP (1-methyl-4-phenyl-1,2,3,6-tetrahydropyridine), a neurotoxin which causes permanent symptoms of Parkinson's disease by destroying dopaminergic neurons in the SNc. MPTP has been used to study disease models in various animal studies. The experimental results show that NIr irradiation protects the SNc cells against the degradation by MPTP (Fig 3) in mice.

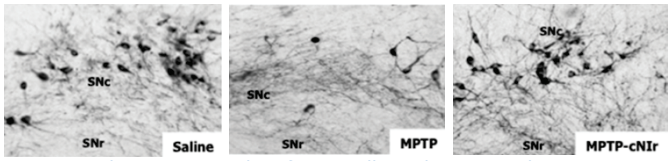

Figure 3: Photomicrographs of TH+ cells in the SNc. Saline: negative control. MPTP: mouse exposed to MPTP. MPTP-cNIr: mouse exposed to MPTP and NIr illumination.

Conclusions: NIr device (without battery) is well tolerated by rodents, does not generate local necrosis, and has sufficient power to protect neurons against toxic insult.

Perspectives:

- performing experiments with larger brain and cranium on monkeys
- designing a device (light source, power supply) compatible with In-Vivo passive implantation.

Related Publications:
[1] Moro C., El Massri N., Torres N., Ratel D., De Jaeger X., Chabrol C., Perraut F.,Bourgerette A., Berger M, Purushothuman S., Johnstone D., Stone J., Mitrofanis J., Benabid A.L.,"Photobiomodulation inside the brain: a novel method of applying near-infrared light intracranially and its impact on dopaminergic cell survival in MPTP-treated mice", 2013 - Journal of Neurosurgery, October 25.

Nano-particles and viruses detection with thin wetting film microscopy

Research topics: Nano-particle detection, virus detection, thin wetting film

Y. Hennequin, C. P. Allier

ABSTRACT: The physical interaction between nano-scale objects and liquid interfaces can create unique optical properties. Here we show that the evaporation on a wetting substrate of a polymer solution containing sub-micrometer or nano-scale particles creates liquid micro-lenses. We characterize the optical properties of these lenses and show that the shape and the condensing power of such liquid lenses can be fine-tuned to enable the detection of nano-particles down to ~100 nm using a low magnification microscope objective, achieving a large FOV of several mm^2. This approach is also applicable to lensfree computational on-chip imaging.

Nano-scale objects are difficult to visualize using optical techniques because of their small size compared to the optical wavelength, resulting in a weak scattering signal from individual nano-particles. To mitigate this challenge, various techniques have been used for imaging sub-100 nm particles and viruses, including near-field optical microscopy, super-resolution microscopy, atomic force microscopy, electron microscopy, and other recently developed imaging techniques. All of these existing approaches for imaging individual nano-particles, however, are relatively complex, bulky and low throughput, with only a limited imaging field-of-view (FOV), typically less than 0.2 mm2.

In 2013 we have described a new high-throughput imaging approach that uses stable and biocompatible thin wetting films to enhance the detection signal of nano-particle by several orders of magnitude. We distinguish two different ways to take advantage of the use of thin wetting film, i.e the formation of microscopic liquid axicon lenses and self-assembled isolated nano-lenses. In the first case the physical origin is a local spatial deformations of a 'continuous' wetting film rather than formation of 'isolated' liquid refractive structures around each particle as in the second case. These two methods have been investigated in close collaboration with the Ozcan Group (UCLA). Together, using lensfree imaging, we achieved the detection of single virus (H1N1) and 100 nm nanoparticle over large field of view exceeding several mm2 [1][2].

At CEA-LETI, we demonstrated the detection and sizing of single nano-particles (100 and 200 nm), CpGV granuloviruses as well as Staphylococcus epidermidis bacteria over a wide field of view of e.g., 5.10×3.75 mm2 using a x5 objective lens with a numerical aperture of 0.15. In addition to conventional lens-based microscopy, this continuous wetting film based approach is also applicable to lensfree computational on-chip imaging. These micro-scale axicon lenses also enable the detection of single 100 nm nanoparticles using computational lensfree imaging, achieving an imaging FOV of e.g., >20-30 mm2. These results could be especially useful for high-throughput field-analysis of nano-scale objects using compact and cost-effective microscope designs.

In sum, we are inventing a path in the realm of diagnostics and pharmacology. In particular this work paves the way for simple bacterial and viral load assays.

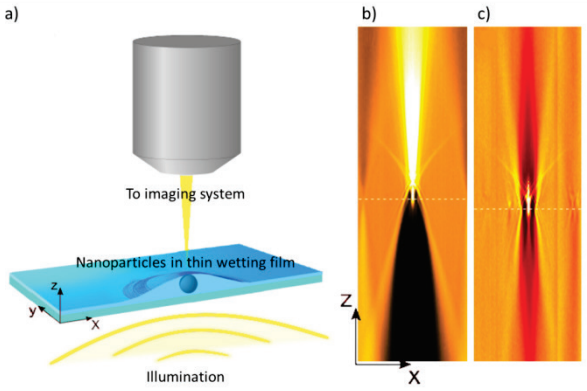

Figure 1: (a) Schematic of a liquid lens consisting of a liquid film wetting a micro-particle (not to scale). The liquid lenses are formed form the evaporation of the water from an aqueous suspensions containing dissolved polymer. This can be realized by simple drop evaporation on glass coverslips. The liquid lenses are able to focus light primarily along the optical axis. (b) Microscopic image of the light cone produced by the liquid lens formed with a 5µm diameter particle and reconstructed from image-stacks. The image dimension is 15 µm × 500 µm and the dash-line indicates the position of the particle. (c) Same as previously but without the wetting film.

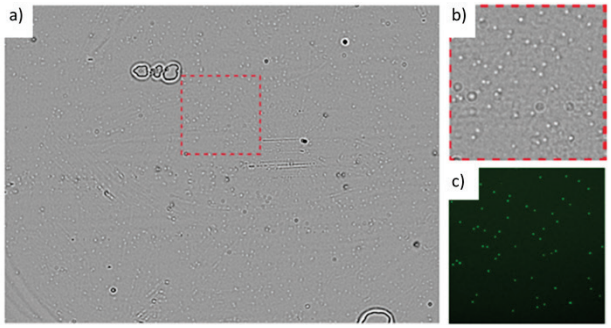

Figure 2: (a) Bright-field microscopic image (objective: ×5, NA = 0.15) of an evaporated drop with polymer and 100 nm particles taken at ~100µm above the drop. Because of the liquid lenses formed by the polymer on top of the particles, the latter can be seen as white spots in the center of the drop despite the low magnification and large field of view (5.10 mm × 3.75 mm). The dashed square has a side length of 0.66 mm a close up of which is shown in (b) in bright-field conditions and in (d) in fluorescence.

Related Publications:
[1] O. Mudanyali, E. McLeod, W. Luo, A. Greenbaum, A. F. Coskun, Y. Hennequin, C. P. Allier & A. Ozcan, "Wide-field optical detection of nanoparticles using on-chip microscopy and self-assembled nanolenses" . Nature Photonics 7, 247–254 (2013) doi:10.1038/nphoton.2012.337
[2] Hennequin, Y., Allier, C. P., McLeod, E., Mudanyali, O., Migliozzi, D., Ozcan, A., & Dinten, J. M., "Optical Detection and Sizing of Single Nanoparticles Using Continuous Wetting Films", (2013), ACS nano, 7(9), 7601-7609.

BacRAM:

Targeting, analysis and classification of bacteria at single-cell level

Research topics: Bacteria detection/identification, Raman spectroscopy, lensfree

E. Schultz, S. A. Strola, C. P. Allier, D. Jary

ABSTRACT: A compact Raman platform has been validated for the rapid identification of single bacterial cells. Targeting of single bacteria is performed via lensfree imaging system. We demonstrated that 1 minute procedure is enough to localize the microorganism and to collect its comprehensive Raman spectrum. With a total of 1200 spectra over 7 bacterial species, we obtained a classification score of about 90%. The speed and the sensitivity of our Raman spectrometer pave the way for high-throughput and non-destructive real-time bacteria identification assays in biomedical, clinical diagnostic and environmental applications.

The results on single bacteria rapid localization and identification obtained with a low-cost and compact Raman spectrometer are shown here.
The localization and the Raman spectrum of a single bacteria is realized in 1 minute procedure and work in progress is still reducing time of these processes. Localization and detection of single bacteria is performed by means of lensfree imaging over a large field of view of 24mm2 [1,2]. An excitation source of 532nm and 30mW illuminates single bacteria to collect Raman signal into a prototype spectrometer (HTVS Tornado's technology). The acquisition time to record a single bacteria spectrum is as low as 10s owing to the high light throughput of this spectrometer [3].

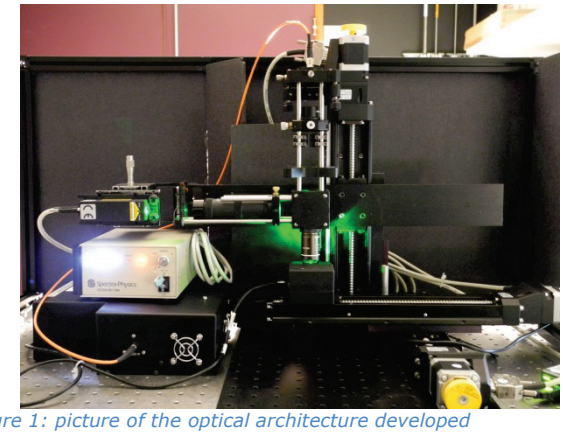

Figure 1: picture of the optical architecture developed

The spectra processing features different steps for cosmic spikes removal, background subtraction, and gain normalization to correct the residual inducted fluorescence and substrate fluctuations. This allows obtaining a fine chemical fingerprint analysis.
We have recorded a total of 1200 spectra over 7 bacterial species (E. coli, Bacillus species, S. epidermidis, M. luteus and S. marcescens). The analysis of this database results in a high classification score (of about 90%) allowing the discrimination at species and families level [3]. Furthermore, a classifications study for E. coli and B. subtilis strains during the different growth phases leads in a classification score of about 95% [4].

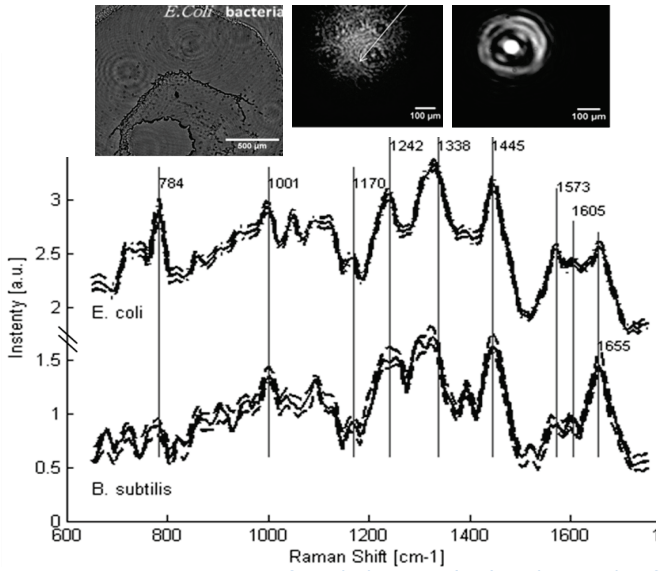

Figure 2: targeting process of single bacteria (top) and example of Raman spectra obtained

We can conclude that our setup enables automatic recognition of single bacteria among 7 different species and discriminates the metabolic responses for 2 different strains. This allows performing the high-throughput and non-destructive real-time bacteria identification assays and susceptibility studies of the bacteria towards antibiotics or drug treatment.
Hence we described our novel Raman spectrometer based on a lensfree imaging scheme that overcomes some of the challenges encountered in Raman microscopy, namely compactness, rapidity and simplicity [5]. The speed and the sensitivity of our Raman spectrometer thus paves the way for the development of the next-generation of compact, low-cost and high performing Raman spectroscopic devices to give benefit in biomedical, clinical diagnostic and environmental applications.

Related Publications:
[1] Allier C.P., Hiernard G., Poher V., Dinten J.M.; Biomed. Opt. Express, 1(3): 762-770 (2010)
[2] Hennequin Y., Allier C. P., McLeod E, Mudanyali O., Migliozzi D., Ozcan A., Dinten J-M.; ACS Nano, 7 (9), 7601–7609 (2013)
[3] Strola S.A., Schultz E., Allier C.P., DesRoches B., Lemmonier J.; Dinten J-M., SPIE Proceedings Vol. 8572, Advanced Biomedical and Clinical Diagnostic Systems XI (2013)
[4] Strola S.A., Schultz E., Perenon R., Simon A-C., Espagnon I., Allier C.P., Claustre P., Jary D., Dinten J-M.; paper 8939-13, BiOS Conference 2014
[5] Schultz E., S. Strola, C.P Allier, M. Dupoy, Patent FR13-50857 (2013).

Optical forward-scattering for label-free characterization of bacteria within microcolonies

Research topics: Bacteria identification, antibiotic susceptibility testing

P. R. Marcoux, E. Schultz, M. Dupoy

ABSTRACT: The development of methods for the rapid identification of pathogenic bacteria is a major step towards accelerated clinical diagnosis of infectious diseases and efficient food and water safety control. Methods for identification of bacterial colonies on gelified nutrient broth have the potential to bring an attractive solution. We show here the possibility of discriminating different bacterial species at a very early stage of growth (6 hours of incubation at 37°C), directly on agar media and in a non destructive way, using light forward-scattering and learning algorithms.

We have been developing since 2008 an innovative way of characterizing bacteria growing on agar medium. This method uses elastic scattering emitted by bacteria when they are illuminated with a laser. When bacteria are assembled in a complex pattern, as they do when they form colonies on agar, forward elastic scattering yields a diffraction pattern. The pattern issued from microcolonies is complex enough to provide us with a fine characterization, in a label-free and non-destructive way. Furthermore, our method uses a low cost instrumentation and can be done without opening lids of Petri dishes. We showed the potential of this method – non-invasive, preventing cross-contaminations and requiring minimal dish handling – to provide early clinically-relevant information in the context of fully automated microbiology labs. [1] Two characterizations are currently under investigation: identification and antibiotic susceptibility testing.

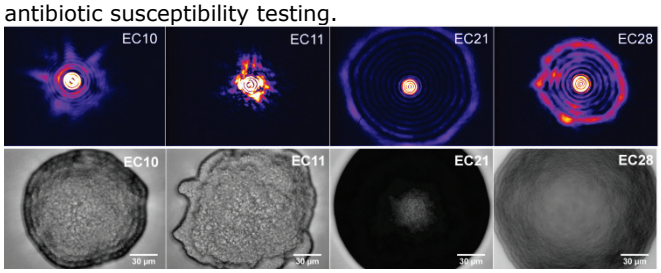

Figure 1 : Typical scatterograms (upper row, reciprocal space) and corresponding images (lower row, direct space; scale bars stand for 30 µm) for 4 different strains of E. coli, grown 6 hours on TSA agar medium at 37°C.

As a proof of concept we chose species from different genera (*Hafnia*, *Enterobacter*, *Citrobacter*, *Escherichia*) within a same family (*Enterobacteriaceae*). The species we selected commonly colonize humans or are associated with human infections. A first database of more than 1000 scatterograms acquired on seven strains from these genera yielded a recognition rate of nearly 80%, after only 6 hours of incubation. [2] We investigated also the prospect of identifying different strains from a same species through forward scattering. We discriminated thus four strains of *Escherichia coli* with a recognition rate reaching 82% (Fig. 1 and Fig. 2). Finally, we showed the discrimination of two species of coagulase-negative *Staphylococci* (*S. haemolyticus* and *S. cohnii*), on a commercial medium used in clinical diagnosis (ChromID MRSA, bioMérieux), without opening lids during the scatterogram acquisition. [2] Our results confirm that the ordered stacking of bacteria within colonies induces a periodic modulation of phase and absorbance in direct space that can be assessed using forward scattering imaging and used for bacterial classification.

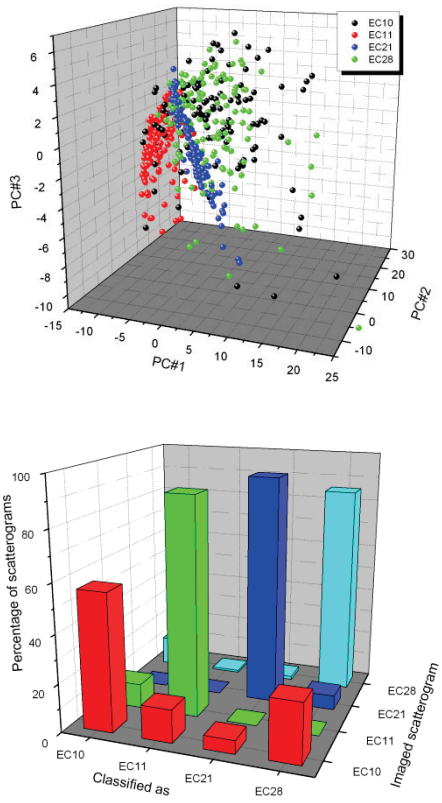

Figure 2 : Unsupervised (a) and supervised (b) learning on the database gathering the scatterograms of the four E. coli strains. (a) Scattering patterns of the four strains of E. coli visualised in the first three principal components plot. (b) Confusion matrix provided by the SMO learning algorithm. The confusion matrix displays an overall classification rate as high as 81.5%.

Related Publications:
[1] P.R. Marcoux, M. Dupoy, A. Cuer, J.-L. Kodja, A. Lefebvre, F. Licari, R. Louvet, A. Narassiguin, F. Mallard, "Optical forward-scattering for identification of bacteria within microcolonies", Award for Outstanding Oral Presentation at the 3rd International Conference on Bio-Sensing Technology, Sitges (Spain) 13-15 May 2013.
[2] P.R. Marcoux, M. Dupoy, A. Cuer, J.-L. Kodja, A. Lefebvre, F. Licari, R. Louvet, A. Narassiguin, F. Mallard, "Optical forward-scattering for identification of bacteria within microcolonies", Applied Microbiology and Biotechnology (2014, *in press*) DOI: 10.1007/s00253-013-5495-4

Skin characterization by spectroscopy

Research topics: Diffuse reflectance spectroscopy, skin characterization

A. Koenig, B. Roig, J.-M. Dinten

ABSTRACT: Diffuse reflectance spectroscopy is a widely used technique to determine optical properties of tissues. We have developed a low-cost optical instrument based upon the spatially resolved diffuse reflectance spectroscopy approach. It is able to detect early inflammation due to tuberculin intradermal injection, even before the onset of visual signs. Comparing the instrumental and classical clinical readings we show that an early reading is possible only 18 hours after the injection of tuberculin whereas usual reading is done 72 hours post injection. This instrument has been used in a new application for skin ageing assessment studying collagen.

The technique we present here is based upon the spatially resolved diffuse reflectance spectroscopy. Changes of absorption or scattering coefficients reflect a difference in concentration of the chromophores (oxyhaemoglobin, deoxyhaemoglobin, lipid and water) present in the skin and thus an alteration of the examined tissue. This alteration can be due to a reaction following the injection of a reagent or to a disease (melanoma). This technique has been validated on a clinical study conducted at Lyon hospital Fig. 1c) to support the diagnosis of tuberculosis. The objective was to establish a new reading method of the tuberculin Mantoux test. The system consists in a tungsten halogen lamp as the excitation source, a fibered probe for illumination and detection coupled to a fibered spectrometer which can decompose and record the spectra of the backscattered light at the surface of the tissue [1,2,3].

We have developed a specific probe which geometry of collection is optimized for clinical measurements (Fig. 1). It is made of an illumination fiber (500 µm diameter core) and a network of optical fibers for detection (300 µm diameter core) located at different distances from the illumination fiber. On the distal end of the probe, six distances from the excitation are collected, each of them by seven fibers placed concentrically around the excitation fiber Fig. 1a). To study local properties of tissues, we chose small source detection separations (500 µm). On the proximal end of the probe Fig. 1b), the seven fibers belonging to a specific distance are arranged into a bundle. A seventh fiber collects light directly from the source.

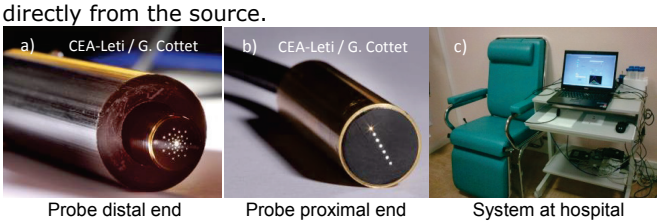

Figure 1 : Fibered probe, detail on the two sides: a) measure on the skin, b) detection on the spectrometer, c) system installed at hospital.

To analyze the recorded spectra, we developed a data processing method based on the deconvolution of the scattering and absorption phenomena. The reflectance decay signal as function of the source-detector distance is compared to a Look up table previously computed with a Monte Carlo algorithm, under the hypothesis of a semi-infinite medium and a range of optical coefficients representative of biological tissues. Finally, knowing the absorption spectrum, and comparing it to a library of chromophore absorption spectra we can deduce the different chromophore concentrations. In this study we consider oxyhaemoglobin, deoxyhaemoglobin, melanin, carotene, water and lipids as main chromophores.

An additional study was conducted in order to demonstrate the potential of DRS to evaluate type I collagen content and to detect structural alterations associated with skin ageing. In vitro and in vivo measurements were carried out respectively on 3D collagen gels and on skin volunteers of different ages. Native type I collagen was extracted from rat tail tendons of different-age animals (young adults of 2 months and old adults of 2 years). Then 3D gels were prepared at final concentrations of 1.5 and 2.5 mg/ml (Fig. 2 a)).The DRS curves shapes acquired on 2 months and 2 years -old rats' collagen hydrogels are shown on (Fig. 2 b)) and (Fig. 2 c)) respectively. They are significantly different. This spectral distinction is essentially due to differences in collagen scattering properties associated with rats' age. This result confirms the suitability of type I collagen scattering properties as an in vivo marker of skin ageing [5].

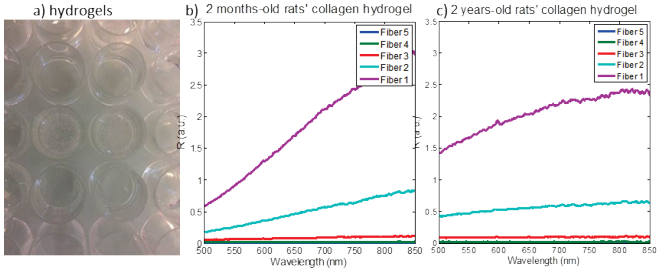

Figure 2 : Typical raw diffuse reflectance spectra acquired on 2 months (b) and 2 years (c)-old rats' collagen hydrogels (a) at concentration of 2.5 mg/ml.

In vitro investigations validate the use of DRS to emphasize collagen alterations associated with age. DRS measurements have been carried out on thirty volunteers ageing from 20 to 60 years old. The examined areas were the maxillary and the inner face of the forearm for control. The contribution of type I collagen to the *in vivo* absorption spectrum is still under investigation. Preliminary results seem to show a correlation between the *in vivo* scattering properties and ageing.

Related Publications:
[1] Koenig A., Nahas A., Planat-Chrétien A., Poher V., Dinten J.-M., "Diffuse Spectroscopy for Tissue Characterization: Application to Skin Tests Reading", Biomed/DH Joint Poster Session (JM3A), Miami, Florida April 28, 2012
[2] Koenig A., Grande S., Dahel K., Planat-Chrétien A., Poher V., Goujon C., Dinten J.-M., "Diffuse reflectance spectroscopy: a clinical study of tuberculin skin tests reading", BiOS, 2 - 7 February 2013, San Francisco, California USA.
[3] B. Roig, M. Guilbert, A. Koenig, O. Piot, F. Perraut, M. Manfait, J.-M. Dinten, "Can diffuse reflectance spectroscopy emphasize skin-collagen alterations due to ageing?", ISBS_SICC October 2013, Milano, Italy.

Multi-wavelength and Time-Domain Diffuse Optical Tomography data processing by using a material basis and Mellin-Laplace Transform

Research topics: Optical tomography, data processing, time resolved imaging

L. Hervé, A. Puszka, A. Planat-Chrétien, M. Berger, J.-M. Dinten

ABSTRACT: Optical tomography is new emerging modality to study some metabolism processes. To eventually translate this technology to clinical diagnosis, we need to be able to address higher thicknesses of tissues. To reach this goal and to separate chromophores on a material basis, we developed a method to process time-domain/multi-wavelengths diffuse optical acquisitions. Validations were performed in the reflectance geometry on phantoms mimicking the spectral behaviors of biological tissues. The method is envisioned to be used for disease detection, for functional imaging or for surgical implant viability follow-up.

Optical tomography consists in illuminating biological tissues with infrared light with a large number of source and detector points and in analyzing the medium response so as to reconstruct 3D optical characteristics.

We previously proposed a method [1-2] based on the data processing of time-domain optical measurements with the Mellin-Laplace Transform (MLT), to reconstruct 3D map of absorption and diffusion coefficients: basically, if *i* is a superindex of the measurements (comprising the source-detector couple index and the MLT order) and m is the index of the position (node) of the reconstruction mesh, it consists in solving a linearized system:

$$Y_i = W_i^m \mu_m$$

Where Y is the set of data built from optical measurements and μ_m is the set of unknown absorption coefficient.
When multi-wavelength acquisitions are performed, we can access to the material content by introducing the specific absorption spectra S_M^λ of material M at wavelength λ and by considering the mixture law : $\mu_m = S_\lambda^M \alpha_{Mm}$. We then have to solve:

$$Y_{i\lambda} = W_{i\lambda}^m S_\lambda^M \alpha_{mM}$$

to get the concentration α_{mM} of material M at node m.
Validation experiments were performed on a diffusive liquid phantoms mimicking deeply buried tumor (with increased deoxygenated blood surrounded by healthy tissues (Figure 1). Black ink, blue dye and intralip were used to obtain the diffusive phantoms with optical properties closed to a biologically relevant situation [3].

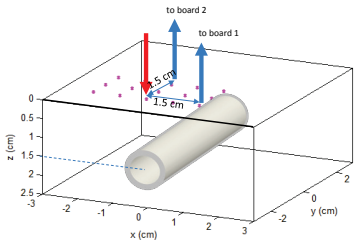

Figure 1: Example of a validation phantom geometry (inclusion at 15mm)

The reconstructions are performed by solving the multi-wavelength equation. It was successful in recovering the inclusion shape, depth and composition (high concentration and low oxygenation). A result is shown in figure 2 for the challenging depth of 15 mm.

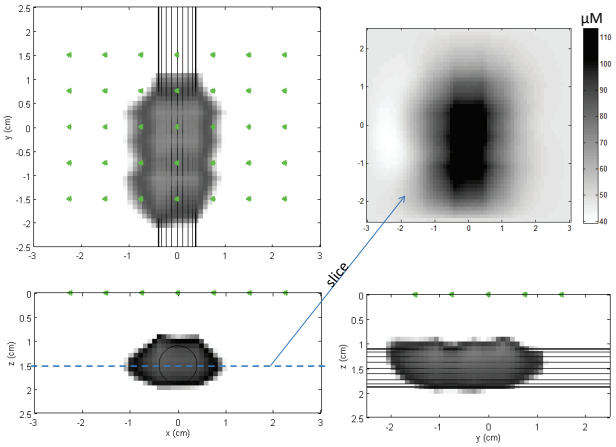

Figure 2: Reconstruction of the tumor-like inclusion (total concentration shown)

The method relies on the use of preliminary "reference" measurements performed on a medium A which may or may not be close to the probed medium B [2-3]. Different scenarios may be envisioned depending on the reference medium:
-from a known medium A, deduce absolute quantification of medium B. Applications are disease detection for example.
-from the unknown medium at time t0 (A), deduce its evolution of quantification for any time t (B). Applications envisioned are functional imaging of the brain or viability diagnosis of implants obtained from optical measurements follow-up.
The second scenario in currently tested with experiments on rat were arterial or venous flows can be stopped with clamping in order to simulate occlusions. By measuring with optical means the evolution of the tissue oxygenation of an implant, we may be able to provide a clinical instrument to follow-up its viability and prevent thrombosis.

Related Publications:
[1] L. Hervé, A. Puszka, A. Koenig, A. Planat-Chrétien and J.-M. Dinten, "Time-Resolved Reflectance Diffuse Optical Tomography by using Mellin-Laplace Transform", Biomedical Optics (2012)
[2] A. Puszka, M. Debourdeau, L. Hervé, A. Planat-Chrétien, A. Koenig, J. Derouard and J.-M. Dinten, "Time-Resolved Reflectance DOT: Experimental Results for Imaging Absorption Contrast in Depth", Biomedical Optics express (2012)
[3] L. Hervé, A. Planat-Chrétien, A. Puszka et al, "Multiwavelengths and Time-Domain Diffuse Optical Tomography data processing by using a material basis and Mellin-Laplace Transform", conference BIOS2014/PhotonicsWest

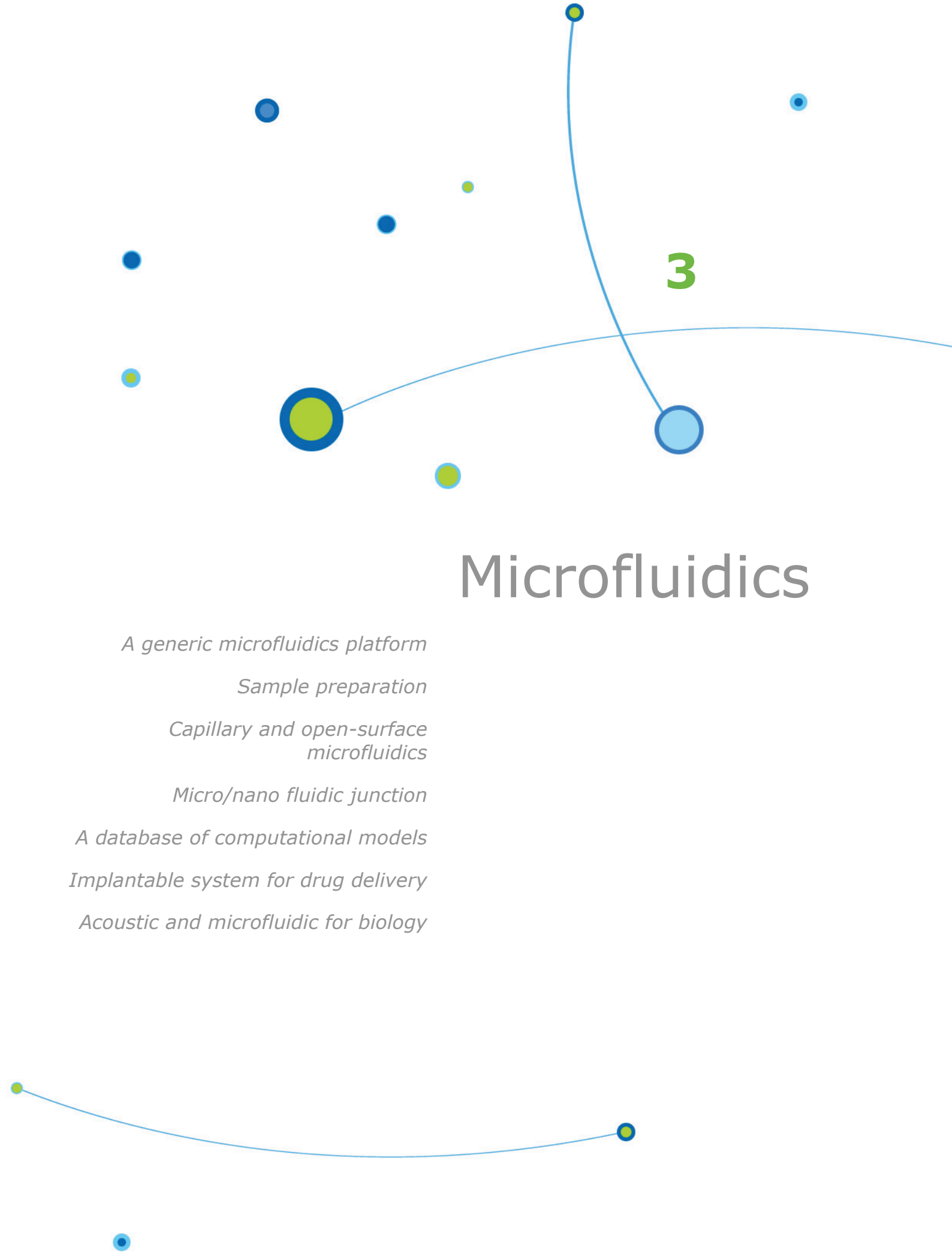

3

Microfluidics

A generic microfluidics platform

Sample preparation

Capillary and open-surface microfluidics

Micro/nano fluidic junction

A database of computational models

Implantable system for drug delivery

Acoustic and microfluidic for biology

FlowPad: a generic microfluidics platform

Research topics: Lab-on-chip, microfluidics, sample preparation, chemical synthesis

D. Jary, A.-G. Bourdat, R. Charles, R. C. den Dulk, N. Verplanck, G. Delapierre

ABSTRACT: The miniaturization and integration of laboratory procedures into lab-on-chip devices is an obvious trend in many fields of application. FlowPad is a generic microfluidics platform developed and patented by CEA that responds to this trend by providing easy fluid handling in single-use cartridges. FlowPad can be adapted to a wide range of applications such as sample preparation, in-vitro diagnostics, cell encapsulation, chemical synthesis, and many more.

FlowPad is a generic microfluidics platform that responds to the need for miniaturization and integration of laboratory procedures into lab-on-chip devices. FlowPad uses pneumatically actuated valves that are integrated in a single-use polymer cartridge (e.g. PMMA or COC) to direct fluids through channels and reaction chambers, which potentially contain embedded reagents. The cartridge is clipped into the system very easily, thereby establishing automatically all fluidic and pneumatic connections. The system includes various hardware modules, such as heating or magnetic actuation, depending on the application.

Figure 1: Prototype of a FlowPad instrument for automated sample preparation.

One example of an application is automated sample preparation. Many biological analysis methods require careful preparation of the raw sample, which is all too often a tedious manual procedure and a cause of variability. We have developed an automated sample preparation system that can extract DNA from highly resistant pathogens (e.g. spores) in environmental samples within 20 minutes.[1] The system allows sample volumes up to several mL and delivers the pathogenic DNA in typically 20 to 50 µl to be compatible with downstream qPCR detection.
Without any intervention of the user, the system concentrates pathogens from a mL volume sample using magnetic particles with a special surface coating, while the excess of sample volume is discarded. Subsequently, the pathogens are released in a µL volume sample and their DNA is extracted by using an integrated mechanical lysis. Starting from raw environmental samples, the system thus allows for detection of down to 100 pathogens per mL by qPCR.

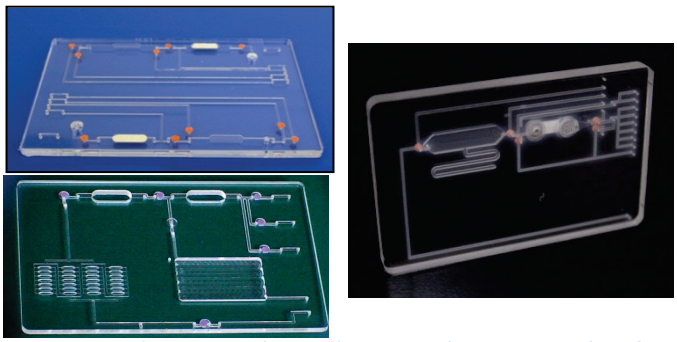

Figure 2: Single-use cartridges with integrated pneumatic valves for automated sample preparation (left top), RNA detection (left bottom), or chemical synthesis (right).

Another example is the detection of ricin intoxication by gene expression profiling of the host response. For this application, qPCR detection has been integrated on the cartridge to obtain a fully integrated system with sample-to-result performance. After chemical lysis of a whole blood sample, the mRNA in the sample is purified and analyzed by RT-qPCR. To be able to monitor 27 different genes simultaneously, the qPCR takes place in 28 separate chambers in parallel.[2]

A final example is the synthesis of radioactive tracers for PET imaging. With a half-life of about 20 minutes, some radiotracers need to be synthesized close to the patient to allow sufficient time for injection and imaging. We are currently developing the synthesis of 11C and 18F radiotracers on the FlowPad microfluidics platform, thus enabling rapid synthesis at the point of care.

These examples show the wide range of applications that are possible on FlowPad, and many more are currently being developed.

Related Publications:
[1] G. Delapierre et al., "Biothreats detection systems: from sampling to integrated sample prep", Leti Innovation Days, June 26th 2013, Grenoble (France),
http://www.leti-innovationdays.com/presentations/AnnualReview/J2SessionA/A02_Leti-innovation-Days-2013_DELAPIERRE.pdf
[2] G. Delapierre et al., "Biomonitoring systems for environmental & national security applications", MicroNanconference, December 12th 2013, Ede (Netherland)
http://www.micronanoconference.nl/images/presentaties/SessieB/B4/guillaume%20delapierre.pdf

Sample preparation of Human samples for qPCR detection in point of care systems

Research topics: DNA purification, point of care, lab on chip

D. Jary, J. Lemonnier

ABSTRACT: In the very competitive field of Point of Care system development, numerous criteria must be fulfilled in order to end up with an attractive product. These criteria include ease of use, quality of the result, reliable and low cost fabrication and robust technology. One key point lies in a robust and alcohol free sample preparation protocol for qPCR analysis, unlike well-established methods, in order to avoid interference of alcohol with materials of the disposable, long term evaporation at the small volumes scale and possibility of air shipment. Such a protocol has been patented and validated with human blood samples.

Development of Lab on a chip for rapid and low cost analyses, which is still a hot topic for in vitro diagnostic players, must fulfill a large panel of criteria in order to be attractive as simple and easy to handle final system coupled to a high quality analysis. To respond to this expectation different strong features must be associated like reliable but low cost disposable fabrication, reagents integration in the disposable, complete automated analysis from sample to answer [Dineva MA, et al., Analyst, 2007, 132, 1193–1199]. In this context the European project Poditrodi aims to develop Point of care tests for tropical diseases, especially for chagas. Indeed, so-called "rapid in-vitro diagnostic (ivD) tests" for single diseases are already on the market, but more complex analytical protocols are necessary to clearly identify a certain tropical disease AND to determine the status of the disease - the latter being crucial for proper treatment - even for geographic regions with poor or low-density medical infrastructure. Such complex analytical protocols would include liquid handling as well as sample preparation like transcription and amplification (PCR) of the virus RNA (dengue, HIV) or the parasite DNA (leishmaniasis, malaria, Chagas). These sample preparation steps are currently only available in laboratories and have not yet found their way in mass-producible, integrated point-of-care diagnostic tests. Thus, in this project, in parallel to technological development for a microfluidic cartridge and associated instrumentation, one key point was to end up with developing an alcohol free protocol for T. cruzi parasite DNA purification in human blood samples, fully adapted to the constraints of the developed microfluidic disposable. CEA leti has expertise on sample preparation for micro-fluidic system and is in charge of this development [1].

The very classical protocols (Boom et al; J. Clin. Microbiol. March 1990, vol. 28, no. 3, 495-503) include sample lysis, to liberate DNA from the cells, followed by DNA purification using a silica solid surface (membrane or magnetic beads) and chaotropic agents. These chaotropic agents are used to bind nucleic acids to the solid surface and thus make a separation of nucleic acids from other components of the sample. In a final step nucleic acids are separated from the surface with a buffer free of chaotropic agents and compatible with qPCR. To achieve DNA precipitation on the solid surface, classical buffers contain alcohol, combined with guanidium salt, which suffer from different disadvantages for final use in a Point of Care context: interference with some kind of plastic disposables, sealing glue dissolution (between different part of the cartridge or from an adhesive sealing film), high constraint for air shipment, long term evaporation at the small volume scale of Point of care systems. For all these reasons alternative protocols without alcohol present high added value.

Such a development has been achieved for both magnetic beads [1] and silica membranes. This protocol has been validated with 200µL human blood samples spiked with bacteria (104 bacteria E. coli and 104 bacteria S. pneumonia per sample) showing good performances comparing to existing very well established commercial kit with alcohol buffers.

Table 1: alcohol free Leti protocol used with magnetic beads for 200µL human blood samples

	E. coli	S. pneumoniae
Dynabeads Silane genomic DNA	45%	80%
CEA protocol	50%	50%

This alcohol free protocol has also been validated by IBMP team from Fiocruz institute (Brazil) using silica membranes and compared to "High pure template preparation kit" (Roche) with alcohol buffers for T. cruzi detection, showing the same sensitivity for both methods.

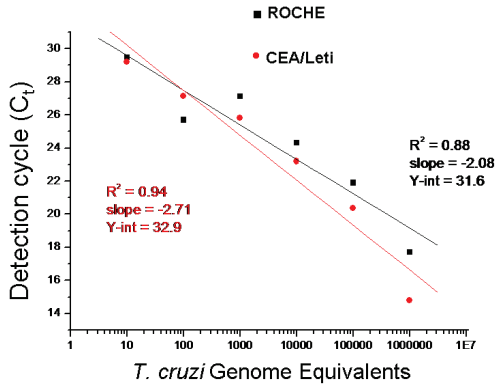

Figure 1 : T. cruzi detection by qPCR with CEA / Leti alcohol free protocol adapted for Roche membrane (red dots) compared to commercial Roche kit using alcohol in DNA purification buffers (black dots).

Related Publications:
[1] C. Delattre, C. P. Allier, Y. Fouillet, D. Jary, F. Bottausci, D. Bouvier, G. Delapierre, M. Quinaud, A. Rival, L. Davoust, C. Peponnet, BIOSENSORS & BIOELECTRONICS, Volume: 36 Issue: 1 Pages:230-235
[2] Patent EN 1357067 "Procédé d'extraction et purification d'acides nucléiques et tampons mis en œuvre"

Capillary and Open-Surface Microfluidics: a solution for Point-Of-Care and Home-Care Systems?

Research topics: Capillarity, spontaneous capillary flow, open-surface microflows

J. Berthier, G. Delapierre

ABSTRACT: Conventional microfluidic systems require auxiliary sources of energy, such as pressure pumps, syringes, or electric potential to motion liquids. Capillary systems do not require auxiliary sources: the motion of the fluid is related to the nature of the materials under the form of surface energy. Such a solution is extremely interesting when systems have to be portable, low-cost and user-friendly. This is particularly the case of Point-Of-Care and Home-Care. Open microfluidic systems, i.e. microflows with a free surface, is especially interesting because it adds the simplicity of fabrication, re-use and accessibility.

Conventional fluidic microsystems require auxiliary sources of energy, such as pressure pumps (like Fluigent®), syringes alone or in parallel, or electrical actuation (in the case of Digital Microfluidics). In all cases, owing to the non-miniaturized auxiliary energy sources, the devices are difficult to transport, need highly trained personnel to run them, and their microfabrication is costly. They bring precise and sensitive solutions when their functioning can be performed in laboratories. Point-of-care or home-care require highly portable, robust, low-cost, user-friendly devices. For most of them, the transport of liquids is based on capillarity.

Closed— or confined —capillary systems have been investigated in the few last years by teams such as that of IBM Zurich, and basic rules for the control of the flow have been stated. The name « Capillarics » has even been attributed to such systems.

More recently, a sub-domain of the general « Capillarics », the open-surface microfluidics (OSM) has been investigated. It provides additional interesting features such as accessibility, easy washing for reuse, and high facility of fabrication.

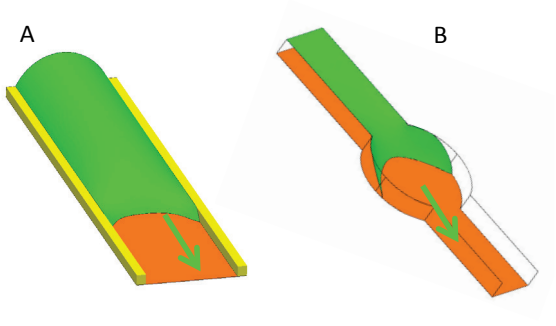

Figure 1: A : capillary flow in a channel limited by two small barriers ; B : capillary flow in a U-groove with a widening. Both figures are obtained with EVOLVER.

Development of OSM has been three-fold : theoretical, numerical and experimental [1-4]. From a theoretical and numerical standpoint the investigations have been conducted using the software EVOLVER for guidance (fig.1).

From an experimental standpoint, preliminary experiments have been conducted using silicon and PMMA substrate. Because the liquids used in biotechnology are most of the time aqueous (water, aqueous polymeric solutions, blood, body fluids, etc.), the channels must have a high surface energy, i.e. a large wettability. Hence surface treatment is necessary (SiO2 layer, or plasma O2 treatment). It has been shown that such liquids can be moved by OSM on very long distances (Fig.2).

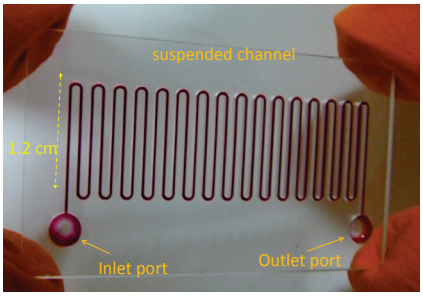

Figure 2 : Water tinted with red dye flows capillary flow on a distance of 35 cm

It has also been shown that whole blood, even if i sis very viscous, can be transported in open-capillary channels (Fig.3).

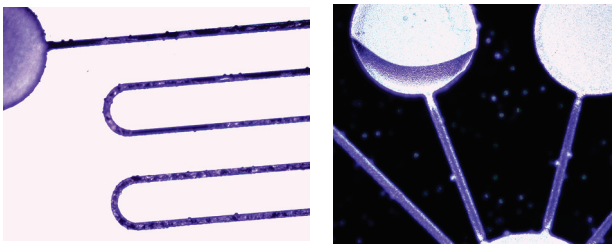

Figure 3: Left : whole blood (with 1% Tween 10) spontaneous capillary flow in a long winding U-channel ; right : PCR Mix « Hawk » self moving in open U-grooves and cylinders etched in silicon. The channels are 50 µ wide and 200 µm deep.

In conclusion, open-surface microfluidics has great potentiality in terms of POC and home-care systems.

Related Publications:
[1] J. Berthier, K. Brakke. The Physics of Microdroplets. Scrivener-Wiley Publishing, 2012.
[2] J. Berthier, K. Brakke, E. Berthier, A general condition for spontaneous capillary flow in uniform cross-section microchannels, Microfluid. Nanofluid., 2013.
[3] J. Berthier, K. Brakke, E. Furlani, I. Karampelas, G. Delapierre, Open-surface microfluidics, Nanotech, 15-19 June 2014, Washington D.C.
[4] B. Casavant et al. , Suspended microfluidics, PNAS, 2013.

Nanoparticles concentration in micro/nano fluidic junction

Research topics: Microfluidics and nanofluidics

K. Aizel, Y. Fouillet, C. Pudda

ABSTRACT: Micro-nanofluidic systems have an important role to play in the detection of bioparticles in several biomedical fields. In particular, the aim of this study is to develop micro-nonofluidic devices for the concentration of nanobeads that could mimic organic particles like viruses or exosomes. Experiment showed that strong enrichment can appear near the micro-nano fludic junction. Steric or ionic effect were investigated using different design configuration in order to enhance the kinetic of enrichment.

The Silicon micronanofluidic devices were fabricated from MEMS based process technology using standard micromachining techniques. Three levels of etching are successively performed for the nanochannels (50 or 100nm), the microchanels (10 µm) and the access fluidic port. The silicon wafer is then bounded to a glass cover plate. After dicing, the chips are then connected to a dedicated fluidic setup. The aim is to characterize the enrichment effect of the 50nm fluorescent nanoparticles (polystyrene or lipidic: Lipidots®) diluted in aqueous solution. The stability and efficiency of the enrichment phenomena were investigated on two categories of devices.

Bypass device. The "Bypass" device, consist in two microchannels bridged by a nanojunction which consist in an array of nanochannel(s). It was shown that steric filtration induced by one bar of pressure across the nanochanels can induce a symmetrical cross-flow configuration which is able to stack nanoparticles in the center of the device [1] (fig1 left). The concentration process can be maintained for several hours and concentration factor as high as ~100 fold have been obtained. An experimental parametric analysis was carried out and results were compared with a simple analytical model. Up to 2000 folds concentration was measured with a new optimized device resulting from this study.

Ring like device. The Bypass device is suitable for experimental studies but can be limited, due to its configuration which needs at least 4 outlet holes, considering its integration into MicroTotal Analysis Systems. Here, we propose a micro-nanofluidic device, called "Ring-like" device [3]. The device is actuated by electrostatic field and particles are concentrated by ionic effects (Fig1-right). Because the Debye layer thickness (λD) is non-negligible compared to the nanochannel thickness, the electrical double layers can overlap inside the nanochannels under certain conditions (appropriate buffer, ionic strength...). Within the influence of an electric field through the nanochannels, a phenomenon called ICP "Ion Concentration Polarization" appears [2]. Near the micro-nanojunction, ion depletion zone at the anodic side (AD) and ion concentration zones at the cathodic side (CC) are created. The CC is generally weak and unstable, nevertheless the AD is used as powerful tool to accumulate species against the depletion zone which acts as an electrostatic barrier to any charged particle, biological particles like viruses. However this depletion zone quickly extends toward the outlets leading to unstable concentration process.

Our Ring like device, which exhibit a circular nanojunctions, was tested to analyse the ICP phenomenon. One interesting result is that cathodic concentration appears to be very stable with this axisymmetrical geometry. A strong and stable cathodic concentration effect was observed when a positive voltage was applied in the center of the device. (Fig1–right).

Finally such results are promising for several biological applications like the early detection of viral agents which have similar size as the nanobeads used here.

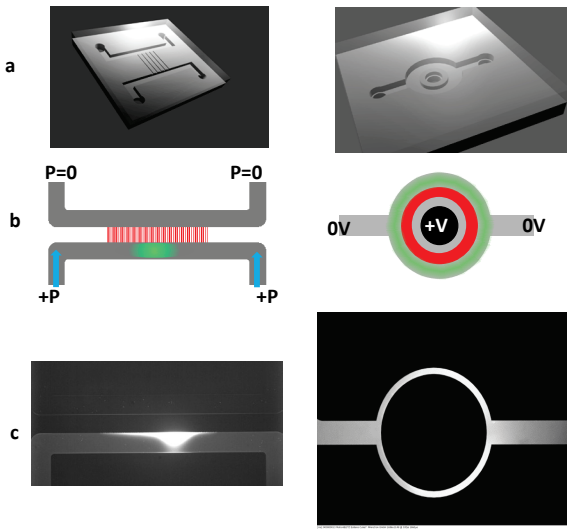

Figure 1: Concentration of nanoparticles with two micronanofluidic designs: the by-pass device (left) and the ring like device (right). a) 3D artistic view. b) top view : microfluidic (10µm in depth) are colored in grey, and nanochannel (100nm) are in red. The green spot is the zone where nanoparticles are concentrated. The bypass is actuated by a pressure of one bar and the ring like device by a voltage of 50V. c) Fluorescence imaging captured after 60 min of concentration operation.

Related Publications:
[1] K. Aïzel, V. Agache, C.Pudda, F. Bottausci, C. Fraisseix, J. Bruniaux, F. Navarro and Y. Fouillet, Enrichment of nanoparticles and bacteria using electroless and manual actuation modes of a bypass nanofluidic device. Lab on a Chip, 2013 (22),4476-4485.
[2] K. Aïzel, Y. Fouillet, C. Pudda, C. Chabrol, I.Texier-Nogues, Investigation of ICP effect on nanoparticles using an original micro-nanofluidic device, Microfluidic conference, Germany, 2012.
[3] K. Aïzel, Y. Fouillet, C. Pudda, C. Chabrol, Concentration of nanoparticles using radial nanofluidic devices. TechConnect World, Washington, US 2013.

A data base of computational models: static and dynamic approaches for multiphysic problems

Research topics: Flow field calculation, transport, diffusion, reactions, interfaces

J. Berthier, P. Pouteau, N. Sarrut, V. Agache, J. El-Sabahy, F. Abeille

ABSTRACT: Whereas the initial approaches to biology and biotechnology have been mostly experimental, the development of numerical methods for the modeling and simulation of phenomena encountered in these scientific domains has seen a steady progress in the recent years. Similarly to other scientific domains, numerical models are becoming a support for the design of new systems, and an appreciable help to the experimenters, designers and engineers.

Owing to the growing trend to back up experimental developments by numerical simulations, an effort has been conducted at the LETI/DTBS, to develop numerical models in parallel with the different experimental approaches.
An on-line data base describing the models, with the guidelines for proper use, has been set up. At the present time, the library contains more than forty models in many different domains: flow field calculation, transport of discrete particles, transport and diffusion of chemical species, chemical and biochemical reactions, as well in the bulk as on the walls. Tutorials for the shape of interfaces are also included in the data base.

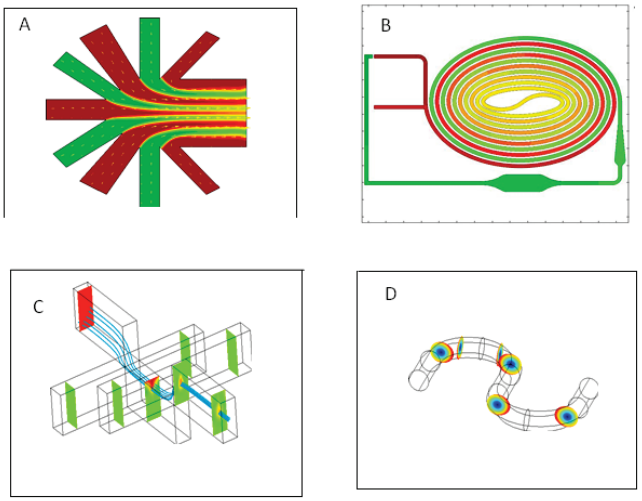

Figure 1: A : Confluence of laminar microflows showing the persistence of flow streams ; B : Pressure profile in a long spiral channel ; C : Focusing of a flow stream by auxiliary sheath microflows ; C : whirling effect in winding channel, sometimes called Dean flow. All figures are obtained with COMSOL, and documented in [1,2].

The numerical approaches are performed with the help of different numerical programs: Finite Element approach with the software COMSOL for the solution of dynamic and multiphysic problems; Surface integral approach with the software Surface Evolver for calculating static or quasi-static interface localization, and Matlab for specific problems that do not fit the preceding softwares.

Figure 1 shows the calculation of laminar flow fields with COMSOL. Figure 2 shows multiphysics problems where the flow field is coupled to other phenomena ; such as dielectrophoresis or mass transfer.

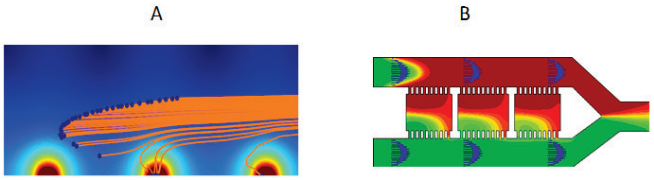

Figure 2: A) Trajectories of particles in a dielectrophoretic field ; B) micro chamber for the culture of cells.

In modern biotechnology, interfaces are often present in microsystems; for example in Flow Focusing Devices [3], or in Digital Microfluidics. Usually, owing to the small dimensions, inertia is negligible and the shape of interfaces can be calculated by a static or quasi-static method. The software Surface Evolver is well suited for such problems (Figure 3) [4].

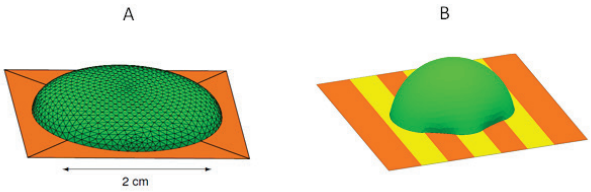

Figure 3: A: shape of a large sessile droplet ; B: shape of a small sessile droplet on a patterned substrate. Software Evolver.

In conclusion, numerical methods are being increasingly sophisticated and can provide very useful help to design new microsystems.

Related Publications:
[1] J. Berthier, Chap 13, Finite Element Method for Micro and Nano-Systems for Biotechnology, S.M. Musa (editor), Computational Finite Element Methods in Nanotechnology, CRC Press 2012
[2] J. Berthier, R. Renaudot, P. Dalle, G. Blanco-Gomez, F. Rivera, V. Agache, COMSOL assistance for the determination of pressure drops in complex microfluidic channels. European COMSOL Conference, Paris, 2010.
[3] J. Berthier, P. Dalle, F. Rivera, R. Renaudot, S. Morales, P-Y. Benhamou, P. Caillat, "The physics of pressure powered micro-flow focusing device for the encapsulation of live cells", Nanotech Conference, Nanotech Conference, 2011, Boston, USA.
[4] J. Berthier, K. Brakke. The Physics of Microdroplets. Scrivener-Wiley Publishing, 2012.

Implantable system for controlled intratumoral drug delivery

Research topics: Drug delivery, micropump

S. Maubert, Y. Fouillet, O. Fuchs, M. Cochet, Y. Colletta, C. Chabrol, N. David, R. Campagnolo

ABSTRACT: An implantable system for controlled low pressure and low flow rate intratumoral drug delivery was developed. A new silicon micropump powered by a specially designed electronics allows for a perfectly localized injection. The system was validated by a one week implantation in swine affected by glioblastoma.

The treatment by systemic drug delivery of some cerebral diseases like malignant tumors, Parkinson disease or epilepsy among others has low efficiency because of the "blood brain barrier" that separates the blood from the brain. One alternative and promising approach requires precise and controlled intra-tissue drug injection, but adapted tools still lack [1]. We developed an implantable, autonomous injection system able to deliver a therapeutic principle into cerebral tumors at low pressure and flow rate in a controlled way (Fig.1).

The heart of the system is a silicon peristaltic micropump based on a piezoelectric actuation. Fluidic characterizations proved its ability to deliver fluids at pressure and flow-rate ranges compatible with intratumoral delivery. Moreover, built-in pressure sensors enable a monitoring of the flow as well as the good functioning of the pump [2].
The pump is powered and controlled by a specially designed low consumption electronics which also collects the data of the sensors. A radiofrequency link allows for a remote control of the system when implanted.
The drug is stored in a collapsible reservoir, and the injection is made through a catheter which is inserted into the heart of the tumor. All the fluidic elements are connected through chirurgical biocompatible tubing.
Finally, the pump, the electronics and the reservoir are enclosed in specially designed biocompatible and hermetically sealed PEEK housings.

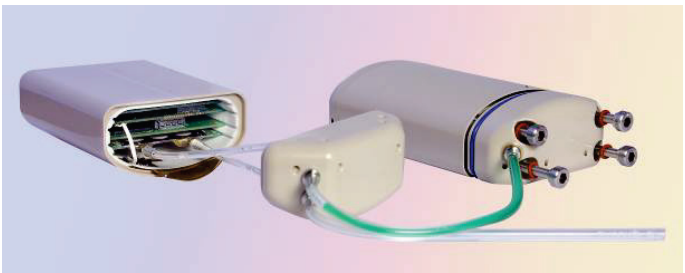

Figure 1: The injection system (left: housing with the electronics and the pump; right: housing with the reservoir inside)

For a real condition test, the system was implanted during one week in swine affected by a model of glioblastoma, a malignant primary brain tumor (Fig 2), and anticancer drug Avastin® was injected at 0.5µl/min. During the implantation, the swine did not show any discomfort nor rejection signs. The system did not present any failure. After one week, the analysis of the tumorous tissues showed a well localized injection without any backflow or leakage of the drug outside of the tumor, which are the main failure reasons of intratumoral chemotherapies (Fig 3).

Our injection system opens new perspectives for drug intra-tissue injection therapies. More efficient treatments with fewer side effects and an improved quality of life for the patients are expected.

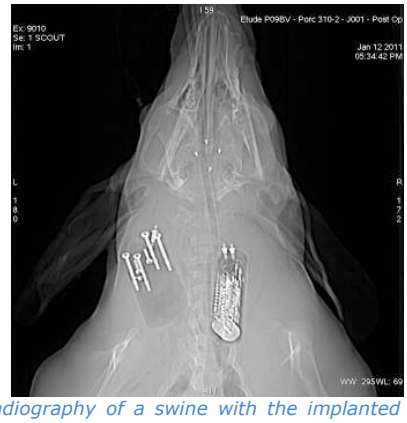

Figure 2: Radiography of a swine with the implanted system (left: reservoir housing; right: pump and electronics housing)

Figure 3: Swine brain and tumor section after one week injection with the implanted system showing intratumoral localized drug delivery (arrow).

Related Publications:
[1] O. Fuchs, "MEMS micropump system for drug delivery", Pharmapack 2013, invited speaker
[2] O. Fuchs, Y. Fouillet, S. Maubert, M. Cochet, C. Chabrol, N. David, X. Médal, R. Campagnolo, "A novel volumetric silicon micropump with integrated sensors", MicroElec. Eng, 97 (2012) 375–378

Acoustic and microfluidic for biology: Radiation Force and Torque

Research topics: Acoustics, microfluidics, biology

D. Rabaud, J.-P. Kleman (IBS), M. Cubizolles, C. Poulain

ABSTRACT: Acoustics waves (i.e. pressure waves) are capable to exert forces and torques upon very small particles such as beads, microbubbles, cells or bacteria. This phenomenon arises from the radiation pressure effect, analogous to the one used in optics with optical tweezers. In the lab, we design, package and implement acoustics on microfluidics chips in order to take advantage of both the statistical approach of successive individual cells, and a non-intrusive and contact less technique to address biological issues like sample preparation (aggregation, separation) and size, density or elasticity based sorting to mention but a few.

When an ultrasound field is imposed on a fluid containing a suspension of particles, the latter will be affected by the so-called acoustic radiation force arising from the scattering of the acoustic waves on the particle. The particle motion resulting from the acoustic radiation force is denoted acoustophoresis and is very similar to the well-known dielectrophoresis and plays a key role in on-chip cell handling. Most work in the literature is devoted to the force but very few to the acoustic torque. We are developing chips in order to concentrate cells in a micro channel by means of acoustic forces on the one hand, and chips to make cells or particle rotate on the other. Our goal is to have a better understanding of both mechanisms at play and consequently be able to implement both effects (i.e. translation and rotation) at will on a dedicated chip.
The first example is a silicon chip that enables to concentrate bacteria in the center of the channel. It is known that bacteria and cells are attracted towards the pressure node of the acoustic field. Using a half wavelength resonance in the transverse direction of the channel, particles (beads or cells) undergoes a radiation force perpendicular to the mean flow, thus allowing the collection of these particles further away in the center of the channel.

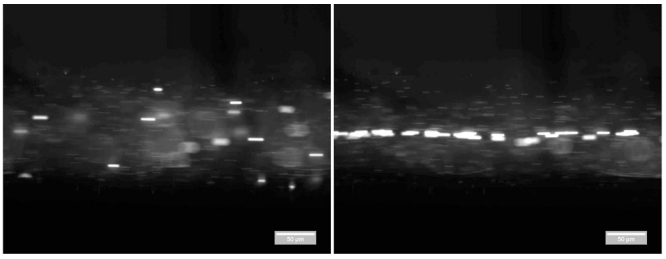

Figure 1: acoustic focusing of bacteria

The second example is what we call the MACS for Microfluidic Acoustic Cell Spinner. The cell flows in a resonator and is excited by two orthogonal standing waves which are out of phase. Doing this, a viscous streaming effect arises and induces a slow rotation of the cell, typically at a frequency of the order of 1 to 10 Hz, for an ultrasound frequency above 30 kHz.

In the work for a better control of the parameters governing the acoustic torque to be able in the future to rotate at a given velocity and stop at a desired

position a cell for addressing applications such as sonoporation or sonofusion of two types of cells. The angular velocity is related to the size, density and elasticity of the cell, and we think this technique could be used to sort cells or bacteria according to one or the other criteria, in a microfluidic chip.

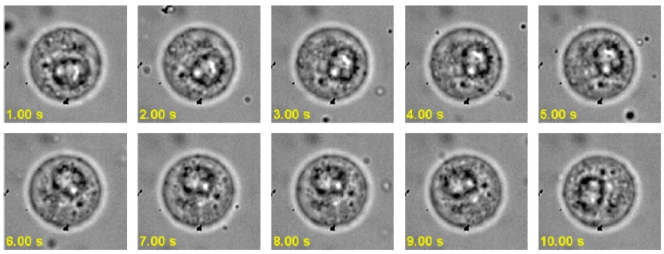

Figure 2: rotation of a 3T3 cell under acoustic excitation

Related Publications:
[1] C. Poulain, D. Rabaud, J.P. Kleman "Acoustic and microfluidic for biology: Radiation Force and Torque", Nano and Micro-Environments for Cell Biology Workshop, 30th January 2014, La Tronche, France

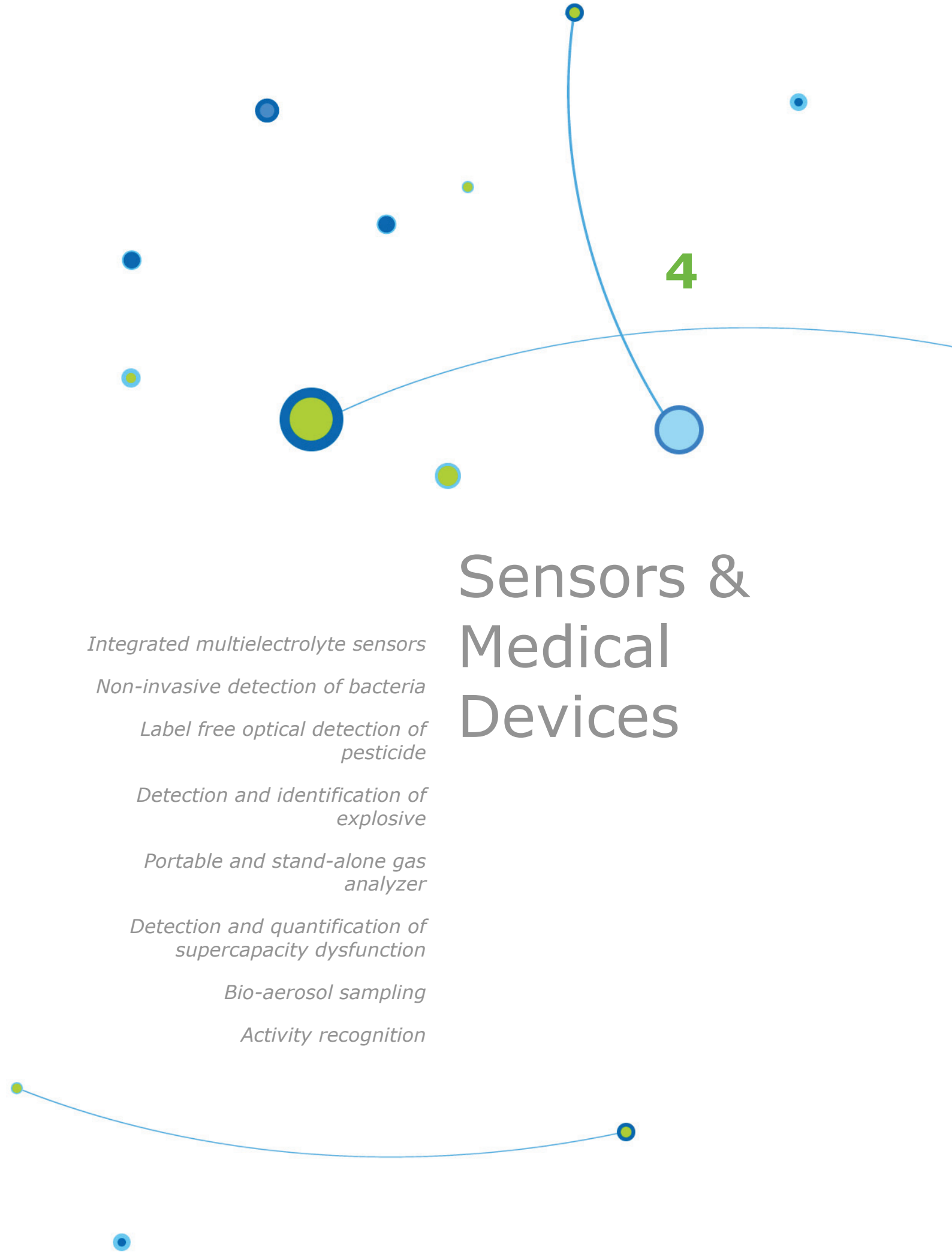

4

Sensors & Medical Devices

Integrated multielectrolyte sensors

Non-invasive detection of bacteria

Label free optical detection of pesticide

Detection and identification of explosive

Portable and stand-alone gas analyzer

Detection and quantification of supercapacity dysfunction

Bio-aerosol sampling

Activity recognition

Integrated multielectrolyte sensors for blood monitoring in chronic liver diseases

Research topics: Biosensors, Ionic Selective Electrodes, bio-artificial organ

C. Goyer, M.-L. Cosnier, F. Revol-Cavalier, J. Fils

ABSTRACT: The European d-LIVER project aims to meliorate the monitoring of chronic liver failure patients. Predictive value of change in patient health status would be improved with more frequent measurements of selected biochemical parameters and more specifically sodium, potassium and ammonium. These sensors have to be integrated within a fluidic disposable cartridge to be used daily by the patient at home.

Chronic liver disease continues to be a frequent problem in the population worldwide. Progressive liver tissue destruction results in inability to perform normal organ function and in turn in development of frequent complications. A possible solution consists to provide a complete solution to improve the management of chronic liver failure patients. Currently outpatient clinic follow-up offers only intermittent review of health status and blood parameters by liver experts on a weekly or monthly basis. Taking into account this situation, the d-LIVER project, a European Integrated Project aims to meliorate the monitoring by means of development of reliable sensor-based patient home systems. More frequent measurement of selected biochemical parameters can improve the predictive value of changes in patient health status.
Among these biochemical parameters, the electrolytes concentrations in blood or serum (sodium, potassium and ammonium) are essential. To monitor these parameters, Ionic Selective Electrodes have been designed to be integrated within a disposable fluidic cartridge containing a total of 8 different sensors which will be used daily in an instrument at patients home (Fig.1).

Figure 1:3D view of the instrument at patients home

Thus many improvements have been made:

- to miniaturize the sensors to have a size of a few millimeters square for integration
- to adapt the detection to a few milliliters of diluted human serum
- to obtain a dedicated fluidic interface
- to have sensors supporting long-term storage (currently few weeks)

The developments have led to a complete test platform containing 3 working electrodes for the 3 electrolytes to detect and an integrated pseudo reference (Fig.2).

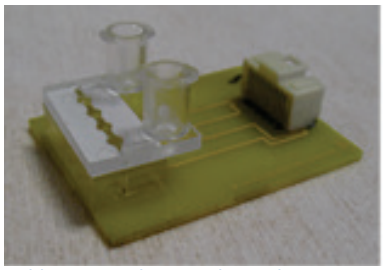

Figure 2: Integrable Ionic Selective Electrodes

The electronic readout setup has been developed by a partner of the project and will allow converting the electrochemical signal to an ionic concentration.

This electrolytes sensors platform has been validated on model solutions with performances meeting clinical requirements of the project.

Reproducibility on animal serum has been evaluated. The reproducibility inter-sensor is from 3 to 6% and reproducibility intra-sensor is 1% [1].
Finally, the platform will be integrated in the complete cartridge to be used among the other sensors. Clinical evaluation is planned next year.

Related Publications:
[1] M.L. Cosnier, LETI Day's, 2013, « Blood monitoring for artificial liver ».

Non-invasive detection of bacteria via the sensing of volatile metabolites

Research topics: Microbial volatile organic compounds, optical detection of gases

P. R. Marcoux, M. Vrignaud, Z. Buniazet, I. Texier-Nogues

ABSTRACT: A low-cost, innovative and non-invasive colorimetric test, is proposed to detect pathogenic bacteria via the simple and fast detection of volatile metabolites (bacterial VOC). The targeted metabolite is either endogenous or exogenous (i.e. released by enzymatic hydrolysis). The gaseous fraction of bacterial metabolite is trapped and accumulated within the nanopores of a xerogel compatible with optical transduction. When the targeted VOC does not have intrinsic optical properties, the xerogel is doped with a probe molecule that reacts with VOC in a fast and specific way, so as to yield a product easy to detect optically.

Sensors are made with sol-gel chemistry and look like glass. This chemistry allows for a large variety of xerogel shapes (Fig. 1a) and surface functionalization. Furthermore, distribution of nanopores is tailored thanks to a porogenous additive. Our sensors efficiently trap the gaseous fraction of targeted VOC (Fig. 1b) as they develop an important surface (between 500 and 1000 m2 per gram of xerogel). As they are transparent in visible domain and do not show intrinsic fluorescence, they perfectly match with the requirements of optical transduction.

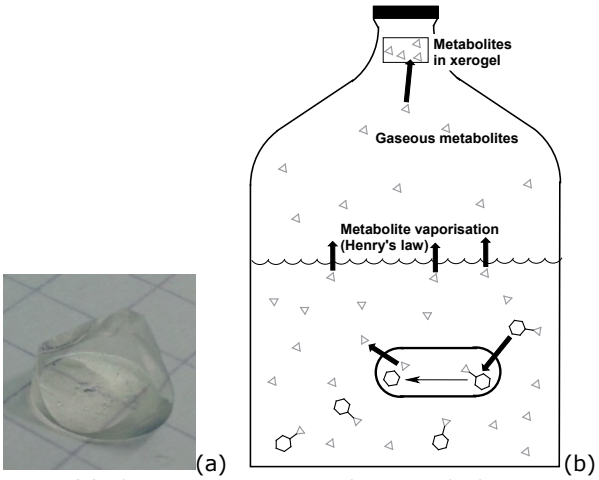

Figure 1: (a) Thans to an innovative drying method, we can make xerogels with complex shapes, such as a trihedral prism (retroreflector). (b) The specimen to be tested is mixed with an aqueous solution of the enzymatic substrate. Viable targeted microorganisms can cleave the synthetic substrate and give rise to a volatile organic compound (VOC) dissolved in the aqueous phase. This VOC has been chosen so as to be detected easily by optical transduction. Because of Henry's law, VOC molecules are released in gas phase where they are trapped and accumulated into a xerogel.

We first worked on the detection of indole, a widespread endogenous VOC produced by a large variety of pathogens, such as E. coli. An aromatic aldehyde was chosen as the selective probe molecule giving a green product in presence of indole. We demonstrated how indole was detected in the gas phase above a bacterial culture, either it is liquid or solid culture medium [1]. Then we extended the proof of concept to exogenous VOC released by enzymatic activity [2,3]. In that case, nitrophenol was chosen as a targeted metabolite as it is intrinsically colored (Fig. 2a) and easy to couple with a sugar so as to form an enzymatic substrate. Accumulation of trapped VOC inside the sensor is easily monitored thanks to spectrophotometry (Fig. 2b).

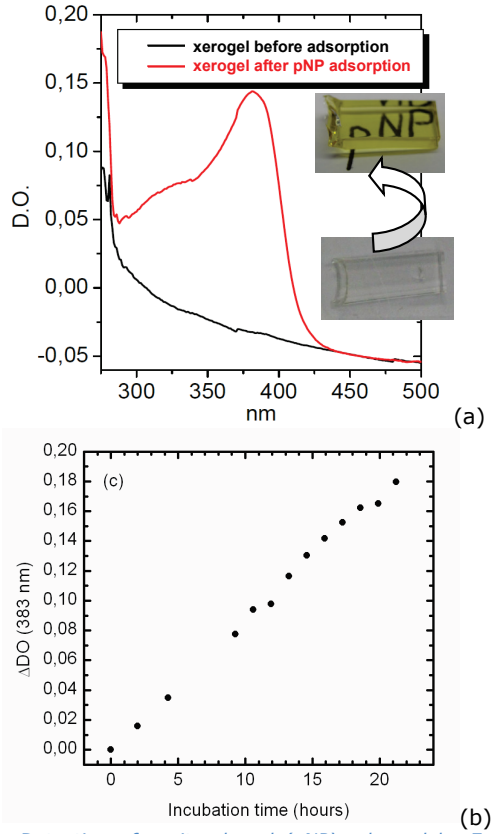

Figure 2: Detection of p-nitrophenol (pNP) released by E. coli (β-glucuronidase enzymatic activity), and trapped in a transparent xerogel (a) UV-visible spectrum of pNP trapped (anionic form) in the xerogel exposed to E. coli culture (initial concentration: 105 cfu/mL). (b) Kinetics of pNP trapping in the xerogel, monitored at 383 nm.

Related Publications:
[1] S. Crunaire, P. R. Marcoux, L.-H. Guillemot, K.-Q. Ngo, F. Mallard, J.-P. Moy, T.-H. Tran-Thi, "Discriminating bacteria with functionalized nanoporous xerogels", Procedia Chemistry 6 (2012) 125-131.
[2] L.-H. Guillemot, M. Vrignaud, P. R. Marcoux, T.-H. Tran-Thi, "Non-invasive detection of bacteria via the sensing of volatile metabolites released by enzymatic activity", 3rd International Conference on Bio-Sensing Technology, Sitges (Spain), 15-17 May 2013.
[3] L.-H. Guillemot, M. Vrignaud, P. R. Marcoux, C. Rivron, T.-H. Tran-Thi, "Facile and fast detection of bacteria via the detection of exogenous volatile metabolites released by enzymatic hydrolysis", Physical Chemistry Chemical Physics 15 (2013) 15840-15844.

Label free optical detection of a pesticide by photonic crystal-shaped Molecularly Imprinted Polymers

Research topics: Molecularly Imprinted Polymers, inverse-opal, label-free sensing

H. Marie, P. R. Marcoux, S. Vignoud, G. Marchand

ABSTRACT: We aim at elaborating a label-free sensor for 2,4-dichlorophenoxyacetic acid, a widely used and toxic pesticide. The detection is performed by Molecularly Imprinted Polymers (MIPs), tailor made synthetic receptors. The optical transduction is obtained by structuring the polymer into a photonic crystal. Opals were manufactured with a new process suitable for large scales (Boostream® from CEA Liten) and opals were used to mold MIPs in inverse opals. Submicron structures are then responsible for the colour of the sensor. A change of colour is triggered by the recognition of the analyte by the polymer (upon swelling).

The developed sensor is based on Molecularly Imprinted Polymers (MIPs) and inverse opal technologies. MIPs are synthetic receptors providing an interesting alternative to biological molecules in sensitive layers of sensors. Indeed, these polymers are generally more robust, more stable and cheaper than their biological counterparts. The polymers display an imprinted cavity, able to recognize the targeted analyte.

We developed here a polymer able to detect selectively 2,4-dichlorophenoxyacetic acid (2,4-D) in water. 2,4-D is a common toxic systemic pesticide/herbicide used in the control of broadleaf weeds. As shown in Figure 1, 2,4-D can be captured by the MIP in methanol/water 4/1 (v/v).

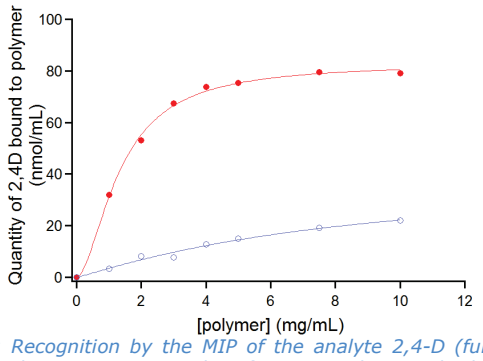

Figure 1: Recognition by the MIP of the analyte 2,4-D (full circles) whereas the non imprinted reference polymer displays little unspecific adsorption (empty circles).

The optical transduction of the sensor is obtained by the structuring of the MIP into an inverse opal. First, opals were synthesized on PMMA substrate, by a novel process called Boostream®. This layer by layer technique enables the continuous deposit of the silica beads on large surfaces. Next, MIPs are synthesized between the beads, thanks to dip-coating followed by UV polymerization. Finally, beads are dissolved and MIPs are structured as inverse opals. Figure 2 shows SEM images of beads multilayers and the inverse opals obtained after beads dissolution.

The sensor, with MIPs structured in inverse opals, can be then used to detect the analyte without labeling. Indeed, due to the senso structuration, a white light incident on the sensor is reflected with a maximum of absorbance (which obeys the Bragg law). Upon analyte recognition, the polymer swells and the maximum of absorbance shifts. This shift (28nm) is observed for the MIP whereas the reference polymer displays barely any shift, Fig#3.

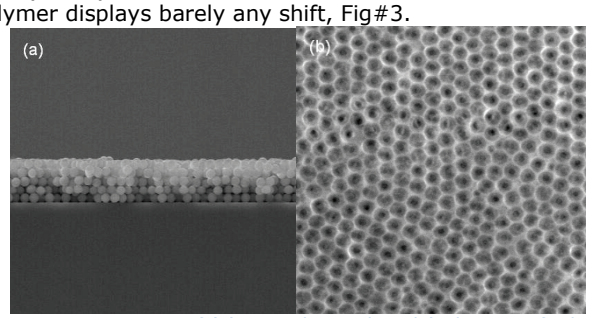

Figure 2: SEM images of (a) a synthesized opal (side view of 5 layers of compact silica beads, diameter 300nm) and (b) the obtained MIPs inverse opals (top view).

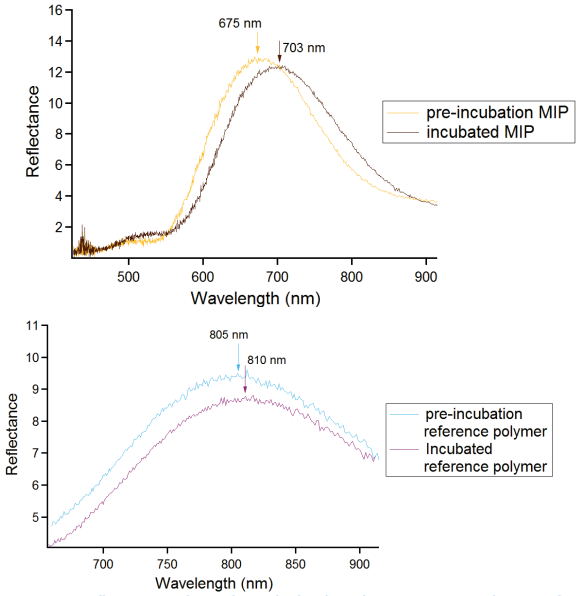

Figure 3: Reflection of a white light by the sensor and its reference, before and after incubation with 2,4-D.

Related Publications:
[1] S. Vignoud-Despond, H. Marie, O. Dellea, P. R. Marcoux, K. Haupt, G. Marchand, "Elaboration of a new sensor combining molecularly imprinted polymers and opal technologies", Materials Research Society Fall Meeting; 2013 December; Boston.
[2] H. Marie, S. Vignoud-Despond, O. Dellea, P. Marcoux, K. Haupt, G. Marchand, "Elaboration of a sensor combining molecularly imprinted polymers and opal technologies" Materials Research Society (MRS 2012), Boston.

An autonomous portable device to detect and identify explosive vapors

Research topics: Electronic nose, gas sensor, explosive detection

R. Rousier, O. Dumas, S. Besnard (DAM), F. Veignal (DAM), F. Pereira (DAM), A. Mayoue (List)

ABSTRACT: A portable device is reported to detect and identify in real time explosive vapors. This device is composed of the multi-sensors chamber with three technologies of explosive vapors detection and identification: Quartz Crystal Microbalance, Surface Acoustic Wave and fluorescence. The multi-sensors chamber was designed and optimized to guaranty an efficient fluidic repartition on each sensor to assure the suitable responses of sensors. A laptop controls the device. An algorithm has been specifically developed to detect and identify gas nature. This device is dedicated to 2nd level control such as checking of abandoned or suspicious luggage.

Both detection and identification of dangerous gas are very important. In a first time, the detection allows to warn the surrounding people if there is a danger and in a second time the identification allows to choose which action has to be taken accurately to neutralize the danger. The association of several and different chemical sensors is an asset in this way, because different sensors bring complementary information to ensure efficient detection and identification of gas nature. The development of this kind of device is known as an electronic nose.

A portable electronic nose (Fig. 1) named T-REX (Technology for the Recognition of Explosives) is presented here. Our device is composed of three existing technologies, 2 gravimetric sensors (QCM, SAW) and fluorescence sensors. This device has 14 sensors: 8 SAW, 4 fluorescent sensors and 2 QCM. A fluidic chamber integrating all sensors has been designed with Solidworks and an add-on for fluidic simulation to optimize the flow. The device includes a pump and a flow rate control. All the electronic boards and power source are inside. A laptop controls the device with a Labview interface. An algorithm has been developed and adjusted to take into account the complementary sensor responses.

Figure 1 : Photography of T-REX

The power consumption of the device is about 20 W. We tested the device with external battery. We obtained a lifetime of about 7 hours with a battery of 111 Wh. This lifetime is comparable to industrial portable devices. So our device satisfies the entire requirement to be electrically autonomous.

With the present sensitive material inside the device, the work has been focused on several targets such as trinitrotoluene (TNT), 2,4 dinitrotoluene (DNT), ethylene glycol dinitrate (EGDN), nitromethane (NM). Three interfering compounds have also been tested: ethanol, dichloromethane (DCM) and methyl ethyl ketone (MEK) to test the robustness of the algorithm. The device has been characterized in laboratory conditions and in real conditions. In the laboratory conditions the sensors were exposed to ambient air during several minutes to obtain a stable baseline. Then a bubbler, filled with liquid or solid analyte, is connected to the device. All the data were processed during the gas exposition in real time with an algorithm. In the real conditions, a bag was filled with TNT (Tolite). The device was initially running to obtain a stable baseline, then the bag was brought close to the device. The device has successfully detected the TNT.

The concentrations were near the saturation vapor pressure of gases. The successful detections and the identifications were in about 1 min to 2 min. The present performance is about 100% for the detection and 80 % to 90% of true identification. We are pursuing the tests and the optimization of the algorithm to improve the performances.

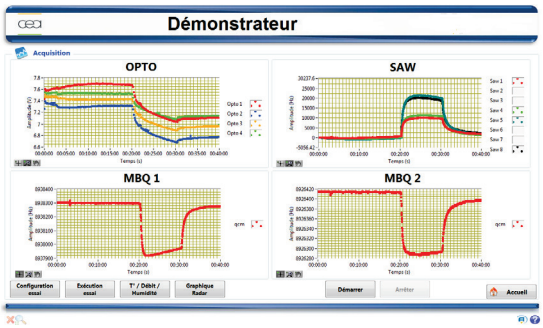

Figure 2 : IHM Labview interface of Ethylene glycol dinitrate (EGDN) acquisition

We report a portable electronic nose device to detect and identify explosive vapors on abandoned or suspicious luggage/people. This device is composed of 14 sensors. These different technologies were successfully integrated on a multi-sensors chamber. The device with the sizes of 300 mm length, 200 mm wide and 180 height and a weight of 6 kg is fully portable. The results are very promising to fight against the terrorism.

Related Publications:
[1] R. Rousier, S. Bouat, T. bordy, H. Grateau, M. Darboux, J. Hue, G. Gaillard, S. Besnard, "T-REX : A portable Device to Detect and Identify Explosives Vapors", Procedia Engineering, V. 47, 2012, p390-393.
[2] R. Rousier, O. Dumas, S. Besnard, F. Veignal, F. Pereira, A. Mayoue, "An autonomous portable device to detect and identify explosive vapors" to be submitted: Sensors and Actuators B, 2013.

The authors thank SGDSN and CEA/DSNP for the financial support.

Towards a portable and stand-alone gas analyzer: Quantification of benzene, toluene and xylene in the 10 ppb range

Research topics: Optical detection, gas analyzer, sol-gel, Volatile Organic Compound

J. Hue, T. Bordy, R. Rousier, S. Vignoud

ABSTRACT: In the framework of a French Joint program COVADIS, an ultra-sensible system for a simultaneous detection of benzene (B), toluene (T) and xylenes (X) in indoor air has been developed. The sensors are nanoporous disks. The detection is based on absorbance measurements over the 250 nm-300 nm range with an uncooled spectrophotometer. For the benzene, a detection of 3 ppb has been successfully achieved within 15 minutes of exposure. In using, thicker but flat sensors, the quantification becomes possible: 21 ppb for the B, 16 ppb for the T and 8 ppb for the X.

Benzene, toluene, and xylenes (BTX) are volatile aromatic monocyclic hydrocarbons of significant health concern. In particular, benzene is a well-known human carcinogen. According to [1], the concentration of airborne benzene is associated with an excess lifetime risk of leukemia of 10^{-4} is 17 µg/m^3 (≈ 5 ppb). Such concentration can be found in indoor air and there is no easy and direct way to detect and quantify these pollutants. Therefore, the development of a fast and sensitive analyzer to measure, on site, a wide range of concentration of BTXs is a significant challenge [2].
The development of a portable stand-alone BTX analyzer based on sol gels sensors is ongoing. Devoted sol-gel sensors have been developed to trap the BTX, especially close to their "interfaces". Indeed, the nanopores size inside the sol-gel is adapted to the BTX molecule sizes (i.e. benzene molecule size ≈ 0.5 nm). The trap selectivity is improved in following the light absorption of the sol gel sensor at specific wavelengths (250nm-300nm) (see Fig. 1).
The laboratory analyzer is built around 3 main components linked together by optical fibers:
a UV deuterium commercial compact lamp, an uncooled spectrophotometer and an home-made modular fluidic chamber to receive the sensors crossed by UV light and continuously exposed to the atmosphere at a control flow rate.
The detection limit is improved in increasing the interface number of the sol gel. Unfortunately, the sol gel sensors without BTX inside, absorb and scatter the UV probe light. Thinner sensors are developed to minimize these effects. Therefore, 18 cylindrical sensors (5.7 mm in diameter) with a central thickness of 230 µm allow detecting 3 ppb of benzene (see Fig. 2). These sensors are similar to planar concave lenses and act as such lenses. The repeatability of these sensors is insufficient to quantify the BTX concentration. To overcome this difficulty, rectangular parallelepiped thicker sensors (1 mm thick) with 2 flat and parallel faces, have been developed. These sensors show a higher degree of reproducibility. At that stage, BTX concentration measurements with 5 of these sensors lead to higher detection limit (DL): 21 ppb for the benzene, 16 ppb for the toluene and 8 ppb for the m-xylene. A measurement typically lasts 1000 seconds. However, due to the small standards deviations of the detection limit (see Fig. 3), this analyzer allows not only to detect the BTX but to quantify them. From these data, it will be possible in the future to simultaneously quantify benzene, toluene and m-xylene concentrations inside a gas mixture.

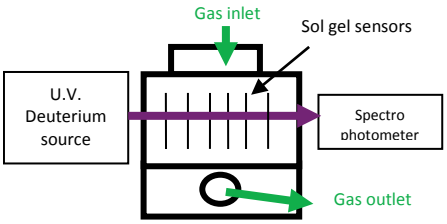

Figure 1: Protocol to determine a given BTX concentration. The light variation is due to the trapped benzene inside the sensors.

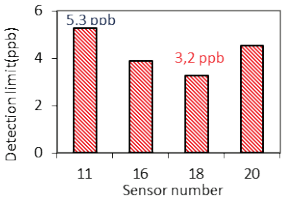

Figure 2: Benzene detection limit (DL) versus the number of sensors. The best detection is obtained with 18 sensors DL ≈ 3ppb

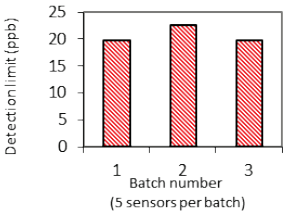

*Figure 3: Repeatability for the benzene detection with 5 * 1 mm "thick" sensors. DL ≈ 21 ppb*

This work was performed in the framework of COVADIS under the auspices of Lyonbiopole, Axelera and Advancity within the 9th FUI project call. A part of this project is granted by OSEO and various territorial collectivities (Rhone Alpes region, Grenoble city…). The thinner sol-gel sensors have been achieved at LETI according the LFP synthesis (T. Tran-Thi: CNRS, DSM, SPAM, URA CEA CNRS 2453, 91191 Gif-sur-Yvette Cedex, France) and the thicker sensors by ETHERA, which is the end user. (T. Caron, P. Karpe, Y. Bigay)

Related Publications:
[1] Air quality guidelines for Europe, 2nd ed. Copenhagen, World Health Organization 2000
Regional Office for Europe (http://www.euro.who.int/data/assets/pdf_file/0005/74732/E71922.pdf).
[2] S. Camou, T. Horiuchi, T. Taga, "ppb level benzene gas detection by portable BTX sensor based on integrated hollow fiber detection cell", IEEE sensors 2006, Daegu, Korea, 22-25 October 2006.

Development of an integrated and portable system to detect and quantify the dysfunction of a supercapacity

Research topics: Supercapacity, gas sensor

S. Vignoud, M. Matheron, T. Bordy

ABSTRACT: In the framework of an European Joint Program HESCAP, the development of suitable sensors is ongoing for specifically monitoring the high energy supercapacitor cell and stacks in order to detect dysfunctions. To reach these safety requirements, a gas sensor is developed that will detect gases emitted during degraded mode of the supercapacitor. The target gases are carbon dioxide (CO2) and hydrogen (H2) in a range of concentration between 100 and 500 rpm.The sensors consist of a gravimetric transducer and a chemical coating. To finish, a prototype is developed integrating all gas sensors.

Supercapacitors (SC) are electrochemical capacitors that have high capacitance and high energy density when compared to common capacitors, and higher power density when compared to batteries. In most commercially available supercapacitors, the electrolyte is either aqueous or organic. Aqueous electrolytes are RoHS and REACH compliant, offer low internal resistance, but limit the voltage to roughly one volt per cell, whereas organic electrolytes are generally based on acetonitrile or propylene carbonate that allow higher voltage per cell, with higher internal resistance[1]. According the literature and gas emission analysis on partner's stacks, two main gases were emitted during electrolyte decomposition: CO2 and H2.

For the detection of gas, we choose mass transducer. Several mass transducers were available and showed different sensibility and resolution.

According to the preliminary results on gas emission of partner's supercapacitor stacks) [2], concentration of emitted gases is between 100 and 500 ppm. For this concentration range to detect, BAW transducers are sufficient because the concentration resolution of such kind of transducer is above 1 ppm. Among the BAW transducers, our choice was focused on Quartz Crystal Microbalance [3]. In order to detect each gas specifically, we develop several chemical coating: polymers (PVP, PEI, PCL…), silanes, porous material, ionic liquids. For each gas, a screening of different sensitive chemical layers has allowed selecting one coating. The sensitive layer was optimized: thickness, coating process, reproducibility repeatability, sensitivity and also robustness. For hydrogen detection, the best layer among all tested is silica functionalized by EBTMOS (0.19 Hz.ppm-1 for 95 nm of porous silica)

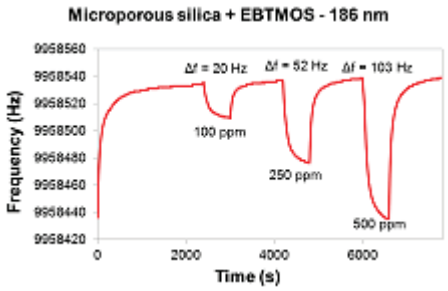

Fig 1: Responses under 100-250-500 ppm H2 exposition of QCM coated with microporous silica functionalized with silane EBTMOS

For carbon dioxide detection, the best layer among all tested for CO2 detection is silica functionalized by HMDS with a sensitivity of 0.07 Hz.ppm-1 for a layer of 43 nm of silica.

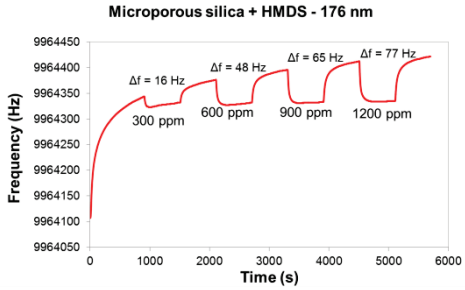

Fig 2: Responses under 300-1200 ppm CO2 exposition of three identical QCM coated with microporous silica functionalized with HMDS

The objective of the HESCAP demonstrator is to provide a system that can afford the detection in the same time of carbon monoxide, carbon dioxide and hydrogen. The demonstrator will include one commercial sensor for the detection of CO and two sensors developed by the LETI for detection of carbon dioxide (QCM 1) and (QCM 2) hydrogen. The demonstrator is piloted by a computer through USB port or by a wireless system. The prototype operates standalone with a rechargeable battery and it is portable and can be placed where desired.

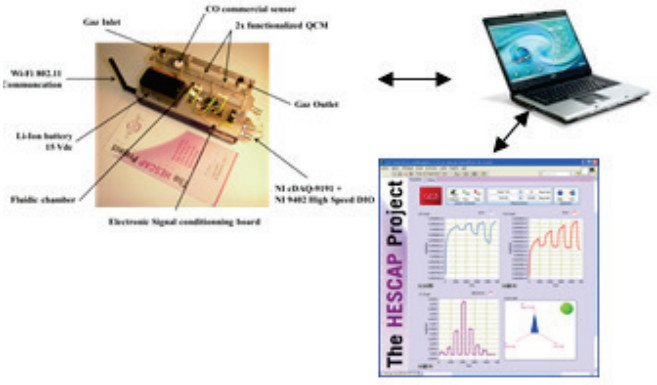

Fig 3: HESCAP prototype

Related Publications:
[1] T. Brousse, M. Toupin and D. Bélanger , "A hybrid activated carbon-manganese dioxide capacitor using a mild aqueous electrolyte., J. Electrochem", Soc. 2004, 151 (4), A614-A622.
[2] P. Kurzweil and M. Chwistek., "Electrochemical stability of organic electrolytes in supercapacitors: Spectroscopy and gas analysis of decomposition products", J. Power. Sources 2008, 176, 555-567.
[3] J-M. Friedt,"Introduction à la microbalance à quartz : aspects théoriques et expérimentaux", IMEC - 3001 Leuven – Belgique.

Bio-aerosol sampling and concentration with an electrostatic air sampler

Research topics: Airborne pathogens, air sampling, biosensors

J.-M. Roux, J.-L. Achard (CNRS-LEGI), G. Delapierre

ABSTRACT: Sensors are more and more sensitive and miniaturized. But analysing dilute analytes such as airborne pathogens remains impossible without a significant and concentrated sample. Original electrostatic bio-samplers are being developed to broaden the range of particles that can be collected and analysed.

Human exposure to airborne biological agents is known to cause various illnesses, infections and allergies. Also, there is a great concern that biowarfare agents can be intentionally released with the purpose of causing public anxiety, sickness and fatalities. Safeguarding a certain area regarding bio-agents demands the detection of pathogenous vegetative bacteria, spores and viruses by sampling and analysing aerosols in a few minutes to trigger an alarm.
Different principles have been used to sample microorganisms: impingement, impaction, filtration and electrostatic precipitation. The first three have been widely used and the interest in the latter has grown in the last ten years. A few studies showed that it is also an efficient and suitable mean of collecting micro-organisms [1].

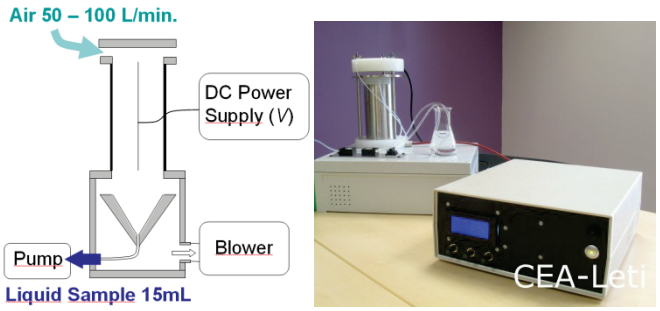

Figure 1: Schematic and picture of the electrostatic bio-sampler

An original electrostatic bio-sampler (Fig. 1) designed and built to broaden the range of particles that can be collected. Its efficiency was evaluated firstly with natural airborne particles and secondly with Bacillus thuringiensis airborne spores inside an aerosol chamber to simulate a release of Anthrax spores [1].

Particles optical diameter (µm)				
0.30-0.35	0.35-0.40	0.40-0.45	0.45-0.50	0.50-0.58
84 +/- 1%	85 +/- 1%	86 +/- 2%	86 +/- 2%	86 +/- 2%

Table 1: Physical efficiency measured on natural airborne particles at a flow rate of 90L/min

At 90L/min., 84% of the 300nm particles are captured by the device (Table 1). Next, after an optimisation of the rinsing protocol, plate counting showed that a biological efficiency of 86% is achievable on Bacillus thuringiensis airborne spores.

Figure 2: Picture of the compact version of the bio-sampler

In parallel, a portable, silent, and autonomous (several hours) bioaerosol collector (BIODOSI) is currently being developed at CEA (Fig. 2) with the final objective to collect very efficiently airborne pathogens such as supermicron bacteria but also submicron viruses which potential is often lacking for existing portable biocollectors. Particles are collected on a dry surface and concentrated afterwards in a small liquid medium to be analyzed by culture, PCR, immunoassays, mass spectrometry, Raman spectroscopy, to name a few. To be efficient with such a wide range of particles, the device is based on electrostatic sampling. And to be representative of individual exposure, the nominal flowrate of the collector is chosen to be closed to human breathing (10 LPM). This low flowrate also meets the compactness required for a portable and silent instrument which gets rid of heavy and noisy pumping systems [2]. 99% of particles from 10nm to a few microns are collected [3].

Related Publications:
[1] JM. Roux, O. Kaspari, R. Heinrich, N. Hanschmann and R. Grunow, "Study of efficient methods to obtain highly concentrated samples of physical and biological aerosols using an electrostatic air sampler", Aerosol Science and Technology, 47:5 (2013), 463-471.
[2] E. Quinton, J-L. Achard, J-M. Roux, "Ionic wind generator issued from a liquid filled capillary pin. Application to particles capture", Journal of Electrostatics, 71:6 (2013) 963-969.
[3] R. Sarda-Estève, J.M Roux, J. Sciare, M.H Nadal and G. Delapierre, "Physico-chemical qualification and refinements of a new portable bio aerosols collector: BIODOSI", Charged Aerosols, 14 novembre, London (England) 2013.

Improving Activity Recognition Using Temporal Coherence

Research topics: Accelerometer data, activity recognition, classifier

A. Ataya, P. Jallon, P. Bianchi (Telecom ParisTech), M. Doron, R. Guillemaud

ABSTRACT: Assessment of daily physical activity using data from wearable sensors has recently become a prominent research area in the biomedical engineering field. In this paper, we present an accelerometer based activity recognition scheme on the basis of a hierarchical structured classifier. A first step consists of distinguishing static activities from dynamic ones in order to extract relevant features for each activity type. Next, two separate classifiers are applied to detect more static and dynamic activities. On top of our activity recognition system, we introduce a novel approach to take into account the temporal coherence of activities. Inter-activity transition information is modeled by a directed graph Markov chain. Accurate results and significant improvement of activity detection are obtained when applying our system for the recognition of 9 activities for 48 subjects.

The objective of the study is to recognize 9 activities of everyday life using one hip-mounted accelerometer. Three static activities or postures are: lying down, slouching and standing. Six dynamic activities are: stamping, cycling, running, slow walking, fast walking and using stairs. The physical activity recognition system is based on a 2-stage organization: first, an instance based classification, where a hierarchical structure distinguishes beforehand between static and dynamic activities; and second, the incorporation of temporal dependencies, where the classification results are reinforced by taking into account the temporal coherence of activities. The feature extraction for the classifiers is based on a 2-second-window with 50% overlapping ratio; the features are different for the static and dynamic activities. Numerous classifiers have been tested: Decision Trees (DT), Random Forests (RF), Support Vector Machine (SVM), k-Nearest Neighbors (k-NN), Gaussian Mixture Models (GMM), AdaBoost Decision Stumps (AdaB-DS) and AdaBoost with Decision Trees (AdaB-DT).

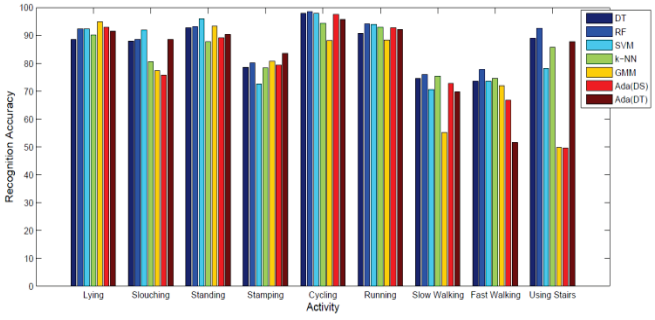

Figure 1: Individual activity recognition accuracies with the proposed graph method implemented.

The graph method idea is to exploit temporal information to improve activity recognition: each activity is modeled by a state in a directed graph Markov chain and the transition probabilities are used to reflect the temporal continuity of activities (this is performed by state proper transition probabilities values close to unity).

The validation database includes 48 subjects (22 women): for which an average of 55 minutes of acceleration data were collected at 200 Hz, using a hip-mounted Motion POD (Movea, containing a built-in triaxial accelerometer). The annotations were performed by a supervising medical team.

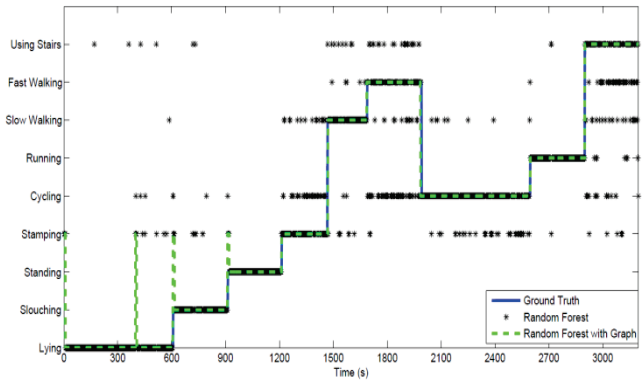

Figure 2: Illustration of detected activity sequence. The effect of the graph is to stabilize the decision in one activity.

The graph based method improves markedly the performances of all classifiers (around 10% in activity recognition). Figure 1 shows the results of the independent classifiers for each of the 9 activities, when the graph method is implemented. Figure 2 shows the impact of the graph method in the stabilization of the activity recognition.

This activity recognition algorithm can be implemented in real-time based on accelerometer data captured at the hip. Possible applications are 1) the lifestyle study in relation with the growing sedentary lifestyle of people and the spreading of overweight and 2) the monitoring of daily activity for isolated elderly.

Related Publications:
[1] A. Ataya, P. Jallon, P. Bianchi and M. Doron, "Improving Activity Recognition using Temporal Coherence", the Engineering in Medicine and Biology Society Conference (IEEE EMBS), Poster presentation, Osaka, Japan, 4-7 July 2013.
[2] M. Doron, T. Bastian, A. Maire, J. Dugas, E. Perrin, F. Gris, R. Guillemaud, T. Deschamps, P. Bianchi, Y. Caritu, C. Simon and P. Jallon, "Estimation of physical activity monitored during the day-to-day life by an autonomous wearable device (SVELTE project)", the Engineering in Medicine and Biology Society Conference (IEEE EMBS), Poster presentation, Osaka, Japan, 4-7 July 2013.
[3] M. Doron, T. Bastian, A. Maire, E. Perrin, L. Oudre, H. Ovigneur, F. Gris, A.-L. Francis, M. Antonakios, R. Guillemaud, C. Villars, J. Dugas, M. Bourdin, T. Deschamps, P. Bianchi, Y. Caritu, C. Simon and P. Jallon, "SVELTE: Evaluation device of energy expenditure and physical condition for the prevention and treatment of obesity-related diseases through the analysis of a person's physical activities", IRBM (34), pp. 108-112, 2013.

5

Neural interfaces

Event-related potential EEG classification

Classification of covariance matrices for BCI Applications

Selective ENG recording

Event-related potential EEG classification of emotional processing

Research topics: BCI, EEG, signal processing, classification

N. Mathieu, A. Campagne, S. Bonnet

ABSTRACT: This paper investigates human emotion recognition based on event-related potentials (ERPs) in EEG elicited by picture presentation. Emotion is manipulated through arousal and valence with a calibrated picture dataset. A classification framework is then designed for single–trial ERP classification. Our results suggest that the discrimination of emotional states is better achieved when it is mainly based on an arousal difference between stimuli rather than on a valence difference.

Brain-Computer Interfaces (BCIs) have been widely developed during the last decade. A related field of interest concerns the automatic emotion recognition from physiological signals. Such emotional BCIs are somewhat different from the previous type since they do not require explicit control. As such, they can enrich the human-machine interface with additional user information in order for the system to adapt to the actual emotional state of the individual. This concept can be enlarged to the monitoring of other mental states like workload or mental fatigue and it has been termed recently under the name of passive BCI.

The aim of this work is to provide a new method for emotion recognition based on event-related potential (ERP) signals instead of most widespread spectral features. ERP are EEG signals that are time-synchronized on stimulus appearance. Indeed many neuropsychology studies have illustrated a high sensibility of ERP components to the different emotional stimuli properties. Moreover ERP analysis can decrease the emotional recognition time which may be of interest in some applications.

The experiment consists in displaying images to participants equipped with EEG sensors. Visual scenes with different valences (negative, positive and neutral) were chosen in order to directly involve the participant. In the experiment, each picture is randomly presented, during 1 second, after a fixation cross. After each picture presentation, the participant is asked to indicate its feeling (well-being, fear or neutral) by using the keyboard.

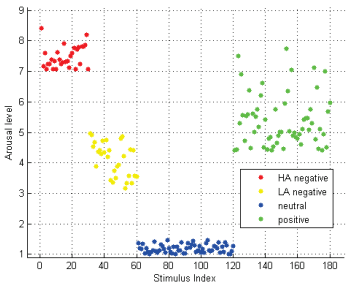

Figure 1: Emotional categorization of pictures. Arousal level is defined on a continuous scale ranging from 1 (calm state) to 9 (excited state).

A classification framework is then set to decode mental state associated to the elicited emotion. Multivariate analysis combines information from different channels. This approach makes it possible to cancel out noise and thereby to enhance the brain signals of interest with higher sensitivity and specificity. A new spatial filtering is proposed to enhance one type of emotional images versus the rest. Once the EEG signals have been filtered, a feature selection technique is employed to keep the most discriminative temporal intervals. Finally, a single-trial classification is performed with a shrinkage linear discriminant analysis. The classifier's performances were evaluated for each participant by a leave-one-participant-out cross-validation method and the results were averaged across participants.

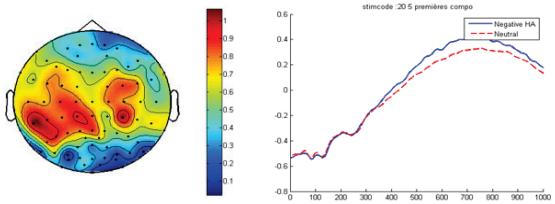

Figure 2: Spatial pattern associated with the P30 component.

It can be observed from fig. 2 left that, the first activation pattern is principally located in centro-parietal regions. Furthermore event-related potential grand-average (fig. 2 right) is well in accordance with the literature regarding to the peak latency of the late-positive-potential (LPP) between 500 and 900ms after stimulus onset. A mean classification accuracy of 87% was obtained when classifying arousal at fixed valence. Lower performances were obtained when attempting to classify either valence or valence at fixed arousal.

The classification methodology described in this work has been explored in emotion recognition applications. It can also be used to deal with other EEG-based ERP paradigms, like P300 spellers or vigilance estimation. Fusion of other EEG features or other physiological signals may improve the recognition rate in the future. Discrepancies between young and older subjects will also be studied.

Related Publications:
[1] N. Mathieu, S. Bonnet, S. Harquel, E. Gentaz, A. Campagne, "Single-trial ERP classification of emotional processing", In 6th International IEEE EMBS Conference on Neural Engineering NER-2013.
[2] N. Mathieu, E. Gentaz, S. Harquel, L. Vercueil, S. Bonnet, R. Guillemaud, M. Ida, A. Campagne, "Brain processing of emotional scenes with age: Effect of arousal context", submitted to Neuropsychologia, 2014.

Classification of covariance matrices using a Riemannian-based kernel for BCI applications

Research topics: BCI, EEG, signal processing, classification

A. Barachant, S. Bonnet

ABSTRACT: This paper presents the use of spatial covariance matrix as a feature for motor imagery EEG-based classification in brain–computer interface (BCI) applications. A new kernel is derived by establishing a connection with the Riemannian geometry of symmetric positive definite matrices. Different kernels are tested, in combination with support vector machines, on a past BCI competition dataset. We demonstrate that this new approach outperforms significantly state of the art results, effectively replacing the traditional spatial filtering approach. This framework can be applied in other BCI paradigms.

Brain-Computer Interfaces (BCIs) based on motor imagery (MI) have been well studied in the literature. For this type of BCI, movements are imagined by the subjects, inducing the activation of dedicated cortical areas in given frequency bands. This approach is well suited for asynchronous BCI applications since the user can potentially perform actions without any stimulus from the exterior world. The standard approach in MI-based EEG signal classification is to perform bandpass frequency filtering, spatial filtering and linear classification.

The aim of this work is to provide a way to take into account the Riemannian geometry for EEG signal classification. This approach has been successfully applied in the past on radar signal processing and image processing. Sample covariance matrices are handled by considering the curvature of the space of Symmetric Positive Definite (SPD) matrices, for which tractable computations can be done.

Furthermore, an original kernel is derived by establishing a connection with the Riemannian geometry of SPD matrices.

This kernel is tested in combination with a support vector machine (SVM). Encouraging results are presented that demonstrate the potential benefit of the approach. Another advantage of the presented method is that it can directly be applied without the need for spatial filtering.

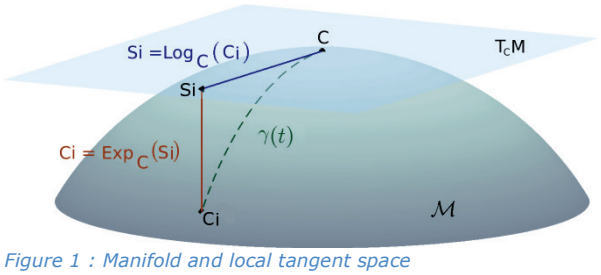

Figure 1 : Manifold and local tangent space

If one is interested in using a covariance matrix $\mathbf{C}$ as a feature in a classifier, a natural choice consists in vectorizing it in order to process this quantity as a vector and then use any vector-based classification algorithms. Due to symmetry, we introduce the modified half-vectorization operator that stacks, with appropriate weighting, the upper triangular part of $\mathbf{C} \in P(E)$ into a $E(E+1)/2$ column vector $\mathrm{vect}(\mathbf{C})$.

The direct vectorization of these matrices do not take into account the relationships that link between them the coefficients of the SPD matrices. The proposed Riemannian kernel (see fig.1) is given by $k_R\left(\mathrm{vect}(\mathbf{C}_i), \mathrm{vect}(\mathbf{C}_j)\right) = \langle \phi(\mathbf{C}_i), \phi(\mathbf{C}_j) \rangle_{\mathbf{C}_{\mathrm{ref}}}$ with $\phi(\mathbf{C}) = \mathrm{Log}_{\mathbf{C}_{\mathrm{ref}}} \mathbf{C}$. See [2] for details.

This kernel can be easily integrated into any kernel-based classification algorithms, like SVM. The reference SPD matrix $\mathbf{C}_{\mathrm{ref}}$ is usually set to the Riemannian-based mean of all covariance matrices. We further have proposed an adaptive update of this reference point in order to deal with EEG non-stationarities intra- or inter-sessions.

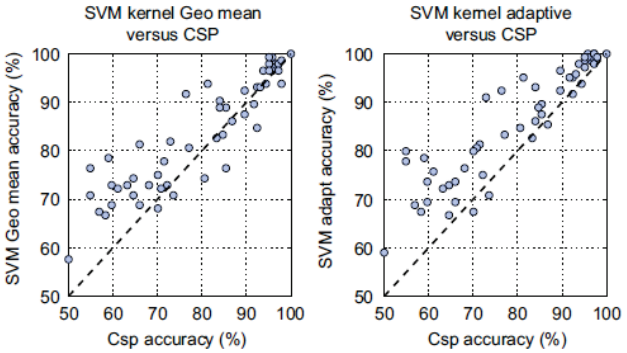

Figure 2 : Comparison between CSP (common spatial patterns) and proposed kernel-based SVM method on individual sessions. Each dot is a binary classification experiment.

It can be seen from fig. 2 that, except for few localized pairs of mental tasks, the proposed algorithm consistently outperforms the state-of-the-art classification results. This remark is especially true for difficult binary classification cases (CSP performance below 80%) where the improvement brought by kernel-based SVM is significant.

The classification methodology described in this work has been explored in motor imagery BCI applications. It is both efficient and natural with respect to the underlying space geometry. It can also be used to deal with other EEG-based BCI paradigms, like P300 spellers, and more generally it can be used in any multivariate signal acquisition technique. Information geometry is indeed a very powerful and intuitive way to handle classification problems and its impact should become important in the future.

Related Publications:
[1] A. Barachant, S. Bonnet, M. Congedo, C. Jutten, "Common spatial pattern revisited by Riemannian geometry", IEEE International Workshop on Multimedia Signal Processing (MMSP) 2010.
[2] A. Barachant, S. Bonnet, M. Congedo, C. Jutten, "Classification of covariance matrices using a Riemannian-based kernel for BCI applications", Neurocomputing 112 (2013) 172-178.
[3] A. Barachant, S. Bonnet, M. Congedo, C. Jutten, "Multiclass brain–computer interface classification by Riemannian geometry", IEEE Trans. Biomed. Eng. 59 (April (4)) (2012) 920–928.

Selective ENG recording with a polymer-based multi-contact cuff electrode

Research topics: ENG, electrode design, neural signal characterization

S. Bonnet, C. Rubeck, A. Bourgerette, O. Fuchs, S. Gharbi, F. Baleras, F. Bottausci, C. Pudda, M. Cochet, V. Agache, F. Sauter-Starace, S. Maubert

ABSTRACT: This paper presents the design, microfabrication, characterization and experimental validation of a 6-contact cuff electrode embedded in a parylene-based flexible support. This type of electrode is well suited for both peripheral nerve recording and stimulation and offers improved spatial selectivity as compared to conventional ring electrodes. Both measured and modeled impedance spectra are compared. An experimental validation is performed on an earthworm. Single fiber action potentials, are discriminated on the 6 contacts. Spontaneous activity is also recorded with burst of spikes.

Electroneurogram (ENG) data are often acquired using cuff electrodes that on one hand isolates the nerve from the surrounding tissues and on the other hand records at metallic contacts extracellular potentials produced by inside-nerve activity. Contacts can be arranged in rings or in small contacts distributed around the section of the nerve. Several challenges arise in ENG recording due to very small amplitude ENG potentials (few microvolts) that can be easily be buried into electrode noise, electronics noise and interferences arising from muscular activity. Small contacts could improve the recording selectivity and record the activity of few fascicles. This could open the way of triggering external devices (like stimulator or functional electric system) by using natural signals.

The aim of this work is to design and validate on an earthworm experiment a multi-contact cuff (MCC) recording electrode with 18 contacts. The microelectrode patterned onto a flexible parylene carrier is interfaced with an assembled acquisition chain comprising a preamplifier, an amplifier and an analogic to digital conversion stage. Single-metal-layer parylene C-based electrode arrays are fabricated using microfabrication techniques. In order to form the electrodes onto the parylene, a metallic bi-layer made of Pt (~ 50-200nm) is patterned by a lift-off process onto a 20nm thick adhesive titanium layer. The MCC electrode is then glued to the inner side of a customized silicone cuff and also to an Omnectics connector. The cuff total length was 11mm while the inner diameter was 1.7mm. Each contact has an exposed surface of 0.72mm². In-vitro impedance characterizations of the MCC were performed with an impedance of 3kΩ at 1kHz (20mVpp). Both measured and modeled impedance spectra were compared and fitted well (not shown).

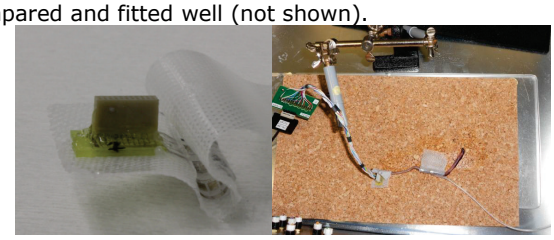

Figure 1: (left) The cuff electrode. (right) The 6-contact MCC recording electrode is located on the left of the worm while the stimulation ring electrode is on the right.

The MCC electrode is used in an earthworm experiment (fig. 1). Indeed this animal model is well suited to validate a MCC design in terms of dimensions (diameter up to few millimeters). Furthermore, only one median giant fiber (MGF) and two lateral giant fibers (LGF) are present in the earthworm with different conduction velocities. It is thus reasonable to consider the earthworm as a peripheral nerve with only 2 fibers. Our experimental setup consists in eliciting neural activity at one extremity of the worm and recording at the other activity the traveling action potential (AP). A low-noise common-reference preamplifier was located close to the MCC for signal amplification (gain 10x, bandwidth [DC-50kHz], input-referred voltage noise: less than 2µVrms in [1Hz-5kHz]). The 6 monopolar signals are then amplified using a second amplifier (gain 1,000x, bandwidth [1-5kHz]) and digitized at 20kHz using the NeuroPXI system from LETI.

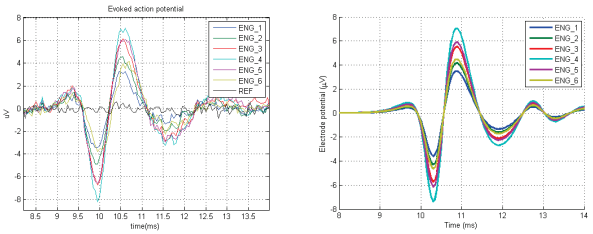

Figure 2: (left) Recorded average Single fiber action potentials (SFAPs), for the different MCC contacts. The reference contact is also shown for control. (right) Simulated SFAP obtained by coupling 1D biological model and 3D electrocinetical model.

It can be seen from fig. 2 left, that, each contact, i.e. each curve, was able to measure an elicited single fiber AP with different amplitude. This can be partly attributed to the geometrical arrangement, as it can be observed in fig. 2 right with predicted potentials at the surface of the nerve (FEM modeling done in COMSOL Multiphysics™). Thanks to this selectivity, inverse problem will be investigated in the future in order to locate the electrical activity inside a nerve from multi-channel ENG.

Related Publications:
[1] S. Bonnet, C. Rubeck, V. Agache, A. Bourgerette, O. Fuchs, S. Gharbi, F. Sauter-Starace, P. Maciejasz, J.L. Divoux, N. Bourquin, C. Henry, S. Maubert, "Selective ENG recordings using a multi-contact cuff electrode", IEEE International Neural Engineering conference (NER) 2013.
[2] S. Bonnet, J.F. Bêche, S. Gharbi et al., "NeuroPXI: A real-time multi-electrode array system for recording, processing and stimulation of neural networks and the control of high-resolution neural implants for rehabilitation", IRBM, vol. 33, pp. 55-60, 2012

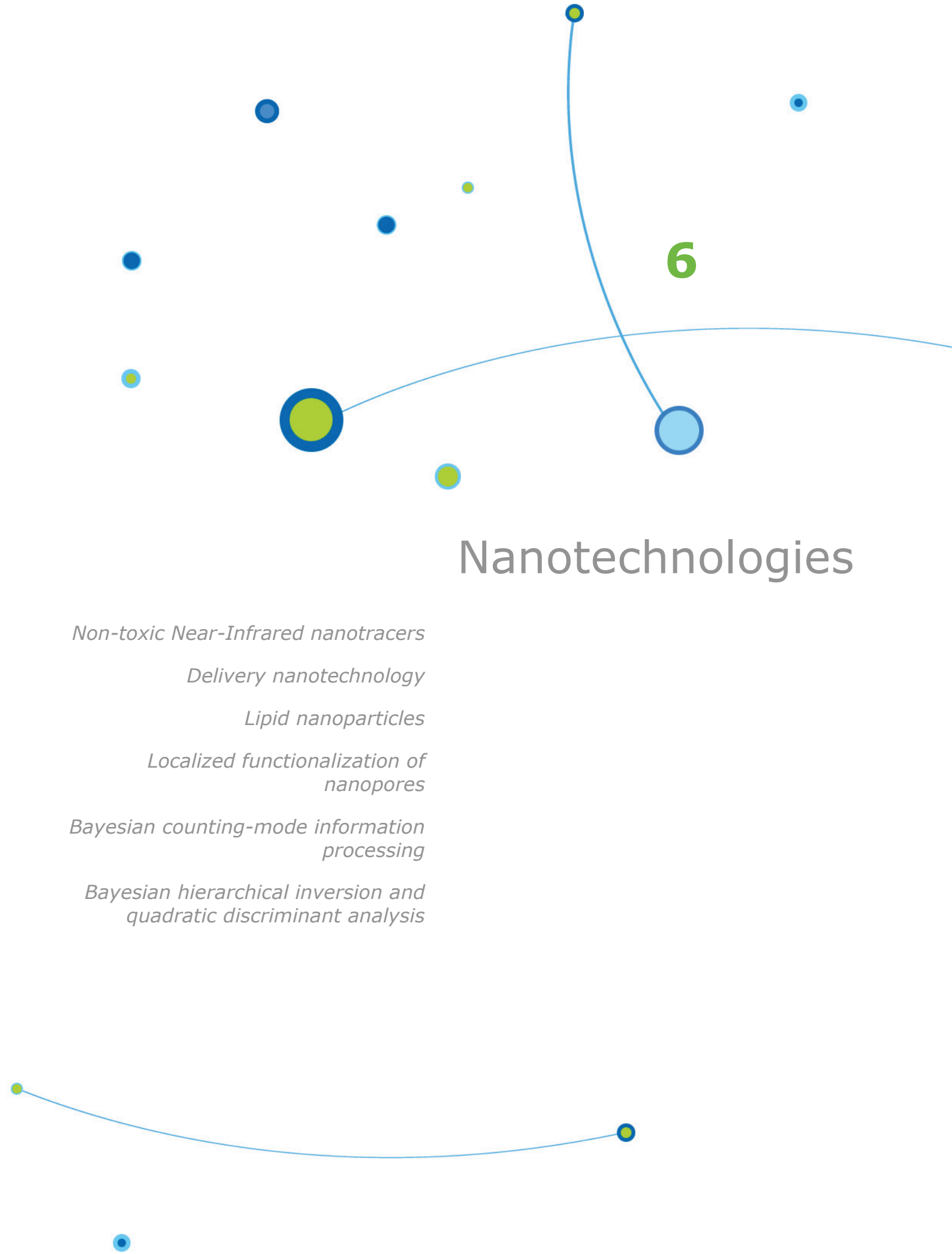

6

Nanotechnologies

Non-toxic Near-Infrared nanotracers

Delivery nanotechnology

Lipid nanoparticles

Localized functionalization of nanopores

Bayesian counting-mode information processing

Bayesian hierarchical inversion and quadratic discriminant analysis

LipImage™ 815, non-toxic near-infrared nanotracers for sensitive imaging: demonstration in rodents and dogs

Research topics: Molecular imaging, lipid nanoparticles, diagnostics

A. Jacquart, E. Heinrich, J. Boutet, A.-C. Couffin, F. Navarro, I. Texier-Nogues, R. Boisgard (CEA, DSV-SHFJ), J.-L. Coll (INSERM, UJF), F. Ponce (Vetagro Sup Lyon)

ABSTRACT: LipImage™ 815, lipid nanoparticles encapsulating a near infrared dye, constitute outstanding fluorescent nanotracers for sensitive in vivo imaging. Their optical properties have been optimized to respond to in-depth tissue imaging. Their high colloidal stability and their manufacturing process ensure they respond to industrialization and commercialization needs. Their harmlessness and imaging efficiency in rodent and non rodent models, as required by regulatory affairs, have been demonstrated.

Lipid nanoparticles encapsulating a near-infrared dye emitting at 815 nm, wavelength for which in-depth tissue imaging can be performed, have been developed.
We demonstrated that the new tracers display suitable properties for in vivo imaging and safe use [1].
- Physico-chemical properties:
The nanotracers display a diameter of 50 ± 2 nm, with a low polydispersity index (0.13 ± 0.02), and a nearly neutral surface charge (zeta potential of -2.5 ± 0.5 mV). Their synthesis is highly reproducible and well mastered. Colloidal suspensions are very stable (> 6 months), which is compatible with the necessary time for commercial distribution and use of diagnostic products.
- Optical properties:
The nanotracers absorb and emit in the near infrared range (793/815 nm), for which a few cm depth imaging in tissues can be performed. Interestingly, the fluorescence quantum yield reflecting the tracer brightness and efficiency is high in aqueous suspension (0.08 ± 0.01) and stable with time.
- Toxicity study:
The potential adverse effects of the nanotracers were looked for in a rodent (rat) and a non-rodent (dog) animal model, as required for regulatory toxicity studies. For this purpose, high doses of nanotracers (30 times the dose necessary for imaging in rat, 1, 5 and 10 times the dose necessary for imaging in dog) were injected intravenously and animal blood parameters were followed. In the animal models and for the tested injected doses, no modification of blood parameters (hepatic enzymes, cell content) have been observed for 14 days (end of the study).
The ability to perform in vivo imaging with the new nanotracers was further explored in healthy mice and dogs, and tumor-bearing mice. In both mice and dogs, the biodistribution of the nanotracers was identical (Fig. 1).
The nanoparticles are uptaken by the liver, organ involved in the lipid metabolism, and cleared by the hepatobiliary pathway (inducing fluorescent signal in the intestine) with a minimal clearance by the renal pathway for dogs (intermediate signal in kidneys). No signal is observed in spleen, as well as heart, brain and lungs (analyzed post-mortem). As previously observed [2], lymph nodes also appear to efficiently retain the fluorescent tracers, probably because of their nanometric size and their lipid nature.

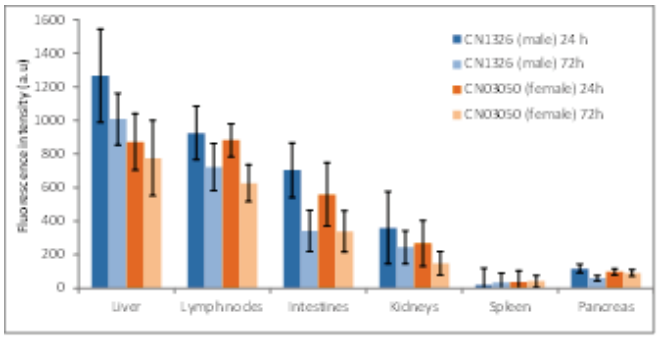

Figure 1: Fluorescence biodistribution in dogs at 24h and 72h post-injection.

The efficient uptake of the nanoparticles in tumor xenografted in mice was then demonstrated. Fig. 2 evidences that following IV injection of the nanotracers in PC3 (human prostate cancer cells) bearing mice, intense and prolonged fluorescence tumor labeling is obtained.

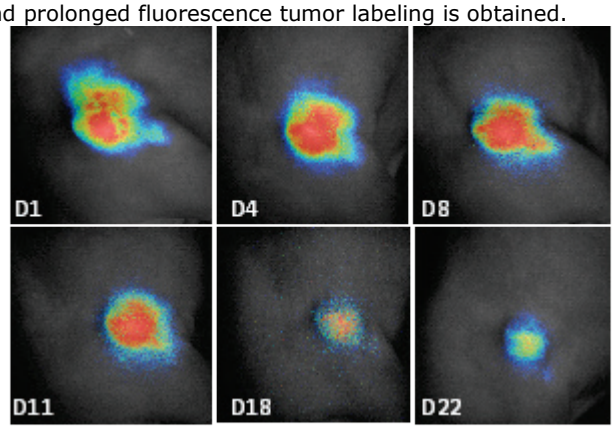

Figure 2: Prolonged tumor labeling 1, 4, 8, 11, 18 and 22 days after LipImage™815 injection.

In conclusion, this new nanotracer, named LipImage™ 815, presents all the characteristics for an efficient and sensitive fluorescent contrast agent dedicated to clinical applications. Next development steps will be dedicated to its scale-up production in GMP conditions to prepare clinical trials.

Related Publications:
[1] A. Jacquart, M. Kéramidas, J. Vollaire, R. Boisgard, G. Pottier, E. Rustique, F. Mittler, F.P. Navarro, J. Boutet, J. L. Coll, I. Texier, "LipImage™ 815: novel dye-loaded lipid nanoparticles for long-term and sensitive in vivo near-infrared fluorescence imaging", Journal of Biomedical Optics 18 (2013) 101311.
[2] F. Navarro, M. Berger, S. Guillermet, V. Josserand, L. Guyon, M. Goutayer, E. Neumann, P. Rizo, F. Vinet, I. Texier, "Lipid nanoparticle vectorization of IndoCyanin Green improves non-invasive fluorescence imaging", Journal of Biomedical Nanotechnology 8 (2012) 730-741.

Delivery nanotechnology for biologicals

Research topics: siRNA, cationic lipid nanoparticles, interference RNA, transfection

J. Bruniaux, I. Texier, M. Menneteau, F. Navarro, (iRTSV Biomics: E.Sulpice, F.Mittler, X.Gidrol)

ABSTRACT: The small interfering RNA (siRNA) shows a specific and effective gene silencing activity through a sequence specific down-regulation of the complementary messenger RNA (interference RNA) in cytoplasm. In this way, interference RNA has emerged as a potent tool to study gene functions for the identification of new biomarkers and/or therapeutic targets. Because of its vulnerability in biological media and its limitations to penetrate across biological barriers, we have recently designed novel cationic lipid nanocarriers for intracellular delivery of small RNAs and use them for RNAi high throughput screening (HTS) purposes.

SiRNA are double-stranded RNA from 19 to 23 nucleotides, enabling effective gene silencing activity through a sequence specific down-regulation of the complementary messenger RNA. Since the discovery of this mechanism, many efforts have been made to broaden perspectives of siRNA in research and clinical work. Naked siRNA are highly sensitive to the degradation enzymes (nucleases) and do not cross the cell membrane due to its large molecular weight (13kDa) and its anionic nature. Thus, delivery systems are highly required to facilitate its distribution to its intracellular sites of action.

Here, multifunctional lipid nanoparticles comprising an imaging contrast agent are emerging as an original and promising approach in the monitored delivery of siRNA. Previously, we have designed lipid nanoemulsions, named Lipidot, entrapping lipophilic cyanine derivatives for in vitro fluorescence imaging purposes [1], as a biocompatible alternative of the well-known quantum dots [2]. Recently, we have adapted the formulation for siRNA delivery purpose by incorporating some cationic compounds (Figure 1).

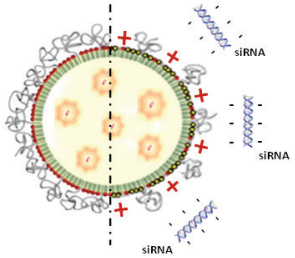

Figure 1: structure of lipid nanoemulsions, namely Lipidots®, before (left) and after (right) incorporation of cationic compounds.

Novel cationic formulations present a high colloidal stability in storage buffer and in biological media, and they are well tolerated by cells in culture. Moreover, their cationic compounds onto the shell confer them the ability to interact through electrostatic bounds with negative charge of siRNA, as demonstrated by gel retardation assay (Figure 2).

Furthermore, siRNA-lipid particle complexes were quickly taken up by cells, as evidenced by Figure 3 through flow cytometry (FC) experiments where most prostate cells were highly positive to green fluorescent siRNA (FITC channel) and red fluorescent lipid particles (APC channel).

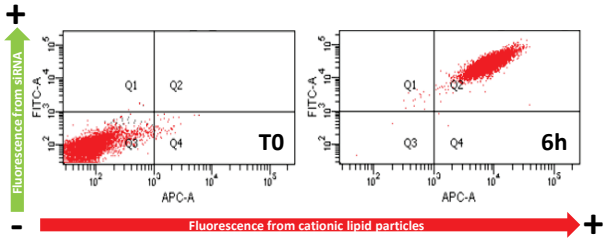

Figure 3: FC analysis of prostate cells incubated 6 h in presence of siRNA/ lipid particle complexes.

Using cell model overexpressing the green fluorescent protein (GFP), we have demonstrated that siRNA/ lipid particle complexes induce a significant inhibition of the targeted GFP expression, characterized by a reduction of green fluorescence emitting from cells (Figure 4).

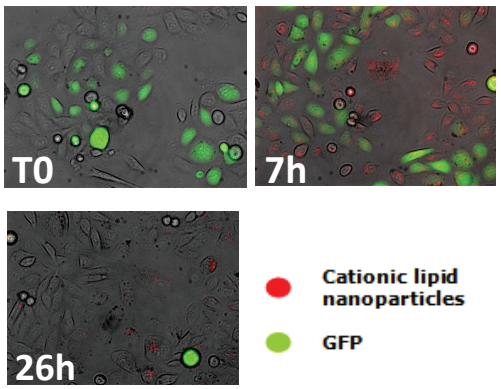

Figure 4: fluorescence imaging of cells overexpressing GFP (T0), after internalization of Lipidot/siRNA complexes (red fluorescence) (7h) and after specific down-regulation of GFP (26h)

Next steps will be dedicated to:

- the performance evaluation of these cationic particles to transfect cells recognized as hard to transfect such as primary cells, neuronal cells,
- the surface functionalization of these particles to improve their internalization,
- their use as innovative tool for RNAi HTS where thousands RNAi should be studied in parallel.

Related Publications:
[1] J. Gravier, F.P. Navarro, T. Delmas, F. Mittler, A.C. Couffin, F. Vinet and I. Texier, Journal of Biomedical Optics 16(9) 2011
[2] F. Navarro, F. Mittler, M. Berger, V. Josserand, J. Gravier, F. Vinet and I. Texier, Journal of Biomedical Nanotechnology 8 2012

Lipid nanoparticles for protein-based antigens delivery

Research topics: Antigen delivery, lipid nanoparticles, immunization, nanotechnology

T. Courant, A. Hoang, I. Texier-Nogues, F. Navarro, H.-L. Reynault (Institut Albert Bonniot), C. Villiers (Institut Albert Bonniot), P. Marche (Institut Albert Bonniot)

ABSTRACT: Nanotechnology presents a great potential for applications in the vaccine field through the controlled manufacturing of synthetic vectors of antigens in the size range of virus. Here, we have developed an original vaccine formulation based-on the grafting of protein antigens onto the surface of lipid nanoemulsions (Lipidots®). These antigens-bearing particles are stable several months at 4°C with marginal protein release over this period. They are very well tolerated *in vitro* and enable the enhancement of the immune responses in mice model using ovalbumin as antigen.

In the near future, novel vaccines are highly anticipated due to the evolution of the society with the increase of elderly and their ageing immune system, the increase of multi-drug resistant strains of pathogens, and also the global warming with the associated spread of tropical diseases in new locations. In parallel, nanotechnology is an emerging field which opens new avenues in medicine for developing innovative diagnosis and/or therapies. In particular, nanoparticles-based vaccine formulations may fight against the spread of infectious diseases where the pathogen is located into the intracellular compartment in host cells or against cancers where a cellular immunity is likely more adapted for reducing tumor growth and metastasis. Moreover, nanoparticles offer the possibilities to combine into the same carrier several kinds of molecules as contrast agents, drugs, proteins, immunomodulatory molecules or antigens. Various examples of protein association to particles can be found in literature. However, the described carriers have several significant drawbacks in terms of colloidal stability and release profile of proteins, reducing thus their ability to induce relevant immune responses.
Here, we have designed a new technology, based on very stable lipid nanoparticles previously described [1, 2], to vectorize protein antigens with lipid nanoparticles. To overcome release issues, we have covalently grafted protein antigens onto particle surface (Figure 1) and demonstrated that resulting particles are highly stable over time and safe.

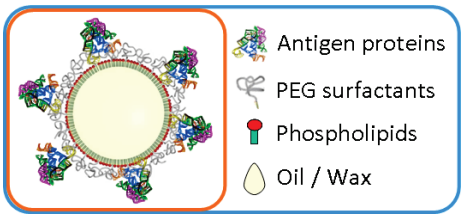

Figure 1: Structure of antigen-bearing lipid nanoparticles

As antigen model, we use ovalbumin, a medium-size protein (~45 kDa), which has been efficiently grafted onto particles, as evidenced by fluorescence measurements and protein bicinchoninic acid titration (coupling yields > 60 %).

Unbounded proteins were efficiently removed by gel filtration chromatography. Ovalbumin content of the lipid nanoparticles can be tuned from several decades up to 400 proteins per particle, leading thus to a maximum loading of 2.9 ± 0.2 % (m/m).

Different formulations of ovalbumin-bearing lipid nanoparticles have been tested for *in vivo* immunizations in mice. We have demonstrated that administration of such particle formulations considerably potentialize the induction of humoral immune response, characterized by a strong enhancement of specific antibodies quantities in blood (**Figure 2**).

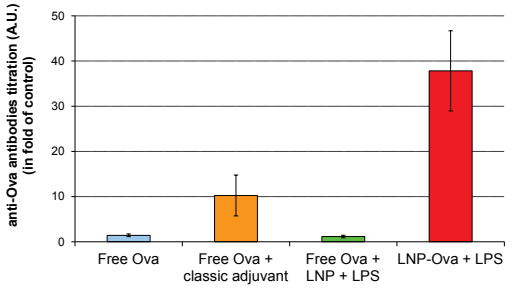

Figure 2: Humoral response after immunization protocol with Ova-LNP in mice. OVA has been injected: as free antigens (in blue), or with the complete Freund adjuvant (classical adjuvant) (in orange) or with ungrafted lipid particles and lipopolysaccharides (LPS) (in green) or grafted onto lipid nanoparticles in addition of LPS solution (in red)

Moreover, levels of IFNγ cytokine which are secreted by collected splenocytes from mice having received particle-based immunization protocol are highly more important, indicating thus the induction of a cellular immunity.
Further experiments are on-going to better characterize the nature of immune responses induced by antigen-bearing lipid particles. At last, these novel antigen formulations will be tested using relevant antigens in appropriate animal models.
These results pave the way to new immunization strategies by using lipid nanoparticles as innovative adjuvant delivery system.

Related Publications:
[1] F. Navarro, M. Berger, S. Guillermet, V. Josserand, L. Guyon, M. Goutayer, E. Neumann, P. Rizo, F. Vinet, I. Texier, I., "Lipid nanoparticle vectorization of IndoCyanin Green improves non-invasive fluorescence imaging", Journal of Biomedical Nanotechnology 2012, 8 (5), 730-741
[2] A. Jacquart, M. Kéramidas, J. Vollaire, R. Boisgard, G. Pottier, E. Rustique, F. Mittler, F.P. Navarro, J. Boutet, J.L. Coll, I. Texier, "LipImage™ 815: novel dye-loaded lipid nanoparticles for long-term and sensitive in vivo near-infrared fluorescence imaging", Journal of Biomedical Optics 2013, 18 (10), 101311.

Localized functionalization of nanopores for biochemical sensing

Research topics: Surface chemistry, biosensing, nanopore.

G. Nonglaton, E. Grinenval, C. Fontelaye, G. Costa, F. Vinet, P. Furjes (MFA, Hungary),
R. E. Gyurcsanyi (BME, Hungary)

ABSTRACT: A process of localized functionalization of nanopores was developed and tested for the fast and label-free detection of molecules of biological interest.

The label-free detection using chemically modified nanopores is an emerging research field. Since 10-15 years, the potential use of nanopores for ultrafast DNA sequencing was a major boost. Nanopore technique is a promising way for very low concentrated molecule sensing. It has been developed from biological nanopore to solid-state nanopore and has a unique property to electrically detect single molecule (Fig.1).

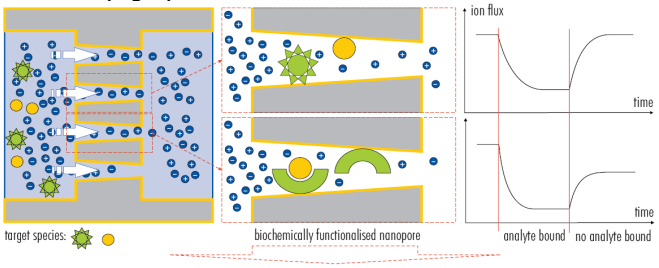

Figure 1: Chemically-modified nanopores for sensing

Indeed, biological molecules are electrokinetically driven through a nanopore by an externally applied electric field. This results in a characteristic obstruction of the ionic current across the pore. When the nanopore is functionalized with bioreceptors, information on interactions with biomolecules can be extracted. To ensure the most sensitive detection to a biomarker, an anti-fouling layer should coat the outer surface of the nanopore while the coupling chemistry to immobilize bioreceptors is deposited inside the cavity. In this study, different organosilane based coatings were evaluated for antifouling or bioreceptors grafting. Coatings were characterized by static contact angle, streaming-current zeta potential measurements, Surface-Enhanced Ellipsometric Contrast optical technique (SEEC), and fluorescence imaging. Effects of activation and functionalization processes on SiO2 and SiNx membranes were studied and characterized by Atomic Force Microscopy (AFM). As a proof of concept, the surfaces were chemically pattern by lithography technique to demonstrate the compatibility between antifouling chemistry and grafting chemistry [1]. Then a process was developed allowing to sequentially functionalize the outer surface, and then after drilling, the inner surface of nanopores (Fig.2).

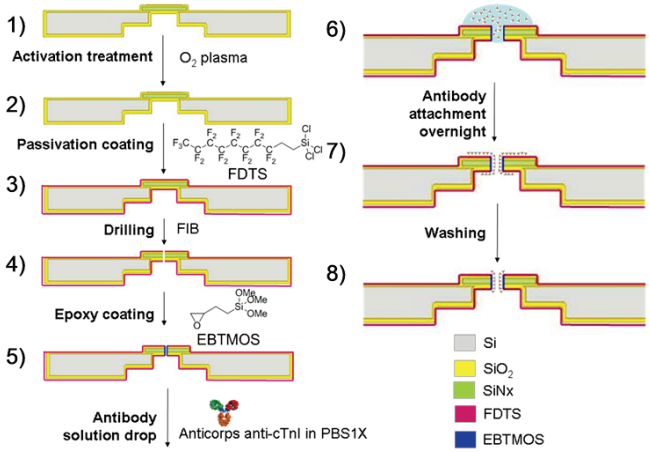

Figure 2: Functionalization process

The antibody immobilization was demonstrated by fluorescence imaging (Fig.3) and characterized by Scanning Electronic Microscopy (SEM).

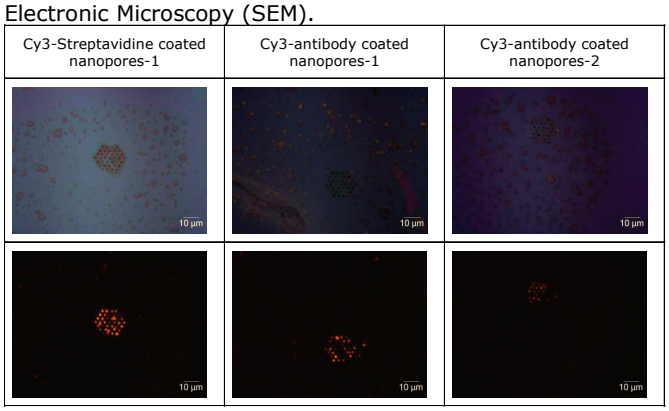

Figure 3: Characterization by fluorescence

The preliminary tests are very promising and show that while the control probes practically do not bind cTnI in the nanopores, in the antibody modified nanopores the cTnI binding causes a significant decrease in the trans-pore ion flux. The first results indicate a 10ng/mL cardiac Troponin I (cTnI) detection [2].

Related Publications:
[1] E. Grinenval, G. Nonglaton, F. Vinet, "Spatially controlled immobilisation of biomolecules: A complete approach in green chemistry" Appl. Surf. Sci., vol. 289, no. 0, pp. 571-580, January 2014.
[2] G. Nonglaton, E. Grinenval, P. Fürjes, R.E. Gyurcsanyi, "Localized functionalization of nanopores for biochemical sensing" International Conference on Solid Surface, Paris, September 2013.

Bayesian counting-mode information processing applied to multi-mode NEMS Mass Spectrometry

Research topics: Statistical signal processing, nanotechnologies, biotechnologies

R. Pérenon, P. Grangeat, A. Mohammad-Djafari (LSS UMR 8506 CNRS),
E. Sage (Leti µDEVICES), L. Duraffourg (Leti µDEVICES), S. Hentz (Leti µDEVICES),
A. Brenac (CEA-INAC), R. Morel (CEA-INAC).

ABSTRACT: This work focuses on an information processing method adapted to NEMS Mass spectrometry. NEMS (Nano-ElectroMechanical Systems) are sensitive enough to detect a single molecule. Thus, it is possible to estimate a concentration profile in a counting-mode which brings a reduced noise and a higher sensitivity. Information processing to build a mass spectrum according to this technology combines three operations, to detect incident molecules, to quantify their masses and to count the molecules.

Mass spectrometry is a science which aims at estimating the mass profile of a given solution. One current application of mass spectrometry is proteomic, entailing the identification and the quantification of proteins, e.g. in order to detect cancers in the early stage.

NEMS are new generation sensors which offer high mass sensitivity. A flow of molecules is oriented toward the sensor. Molecules land sequentially on the sensor according to an adsorption principle. The adsorption generates a sharp change in resonant frequency, depending on the mass of the molecule and the adsorption location (landing position). This sensor resonant frequency is tracked by an electronic Phase-Lock Loop. To handle the indetermination between the mass and the position of the molecule, resonant frequencies are observed on numerous vibration modes. The resulting signals are smooth ones with fast decreasing steps, each step size being related to the mass and the landing position of the adsorbed molecule.
CEA-Leti µDEVICES teams develop this new technology in collaboration with Caltech. In association with CEA/INAC, a platform for acquiring experimental data has been created.

We model the acquisition system through a Bayesian model, as described in Fig. 1. This model links to the observed signal the unknown parameters: N (the number of adsorbed molecules) and t, m and z (respectively adsorption time, adsorbed mass and landing position for each molecule).

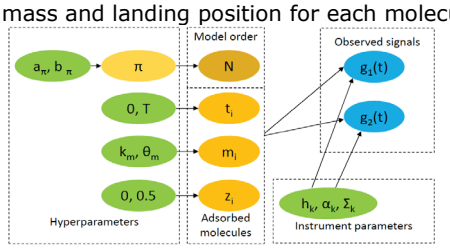

Figure 1: Bayesian hierarchical model of the acquisition system for 2 observed harmonic signals g_1 and g_2.

To process the system output signal and so to estimate the mass of each individual molecule, we propose to use a Bayesian model choice algorithm, inspired by impulse deconvolution Bayesian method described in [1,2]. This algorithm relies on the Reversible-Jumps Monte-Carlo Markov Chain algorithm [2, 3].

We compare the results in terms of detection capability on simulated data, as given in Fig. 2.

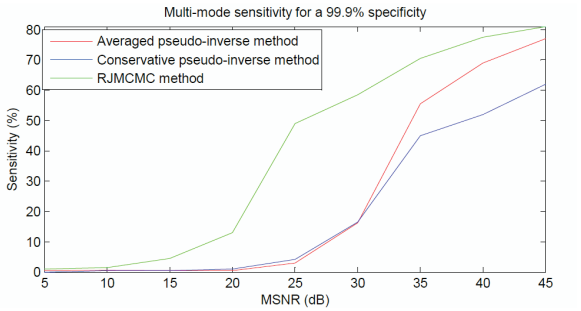

Figure 2: Comparison of detection capabilities of the Bayesian model choice and pseudo-inverse algorithm.

For a given specificity, our Bayesian algorithm offers higher sensitivity than pseudo-inverse ones.
We also test our method on Tantalum nano-aggregates experimental data. The nominal diameter given by a Time of Flight Mass Spectrometer is 6.5 nm. Fig. 3 illustrates the experimental signals (in blue) for the 2 harmonics and the estimated frequency changes (red arrows).

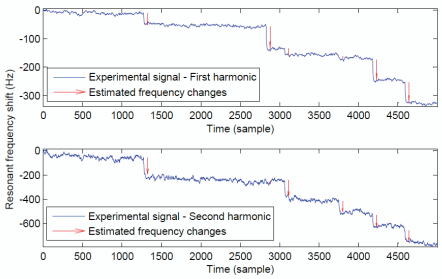

Figure 3: Detection of frequency changes (red arrows) on 2 observed harmonic signals g_1 and g_2 (in blue) on Tantalum nano-aggregates experimental data.

The mean of estimated diameters is 6.53 nm, which is very close from the Time of Flight estimation.
Further work includes speeding-up the computing in order to process more molecules with a higher counting rate.

Related Publications:
[1] R. Pérenon, A. Mohammad-Djafari, E. Sage, L. Duraffourg, S. Hentz, A. Brenac, R. Morel, P. Grangeat. (2013), "MCMC-Based bayesian estimation algorithm dedicated to NEMS Mass Spectrometry", 32nd International Workshop on Bayesian Inference and Maximum Entropy Methods in Science Engineering, Garching near Münich, Germany, 15 - 20 July 2012, AIP Conference Proceedings, Vol. 1553, 46-53.
[2] R. Pérenon (2013), Traitement de l'information en mode comptage appliqué aux détecteurs spectrométriques, Grenoble University Ph.D. Thesis.
[3] R. Pérenon, E. Sage, A. Mohammad-Djafari, L. Duraffourg, S. Hentz, A. Brenac, R. Morel, P. Grangeat (2013), "Bayesian Inversion of Multi-Mode NEMS Mass Spectrometry Signal", 21st European Signal Processing Conference 2013 (EUSIPCO 2013), Marrakech, Morocco.

Bayesian Hierarchical Inversion and Quadratic Discriminant Analysis for protein biomarkers evaluation by mass spectrometry

Research topics: Statistical signal processing, inverse problem, in-vitro diagnosis

L. Gerfault, P. Szacherski, J.-F. Giovannelli (IMS, Univ. Bordeaux), A. Giremus (IMS), P. Mahe (bioMérieux), A. Klich (HCL, Service de Biostatistique, Univ. Lyon I), C. Mercier (HCL), P. Roy (HCL), J.-P. Charrier (bioMérieux), B. Lacroix (bioMérieux), P. Grangeat

ABSTRACT: As an example of LC-MS-MRM data processing, we compare the protein quantification and serum sample classification performances of an automated Bayesian Hierarchical Inversion method developed on the BHI-PRO project and a supervised Non-Linear Processing one, both associated with a quadratic discriminant analysis. Evaluation is carried on a colorectal cancer research cohort, including 170 patients, using LFABP and PDI proteins as biomarker candidates.

Quantification and classification are key points for differential analysis of proteomic studies and diagnostic tests [1,2]. High resolution analytical chains combining Liquid Chromatography and Mass Spectrometry (LC-MS) in Multiple Reaction Monitoring (MRM) mode are foreseen as multiplex quantification platform for reliable diagnosis. Key questions are how to infer protein concentration and class label (case/control) from large, noisy measurements [2].

To replace an operator-supervised Non-Linear Processing (NLP), we have developed on the BHI-PRO project (ANR 2010 BLAN 0313) a Bayesian Hierarchical Inversion (BHI) method. A LC-MS-MRM analytical chain is a cascade of molecular events depicted by a graph structure, each node being associated to a molecular state such as protein, peptide or fragment, each branch to a molecular processing. Each protein is linked to a set of transitions. BHI estimation delivers automatically protein concentration, taking into account AQUA labelled peptides and control quality samples [1,2]. For NLP, an operator-supervised selection of peak position is achieved and transition value is computed from the ratio between native and labeled transition peak area. Then, the median over all transition values is assigned as protein concentration. In both cases, classification is achieved using Quadratic Discriminant Analysis.

We have selected LFABP and PDI proteins out of a list of biomarker candidates issued from a first colorectal cancer research cohort. Quantification and classification performances are evaluated on a second colorectal cancer cohort which includes 72 control cases and 98 colorectal cancer cases starting from grade 1 up to grade 4 [1-3]. MRM acquisitions have been achieved using an AB Sciex QT5500 Triple Quadripole mass spectrometer in MRM mode. For LFABP, 8 transitions and 3 peptides have been considered, and for PDI, 3 transitions and 1 peptide.

For quantification, we observe on figure 1 a good agreement between both methods, for both LFABP and PDI proteins. For LFABP, we get also a good correlation with ELISA measurement. For classification, the ROC curve on figure 2 demonstrates nearly the same performances. The ROC curve region associated with high specificity, typically 0.95, is the most important for screening method.

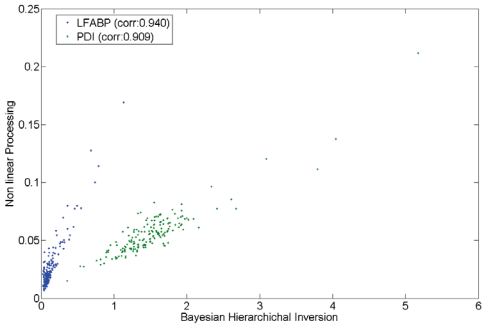

Figure 1: correlation between quantification values obtained by the NLP and BHI methods

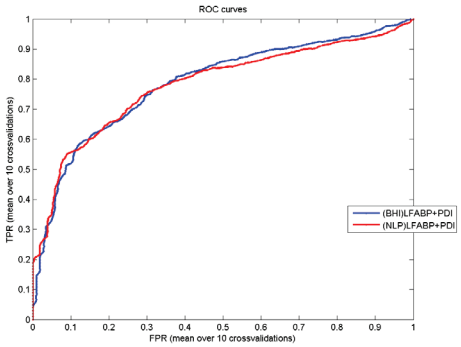

Figure 2: mean ROC curves for the NLP and BHI obtained using ten 10-fold cross validations of Quadratic Discriminant Analysis.

These results demonstrate that using the Bayesian Hierarchical Inversion method, we are able to quantify serum protein concentration in an automatic way with the same or even better performance than the operator-supervised Non-Linear Processing currently used. The BHI algorithm is able to manage the technological variability. This opens the way towards robust automatic processing of larger cohorts, enhance statistical power of biomarker studies and automatic test for diagnosis.

Related Publications:
[1] P. Szacherski et al (2013), "MRM protein quantification and serum sample classification", 61st ASMS Conference on Mass Spectrometry and Allied Topics, Minneapolis, Minnesota, USA, 9 - 13 June 2013.
[2] P. Grangeat et al (2013), "Convergence entre l'analyse biostatistique et les méthodes d'inversion hiérarchique bayésienne pour la recherche et la validation de biomarqueurs par spectrométrie de masse", XXIVème Colloque GRETSI, 3-6 septembre 2013, Brest, France.
[3] L. Gerfault et al (2013), "Assessing MRM protein quantification and serum sample classification performances of a Bayesian Hierarchical Inversion method on a colorectal cancer cohort", EuPA 2013 Scientific Meeting, Saint-Malo, France, 14 – 17 October 2013.

7

PhD Degree Awarded

AÏZEL Koceila

ATAYA Abbas

BISCEGLIA Emilie

BUIS Camille

CHONG Céline

MARIE Hélène

MATHIEU Nicolas

PERENON Rémi

PUSZKA Agathe

RENAUDOT Raphaël

PhD degree awarded in 2013

AÏZEL Koceila
Université de Grenoble

Developments of micro-nanofluidic systems applied to filtration and preconcentration

The research conducted during this thesis consists in a first step for the development of experimental methods applied to the concentration of nanoparticles using silicon micro-nanofluidic devices. The main aim is to explore different system architectures where the preconcentration step is achieved using steric and/or ion exclusion under the influence of a pressure and/or electric field. A special attention is directed toward the characterization methods including Micro-Particle Image Velocimetry (micro-PIV) and fluorescent microscopy in order to measure the nanoparticles distribution and to quantify the concentration folds.
The study is organized according to two main parts. The first part of the research deals with the preconcentration of nanoparticles within classical « Bypass-like » architectures, often found in the literature. Hydrodynamic steric filtration, electrokinetic preconcentration and the coupling of both will be studied. The second part is dedicated to the conception and utilization of original micro-nanofluidic configurations.

ATAYA Abbas
Université de Grenoble

Physical activity estimation using wearable sensors

Recent advances in technology have led to the miniaturization of motion sensors, facilitating their integration in small and comfortable wearable devices. Such devices are of great interest in the biomedical field especially for applications aimed at estimating the daily physical activity of people. In this thesis, we propose signal processing algorithms allowing better interpretation of sensors measures and thus their mapping to different activities. Our approach is based on the fact that activities have strong temporal dependencies. We propose an activity recognition system that models the activity sequence by a Markov chain. In addition, our system relies on parametric and non-parametric classification methods. The soft output of classifiers permits the construction of confidence measures in the activities. These confidence measures are later used as input to a Viterbi algorithm that gives the final estimation of the activity sequence. We validate our algorithms using a database containing 48 subjects, each of whom having carried out different activities for more than 90 minutes. Moreover, this thesis aims at providing practical answers to challenges concerning the development of a system for activity recognition. First of all, we wonder about the optimal sensor placement on the human body, and about the number of sensors needed for a reliable estimation of activities. We also approach the problem of selecting relevant features for the classification. Another crucial issue is related to the estimation of sensor's orientation on the body: this involves the problem of the sensor calibration. And finally, we provide a "real-time" implementation of the proposed recognition system, and collect a database under realistic conditions in order to validate our implemented real-time demonstrator.

PhD degree awarded in 2013

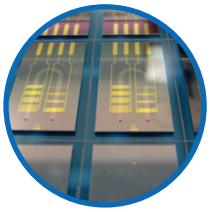

BISCEGLIA Emilie
Université Paris Sud

Physical methods to extract micro-organisms from blood samples using microsystems

Extraction of pathogens from a biological sample is a key step for efficient diagnostic tests of infectious diseases. For bloodstream infections, current diagnostic methods are usually based on bacterial growth and take several days to provide valuable information. An accelerated result would have a high medical value to adjust therapeutic strategies. The aim of this study is to design a new approach for separation and concentration of microorganisms directly from a blood sample, to avoid time-consuming growth stages. We report a method based on two different microsystems connected in series: it combines modification of conductivity and osmolarity of the sample with generic capture of microorganisms by dielectrophoresis. First we explore the impact of conductivity and osmolarity on the dielectric properties of blood cells and microorganisms.
Dilution and acoustic forces are both analyzed to transfer blood cells and microorganisms to the optimized buffer. Then we demonstrate the feasibility of achieving the dielectrophoretic separation of microorganisms from blood cells in a low conductivity and low osmolarity medium inside a fluidic device. The structure of the device is optimized with numerical simulations and experiments performed on blood samples and various microorganisms (E. coli, S. epidermidis and C. albicans).The generic capture of microorganisms is validated, and we achieved a separation of 97% efficiency with E. coli, with an optimal inlet velocity around 100-200 $\mu m.s^{-1}$. Finally, we propose an improved microsystem to perform the sample preparation step on a larger volume (1-10mL) in a few hours, in order to fit the medical need

BUIS Camille
Université Jean Monnet – Saint Etienne

Study of the correlation between the structural defect and the spatial inhomogeneities of CdTe based X-ray detectors for medical imaging

In the present Ph.D. thesis, we investigate microstructural defects in a chlorine-doped cadmium telluride crystal (CdTe:Cl), to understand the relationship between defects and performance of CdTe-based radiation detectors. Characterization tools, such as diffraction topography and chemical etching, are used for bulk and surface investigations of the distribution of dislocations. Dislocations are arranged into walls. Most of them appear to cross the whole thickness of the sample. Very good correlation is observed between areas with variations of dark-current and photo-current, and positions of the dislocation walls revealed at the surface of the sample. Then spectroscopic analysis of these defects was performed at low temperatures. It highlighted that dislocation walls induce non-radiative recombination, but it didn't show any Y luminescence usually attributed to dislocations in the literature. Ion Beam Induced Current (IBIC) measurements were used to evaluate the influence of dislocation walls on charge carrier transport properties. This experiment shows that they reduce the mobility-lifetime product of the charge carriers. A very clear correlation was, in fact, established between the distribution of the dislocation network and the linear defects revealed by their lower CIE on the device.

PhD degree awarded in 2013

CHONG Céline
Université Claude Bernard Lyon 1

Synthesis of functionalized magnetic nanoparticles for biological samples preparation

This thesis describes the synthesis of magnetic latexes which are able to capture and release various microorganisms via non-specific and electrostatic interactions. Cationic iron oxide nanoparticles stabilized by nitrate counterions were synthesized by the co-precipitation of iron salts in water. The surface of the as-obtained maghemite was then modified by a sol-gel process using methacrylate-functionalized organosilane, in order to incorporate the iron oxide nanoparticles into latex particles by copolymerization reactions.
Magnetic particles were obtained by dispersion, emulsion or miniemulsion polymerization of styrene or metyl methacrylate, performed in the presence of iron oxide. Due to the interaction between the stabilizers and iron oxides, dispersion polymerization was not a suitable approach. On the other hand, (mini-)emulsion polymerization led to a large range of particles diameters (140-650 nm), according to the process used to disperse iron oxides prior to the polymerization. These latexes contained between 2 and 37 % of magnetic particles, incorporating up to 91 % of iron oxide. But the size distribution remained quite broad in all cases.

The functionalization of as-prepared magnetic particles was then undertaken by the introduction of either a charged co-monomer or polyelectrolytes or polyampholytes reactivable during the polymerization process. These kind of polymers were synthetized by RAFT polymerization. Their ability to capture and release microorganism was tested on silica-based model systems. Polyampholytes displayed good results on several microorganisms.

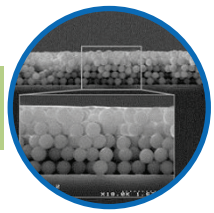

MARIE Hélène
Université de Technologie de Compiègne

Elaboration of a new sensor based on Molecularly Imprinted Polymers for the detection of molecules in physiological fluids

This thesis aimed at elaborating an optical sensor to detect molecules in a biological fluid. Two steroids and a xenobiotic were identified as biomarkers released in some body fluids: cyproterone acetate, cortisol and 2,4-dichlorophenoxyacetic acid respectively.
On one hand, detection was performed by Molecularly Imprinted Polymers (MIPs). These tailor-made synthetic receptors display numerous qualities that foster their integration in sensors. MIPs were therefore developed against the targeted analytes. Formulation optimization was led thanks to experimental designs.

On the other hand, optical transduction was made possible thanks to the structuring of a polymer into a photonic crystal. Opals were manufactured with a new process suitable for large scales and were used to mold MIPs in inverse opals. Thus, submicron structures of the polymer are responsible for the color of the sensor. A change of color is triggered by the recognition of the analyte by the polymer (upon swelling). Polymers studied displayed sufficient swelling observed by spectrophotometry.
Finally, the work of this thesis consisted in elaborating polymer formulations and their integration in a sensor so as to detect an analyte with direct, rapid and unobtrusive means.

PhD degree awarded in 2013

MATHIEU Nicolas
Université de Grenoble

Neurocognitive processing of emotions with aging: study of positivity effect and its consequences

With aging, the preference for positive stimuli increases compared to negative stimuli. This is called "positivity effect" and it may be observed in both behavior and brain activity. The main goal of this work was to characterized age effects on emotional processing to improve our understanding of this positivity effect. The second goal was to evaluate in which conditions these effects could make older people more vulnerable when they are confronted to threatening situations. A first EEG study revealed that the attentional engagement decreased with age for negative stimuli, regardless of their activation level, in an affective categorization task. Conversely, the processing of positive stimuli was preserved with age and, consequently, a reduction of the negativity bias was observed. In a second EEG study, using a similar paradigm to study 1 with the exception of the task which was an "action tendency task", we observed a preservation of the negativity bias. A third study revealed that the voluntary attention on interest situations for aged adults (positive) and on appraisal process modulated with age was requisite to observe positivity effects. Parallel to this work, a new method was proposed to recognize and classify emotional states based on EEG signals. We obtained encouraging results which suggest the possibility to use this method to elaborate brain-computer interfaces to protect old people against a potential vulnerability due to positivity effect. Taken together, these results demonstrate that positivity effect is due to motivational shifts with age. Older people would be motivated to increase their well-being and would regulate their emotions by reducing the impact of negative stimuli, provided no other more important motivations are absent.

PERENON Rémi
Université de Grenoble

Counting-mode information processing applied to spectrometric detectors

The miniaturization of electronic components drives the development of very sensitive sensors. In particular, NEMS (Nano ElectroMechanical Systems) are now sensitive enough to detect single molecules. This enables to use these sensors in order to design mass spectrometry devices, in an individual molecules counting mode. Our objective is to reconstruct the mass spectrum of the analyzed solution, based on the NEMS output signals.
We use inverse problems approach and Bayesian framework. We model the acquisition system linking the unknown parameters to the observable signals with a hierarchical graphical model. We propose a marked-point process model of signal that we compare with discrete-time process one.
We develop an impulse deconvolution algorithm which relies on a model exploration scheme. This enables us to detect the molecules, to quantify their mass and to count them in order to estimate the mass spectrum of the analyzed solution.
We show results on simulated data and on experimental ones acquired in CEA/INAC using Tantalum nano-aggregates and devices developed in CEA-Leti/DCOS. Compared to state-of-the-art, our method offers high counting rate and keeps a low false detection rate. It also permits the computation of uncertainties on estimated values. Finally, we propose a derivation of the method to deal with the reconstruction of discrete mass spectra.

PhD degree awarded in 2013

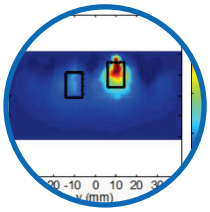

PUSZKA Agathe
Université de Grenoble

Diffuse optical tomography: a time-resolved approach for reflectance measurements at short source-detector separation

Diffuse optical tomography (DOT) is an emerging medical imaging technique using near-infrared light to probe biological tissues. This technique can retrieve three-dimensional maps of absorption and scattering coefficients inside organs from non-invasive measurements.
For some clinical applications, it is desirable to carry out the measurements for DOT with a compact probe including all sources and detectors. However, the depth sensitivity is a real challenge in this configuration. We propose to tackle this challenge by using time-resolved measurements.
A time-resolved approach is developed which involves methodological aspects including the processing of time-resolved signals by DOT algorithms based on the Mellin-Laplace transform. Then, this approach consists in optimizing the detection chain on two aspects for enhancing the detection and localization of absorption contrast in depth in diffusive media. First, the impact of the temporal response of the detector is studied with commercially available single-photon detectors (classical and hybrid photomultipliers). Second, the enhancements in probed depth permitted with fast-gated single-photon avalanche diodes are explored in a joint work with the Politecnico di Milano. To finish, a study is carried out to illustrate the performance of the proposed approach with respect to spatial resolution in depth for different configurations of sources and detectors in the optical probe.
Probes with a width limited to a few centimeters open the gate to multiple clinical interests. They could access intern organs like the prostate or facilitate the measurements on extern organs like the breast or the brain. This thesis has benefited of the Support of Politecnico di Milano, LASERLAB-EUROPE (grant agreement n° 284464, EC's Seventh Framework Program) and Région Rhône-Alpes (France).

RENAUDOT Raphaël
Université de Grenoble, Joseph Fourier

Programmable and re-configurable microfluidic chips

In the field of lab-on-a-chip (LOC) systems, the channel geometry of a microfluidic chip is often specific to perform a given protocol. The chip geometry is hence defined at the design step, before the fabrication steps (generally time consuming and expensive) and cannot be thereafter modified. This fact becomes an issue when the geometry does not fit satisfactorily to the specifications and a new batch of fabrication has to be started, to size afresh the microfluidic chip. To overcome this drawback we propose to develop a new generation of microfluidic chips with a programmable and reconfigurable geometry. This concept is widely based on both digital microfluidic techniques, the electrowetting on dielectrics (EWOD) and the liquid dielectrophoresis (LDEP) actuations.

This thesis is dealing with the programmable and reconfigurable geometry concept, thanks to microfluidic platforms which integrates both EWOD and LDEP technologies onto a same component. Firstly, the microfluidic platform in a single plate configuration allows providing master molds with a programmable geometry for the PDMS microfluidic chip fabrication. The results about this promising study lead to the processing of complex channels geometries, typically used in the microfluidic field. Secondly, the more exciting results are exposed about the programmable and reconfigurable microfluidic concept, by using advantageously the paraffin material. A specific protocol which takes advantages of LDEP and EWOD liquids displacements produces a lot of various and different microfluidic chips with complex channels shapes. For both applications, a single generic microfluidic platform can generate a wide number of different geometries, which can be modified partially or totally thereafter.

Greetings

Editorial Committee
Béatrice Icard
Jean-Marc Dinten
Loïck Verger
Guillaume Delapierre
Gilles Marchand
Raymond Campagnolo
Hélène Vatouyas
Sandra Barbier
Pierre Grangeat

Graphic Art
Hélène Vatouyas / Valérie Lassablière

Special Thanks
Bénédicte Messina

Photos
©CEA-LETI / G. Cottet

Contacts

Daniel Vellou
Head of « Microtechnologies for Biology and Healthcare » Division
daniel.vellou@cea.fr

Raymond Campagnolo
Chief Scientist
raymond.campagnolo@cea.fr

Eric Gouze
Business Development - Medical Devices
eric.gouze@cea.fr

Sandrine Locatelli
Business Development - Environment Monitoring
sandrine.locatelli@cea.fr

Patrick Boisseau
Business Development - Nanomedecine
patrick.boisseau@cea.fr

Claude Vauchier
Business Development - Systems for Process Monitoring
claude.vauchier@cea.fr

Francis Glasser
Business Development - Medical Imaging
francis.glasser@cea.fr

Alexandre Thermet
Business Development - In vitro Diagnostic
alexandre.thermet@cea.fr

CEA - Leti - DTBS
CEA Grenoble
17, rue des Martyrs
F-38054 GRENOBLE Cedex 9
Tel. (+33) 4 38 78 42 36
www.leti.fr